Assessment of Post-printing Component Cleaning Solutions for Lithography-based Metal Additive Manufacturing

Noel Bergvall, Jakob Pölder,
Måns Nilsson, Linus Thorstensson

June 3, 2026

IMSX16-14
Instutionen för industri- och materialvetenskap.
Chalmers University of Technology
Supervisor: Erika Tuneskog
Examiner: Lars Nyborg

Utvärdering av rengöringslösningar för komponenter efter utskrift inom litografibaserad additiv tillverkning i metall

Noel Bergvall, Jakob Pölder,
Måns Nilsson, Linus Thorstensson

June 3, 2026

IMSX16-14
Instutionen för industri- och materialvetenskap.
Chalmers University of Technology
Supervisor: Erika Tuneskog
Examiner: Lars Nyborg

Preface

This project has been conducted to support future research and projects that aim to utilize Lithography-based Metal Manufacturing (LMM). Erika Tuneskog has been consistently available and highly supportive throughout the work, and her assistance and teaching have been invaluable. We would therefore like to express our sincere gratitude and wish her the best of luck in future projects.

We would also like to express our gratitude to the postdoctoral researchers and doctoral candidates working in the laboratory for helping us understand the broader context and applications of this project. In particular, we would like to thank the following individuals for their contributions.

We would especially like to thank Florian Jürries for his insight into the complex shapes found in nature, and Sanjana Erravelli for her continuous support in starting prints and for giving us additional opportunities to test our methods on components beyond the scope of this bachelor thesis.

We also thank Antonio Mulone for his assistance in the materials laboratory, particularly in sectioning our components to obtain high-quality cross-sections, and Gabriele Muraca for his inspiration and valuable insight into another type of printer within the VPP category.

Special thanks to Nils Emil Fredrik Nordström for teaching us how to operate the microscopes and helping us troubleshoot image quality issues. This was essential for obtaining observable results.

Finally, we would like to thank Lars Nyborg for proposing this project and creating the opportunity for our bachelor thesis work.

Abstract

Additive Manufacturing (AM) enables the production of highly detailed components with complex internal geometries difficult to manufacture conventionally. Lithography-based Metal Manufacturing (LMM) is one such novel AM method, and the subject of investigation of this thesis.

Post-processing of LMM components with internal features smaller than 1.5 mm presents significant cleaning challenges. During de-caking, heat is applied to liquefy and drain excess feedstock. However, capillary forces and surface films trap viscous excess feedstock within internal features, making removal difficult. The current cleaning procedure produces defects and lacks standardization. This thesis aims to develop a standardized post-processing method minimizing cleaning-induced defects and yielding reliable cleaning results.

Ten batches of stainless steel 316L test components containing channels, junctions, and narrow fin arrays were manufactured and cleaned iteratively to identify defect-causing parameters. These parameters were validated through additional batches to establish a complete cleaning procedure.

Mechanical and chemical agitation proved most effective for feedstock removal. The optimal method involved inverted printing to avoid flow restrictions caused by the build plate, followed by a 15-minute de-caking stage and intermittent cleaning cycles using pressurized air and heated proprietary solution IncuSOL. A final 60 second exposure to the ultrasonic bath in heated IncuSOL is used to clear residual feedstock from components. Since polymerization begins immediately after printing and is accelerated by heat, cleaning must start directly after the print, conclude within 30 minutes, with the heating temperature limited to 60 °C.

Using this method, straight internal channels as small as 0.8 mm in diameter and 5 mm in length were successfully cleared. Further research is required to evaluate process consistency for other materials.

Sammandrag

Additiv tillverkning möjliggör tillverkning av detaljerade komponenter med komplexa interna geometrier som är svåra att framställa konventionellt. Litografi-baserad Metalltillverkning (LMM) är en ny additiv tillverkningsmetod och undersöks i denna rapport.

Rengöring av LMM-komponenter med interna geometrier mindre än 1.5 mm är problematiskt. Under de-caking appliceras värme för att smälta och avlägsna överbliven printmassa. Dock hindrar ytfilmer och kapillära krafter den viskösa printmassan från att avlägsnas från interna geometrier, vilket försvårar rengöring. Den nuvarande rengöringsmetoden resulterar i defekter och saknar standardisering. Denna studie ämnar att skapa en standardiserad rengöringsmetod som minimerar defekter som uppstår till följd av rengöring och som uppnår tillförlitliga rengöringsresultat.

Tio batcher av rostfritt stål 316L, som hade kanaler, flänsar och korsande kanaler, tillverkades och rengjordes iterativt för att identifiera parametrar som skapar defekter. Dessa parametrar validerades genom ytterligare batches för att etablera en komplett rengöringsmetod.

En kombination av mekanisk och kemisk bearbetning visade sig vara mest effektiv för att avlägsna printmassa. I den optimala metoden skrivs komponenter ut inverterade, för att undvika flödesrestriktioner orsakade av byggplattan, efterföljd av de-caking under 15 minuter och intermittenta rengöringscykler med tryckluft och en uppvärmd proprietär lösning vid namn IncuSOL. En avslutande ultraljudstvätt i uppvärmd IncuSOL under 60 sekunder används för att avlägsna kvarbliven printmassa från komponenter. Eftersom en polymerisationsprocess påbörjas efter utskrift och påskyndas av värmning måste rengöring påbörjas omedelbart efter utskrift, vara slutförd inom 30 minuter och uppvärmningstemperaturen begränsas till 60 °C.

Med denna metod möjliggörs rengöring av raka kanaler ner till 0.8 mm och 5 mm i längd. Fortsatt efterforskning krävs för att undersöka metodens tillförlitlighet.

Contents

1 Introduction **1**
- 1.1 Lithography-based Metal Manufacturing (LMM) . . . 1
- 1.2 Problem Description . . . 2
- 1.3 Motivation . . . 2
  - 1.3.1 Problem Statement . . . 2
- 1.4 Scope Limitations . . . 3
- 1.5 Methodology . . . 3

2 Theory **5**
- 2.1 Hammer Lab35 . . . 8
- 2.2 Post-printing Processing . . . 9
  - 2.2.1 Ultrasonic Cleaning . . . 9
  - 2.2.2 Airbrush Cleaning . . . 10
- 2.3 Interview with Incus . . . 10

3 Method **11**
- 3.1 Test Geometries and Sample Design . . . 11
- 3.2 Evaluation Criteria and Documentation . . . 13
- 3.3 Development of the Cleaning Procedure . . . 14
  - 3.3.1 Baseline Evaluation of the Existing Cleaning Method - Batch One . 15
  - 3.3.2 Baseline Evaluation of the Existing Cleaning Method with Minimized Handling - Batch Two . . . 16
  - 3.3.3 De-caking Parameter Study - Batch Three . . . 17
  - 3.3.4 Solvent-Assisted Cleaning Experiments - Batch Four . . . 19
  - 3.3.5 Impact of Delayed Post-Processing - Batch Five . . . 20
  - 3.3.6 Airbrush Cleaning Experiments - Batch Six . . . 21
  - 3.3.7 Ultrasonic Cleaning in IncuSOL - Batch Seven . . . 21
  - 3.3.8 Inverted Printing, Airbrush - Batch Eight . . . 23
  - 3.3.9 Airbrush without IncuSOL before Ultrasonic Cleaning - Batch Nine 24
  - 3.3.10 Final Method Validation with Incus Recommendations - Batch Ten 26

4 Results and Discussion **27**
- 4.1 Baseline Evaluation of the Existing Cleaning Method - Batch One . . . 27
- 4.2 Baseline Evaluation of the Existing Cleaning Method with Minimized Handling - Batch Two . . . 29
- 4.3 De-caking Parameter Study - Batch Three . . . 30
- 4.4 Solvent-Assisted Cleaning Experiments - Batch Four . . . 32
- 4.5 Impact of Delayed Post-Processing - Batch Five . . . 34
- 4.6 Airbrush Cleaning Experiments - Batch Six . . . 36
- 4.7 Ultrasonic Cleaning in IncuSOL - Batch Seven . . . 39
- 4.8 Inverted Printing, Airbrush - Batch Eight . . . 42
- 4.9 Airbrush without IncuSOL before Ultrasonic Cleaning - Batch Nine . . . 45
- 4.10 Final Method Validation with Incus Recommendations - Batch Ten . . . 49
- 4.11 Method Limitations . . . 54
- 4.12 Future Work . . . 54

5 Conclusions **57**
5.1 Design for Cleaning and Handling 57
5.2 Optimal Cleaning Process 57
5.3 Defect Identification and Categorization 59

A Hammer Lab35 Specification **63**

B Materials and Equipment **65**
B.1 Laboratory Equipment 65
B.1.1 Cleaning Solutions 67
B.2 Additional Equipment Introduced During the Study 68
B.2.1 Borrowed Equipment 68
B.2.2 Purchased Equipment 69
B.2.3 Custom-Made Equipment 71

C Defects **73**
C.1 Residual Feedstock 73
C.2 Cracks 74
C.3 Rounded Edges 75
C.4 Surface Scratches 76
C.5 Delamination 77

D Advantages and Disadvantages of the Different AM-methods **79**
D.1 VPP 80
D.2 MEX 81
D.3 PBF 82
D.4 MJT 83
D.5 BJT 84
D.6 DED 85
D.7 SHL 86

E Cleaning Guide - LMM **87**

F Drawings of test components **97**

Nomenclature

Institutions:

- Chalmers University of Technology - Chalmers
- Loughborough University Additive Manufacturing Research Group - (LU-AMRG)
- Research Institute of Sweden - RISE

Additive Manufacturing Subcategories and Terms

- Acrylonitrile Butadiene Styrene - ABS
- Additive Manufacturing - AM
- Binder Jetting Technology - BJT
- Computer Aided Design - CAD
- Computer numerical control - CNC
- Digital Light Processor - DLP
- Directed Energy Deposition - DED
- Direct Metal Laser Sinterin - DMLS
- Fused Deposition Modelling - FDM
- Electron Beam Melting - EBM
- Fused Filament Fabrication - FFF
- Laminated Object Manufacturing - LAM
- Lithography-based Metal Manufacturing - LMM
- Material Extrusion - MEX
- Material Jetting Technology- MJT
- Metal Injection Moulding - MIM
- Polycarbonate - PC
- Powder Bed Fusion - PBF
- Powder Bed Fusion Electron Beam - PBF-EB
- Powder Bed Fusion Laser Beam - PBF-LB
- Selective Heat Sintering - SHS
- Selective Laser Melting - SLM
- Selective Laser Sintering - SLS
- Sheet Lamination - SHL
- Ultrasonic Additive Manufacturing - UAM
- Ultraviolet radiation - UV
- Vat Photopolymerization - VPP

1 Introduction

Additive Manufacturing (AM), commonly known as 3D printing, enables the production of complex geometries that are difficult or impossible to achieve using conventional subtractive manufacturing methods. Using AM, components are built layer by layer, in contrast to subtractive manufacturing where material is removed to create components. The ability to rapidly iterate and modify components through changes to a digital model has the potential to simplify design steps in product development. Today, the method is used to a limited but growing extent in sectors such as the aerospace industry, medical technology, the space industry, and more [1].

1.1 Lithography-based Metal Manufacturing (LMM)

LMM is a subcategory of Vat Photopolymerization (VPP), a process where photopolymer resins are selectively cured using light [2]. Unlike other VPP methods, LMM uses a raw material that is solid at room temperature. This raw material, referred to as feedstock, consists of a mix of a photosensitive polymer, organic additives and metal particles [3]. The material is melted and spread, using a blade heated to 85 °C, over a build plate that descends as the building proceeds. The building chamber has a controlled temperature of 15 °C to 19 °C, allowing the material to solidify on the build plate.

Using LMM printing, the terms "brown body" and "green body" are used to denote the physical state of the component before it becomes a solid metal part. The green body refers to the component directly after printing and throughout the cleaning process, when a cured polymer binder still holds the metal powder together. Once this binder is completely removed, the part becomes a brown body and is ready for sintering [3].

After a completed print, the resulting green body undergoes a series of post-processing steps before sintering. The first step is heating the component to about 45 °C - 60 °C until the feedstock melts and drains from the component. This leaves residual feedstock material inside geometries such as channels and between fins, requiring further cleaning.

LMM can produce complex internal channels and small intricately detailed geometries (typically with feature sizes below 1 mm). However, these same features introduce significant challenges during post-processing, particularly in achieving effective cleaning of internal structures. In practice, the cleaning procedures are manually performed, lack standardization, and do not ensure repeatability nor avoid cleaning induced defects.

1.2 Problem Description

The current cleaning procedure comprises three main stages: de-cake, ultrasonic cleaning, and drying. Each stage contains process parameters that influence cleaning effectiveness, repeatability, and the risk of component damage.

During the de-cake stage, excess feedstock is removed to reveal the final geometry. However, the current use of manual heating results in uneven temperature distribution, increasing the risk of geometric deformation and incomplete removal of feedstock, particularly in internal features. In addition, the procedure does not provide a reliable method for verifying cleaning effectiveness.

Further cleaning is performed using ultrasonic treatment in a solvent. Exposure time and temperature are critical parameters, as insufficient treatment may leave residual feedstock, while excessive treatment may cause surface defects. The optimal process settings remain unclear and are likely dependent on component geometry.

In the final drying stage, residual solvent is removed using either evaporation or compressed air. This step relies heavily on manual handling and operator controlled parameters, which reduces repeatability and increases the risk of damage to fragile structures.

The interaction between multiple process parameters complicates the identification of defect mechanisms. As a result, the absence of a documented and standardized cleaning process makes it difficult to achieve consistent results and to understand the relationship between the cleaning process and defect formation.

1.3 Motivation

The aim of this study is to develop a standardized and reproducible cleaning process for small, intricately detailed components manufactured using LMM technology. Furthermore, the study aims to identify and categorize surface defects and structural damage, as well as to investigate the geometric limitations associated with the cleaning process.

1.3.1 Problem Statement

- How can a standardized and reproducible cleaning process be established to minimize the risk of structural damage and surface defects in a range of small, intricately detailed geometries manufactured using LMM technology?
- How can the development of such a standardized cleaning process enable the identification and categorization of arising defects and their causes?

1.4 Scope Limitations

This study focuses exclusively on LMM, as the cleaning process is intended to be specifically adapted to this type of AM. In addition the following delimitations apply:

- Printing parameters are determined by doctoral candidates and postdoctoral researchers.
- Components manufactured from other materials are tested and used only when provided by doctoral candidates and postdoctoral researchers at the laboratory who produced the components themselves. Otherwise stainless steel 316L is used.
- No specialized cleaning equipment beyond what is available to Chalmers personnel is considered.
- The sintering process is not included within the scope of this project and its parameters will not be analysed.
- Test geometries are limited to that which fits in the medium sized build plate of the printer with the dimensions $46x28$ mm.
- Available number of print batches is limited to a total of 10, with an unspecified number of components allocated by doctoral candidates and postdoctoral researchers.

1.5 Methodology

This project consisted of the following steps: design of test components, evaluation of the current cleaning method, breakdown of individual steps in the cleaning process, and finally the combination of these steps into a complete cleaning procedure.

Based on discussions with doctoral and postdoctoral researchers, test components were designed to evaluate challenges associated with the cleaning process. These components were first processed using the existing cleaning method to establish a baseline for comparison in subsequent tests.

By separating the cleaning process into individual steps, each stage could be evaluated independently to identify both effective parameters and those causing damage. Following this breakdown, combinations of the steps were tested to develop a complete cleaning procedure for the test components. During these tests, damage to the components was observed and documented.

The evaluation of cleaning performance was conducted through visual inspection and analysis using stereo microscopy. Images were captured from multiple orientations for each component, and additional images were taken when defects or irregularities were observed. Cleaning efficacy was assessed based on the removal of residual feedstock, preservation of geometric features, and the occurrence of defects.

2 Theory

AM encompasses a range of manufacturing technologies that enable the production of components through layer-by-layer material deposition. These methods differ significantly in terms of working principles, material compatibility, achievable resolution, and post-processing requirements. As a result, each AM method presents distinct advantages and limitations depending on the intended application. The advantages and disadvantages are shown in appendix D *Advantages and disadvantages of the different AM - methods*. Understanding these differences is essential when selecting a suitable manufacturing method, particularly for components with complex internal geometries where both manufacturing and post-processing constraints must be considered.

The current AM methods are separated into seven categories [1, 4]. These methods differ in areas such as quality, speed, suitable application range, build size, cost, material compatibility, structural properties, support requirements, and post-processing. The following sections provide a brief overview of these methods, followed by a more detailed discussion of the theoretical background specific to LMM.

- Vat Photopolymerization (VPP) – A process based on a liquid resin or slurry containing photosensitive material that is selectively cured using UV light or a digital light projector. The geometry is built layer by layer by projecting the cross-section of each layer onto the material until a solid structure is formed [1, 2].

  VPP enables high resolution and smooth surface finishes, but typically requires post-processing to remove uncured material. While conventional VPP processes are not surrounded by raw material, LMM, used in this study, differs in that the printed components are embedded in surrounding feedstock during printing[2].

- Material Extrusion (MEX) – A process in which a thermoplastic material is fed as a filament and extruded through a heated nozzle to build components layer by layer. The material is typically supplied on a spool, melted during extrusion, and deposited according to the desired geometry [1, 5].

  MEX is a cost-effective and widely used AM method [5]. However, its limited resolution makes it less suitable for producing the small, intricate geometries investigated in this study.

- Powder Bed Fusion (PBF) – A process in which a thin layer of powder is spread across a build platform and selectively fused using a laser or electron beam to form solid structures layer by layer [1, 6]. The ASTM/ISO standard definitions are powder bed fusion laser beam (PBF-LB) and powder bed fusion electron beam (PBF-EB). Common descriptions set by different PBF equipment providers include Selective Laser Sintering (SLS), Electron Beam Melting (EBM), Direct Metal Laser Sintering (DMLS), and Selective Laser Melting (SLM) [6].

  PBF enables the production of strong and complex components. Similar to LMM, it requires removal of excess material after printing, as surrounding powder must be cleared. This makes internal channels difficult to clean and highlights challenges associated with small internal geometries [6].

- Material Jetting Technology (MJT) – A process in which droplets containing material are selectively deposited onto a build surface and solidified using UV light to form components layer by layer [1, 7]. The process allows for high resolution and the ability to combine multiple materials within a single print [1, 7].

  MJT produces components with high surface quality and typically requires minimal post-processing beyond support removal [8]. In contrast to LMM, MJT does not involve surrounding excess material that must be removed, making it less affected by cleaning challenges in internal geometries.

- Binder Jetting Technology (BJT) – A process in which a liquid binder is selectively deposited onto a powder bed to bond powder particles together and form components layer by layer [1, 8]. The surrounding powder supports the geometry during printing, eliminating the need for additional support structures [8].

  BJT enables the production of complex components at relatively low cost but typically requires post-processing such as curing and sintering to achieve final properties [8]. Similar to LMM, excess material must be removed after printing, as surrounding powder needs to be cleared, making internal features challenging to clean.

- Directed Energy Deposition (DED) – A process in which material, supplied as powder or wire, is melted by a focused energy source such as a laser, electron beam or plasma arc and deposited layer by layer onto a substrate or existing component [1, 9]. The process is typically performed using multi-axis systems, enabling the addition of material in multiple directions [9].

  DED is commonly used for repair, coating, and the addition of features to existing components, as well as for producing larger parts with high strength requirements [1]. In contrast to LMM, the process does not involve surrounding excess material that must be removed, making it less affected by cleaning challenges in small internal geometries.

- Sheet Lamination (SHL) – A process in which sheets of material are cut to shape and bonded together layer by layer to form a three-dimensional component [1, 10]. Variants include Ultrasonic Additive Manufacturing (UAM), which uses metal sheets joined by ultrasonic welding, and Laminated Object Manufacturing (LAM), which typically uses paper-based materials bonded with adhesive [10].

  SHL is suitable for producing larger components quickly and at low cost. However, the layer-wise bonding of sheets limits the ability to create fine internal geometries [1, 10]. In contrast to LMM, SHL does not involve removal of viscous or trapped material, making it less relevant for studying cleaning challenges in small and complex internal features.

Table 1: Simplified comparison of main AM categories based on appendix D*Advantages and disadvantages of the different AM- methods.*

Method	**Resolution**	**Strength**	**Post-processing**	**Relevance to LMM study**	**Internal features <1mm**
VPP (LMM)	High	Low (green state)	Resin/feedstock removal required	Focus of study – cleaning of internal features	Yes
MEX	Low	Moderate	Minimal	Limited resolution – not suitable for small internal geometries	No
PBF	Medium to High	High	Powder removal required	Similar cleaning challenges in internal channels	Limited
MJT	High	Low	Minimal	No trapped material – limited cleaning relevance	Yes
BJT	Medium	Low (pre-sintering)	Debinding + sintering	Powder removal creates similar cleaning challenges	No
DED	Low to Medium	High	Minimal	No surrounding material – limited cleaning relevance	No
SHL	Low	Low–Medium	Minimal	Limited internal geometry capability	No

As seen in Table 1, only a few AM technologies are capable of reliably producing intricate internal features smaller than 1 mm. Most methods fail at this scale for several reasons. MEX fails because the solid supports it creates require mechanical removal, which in most cases is impossible with these features, while DED and SHL ultimately fail due to the inherently low precision of the methods [5, 9, 10].

BJT and medium resolution PBF avoid solid support structures by utilizing the surrounding powder bed. However, they fail to achieve these internal features due to print resolution [6, 8].

Consequently, MJT and high-resolution PBF remain the primary alternatives capable of achieving these internal features. While MJT can achieve this high resolution, it relies on dedicated support materials, bypassing the specific challenge of trapped raw material. PBF presents a similar post-processing challenge to LMM, as unfused metal powder must be evacuated from cavities. However, post-processing LMM components remains uniquely difficult due to the highly viscous feedstock [6, 7].

2.1 Hammer Lab35

The experimental work in this project is based on the Hammer Lab35, see appendix A for specifications, manufactured by Incus. Incus developed the LMM process (a subcategory of VPP) to enable prototyping and small-scale production of AM components [11].

The feedstock is loaded onto the material piston. The piston raises the feedstock layer by layer, which in turn is moved and evenly distributed across the platform by a heated blade. Once distributed, a Digital Light Processor (DLP) flashes the relevant 2D cross section onto the layered feedstock and hardens the polymer in certain areas according to the sliced CAD model. The build piston is lowered, allowing for a new layer of feedstock to be distributed on top of the building platform and the process repeats until a complete model has been created. Once completed, the building piston extends fully allowing for the removal of the block containing the green bodies from the printer [3].

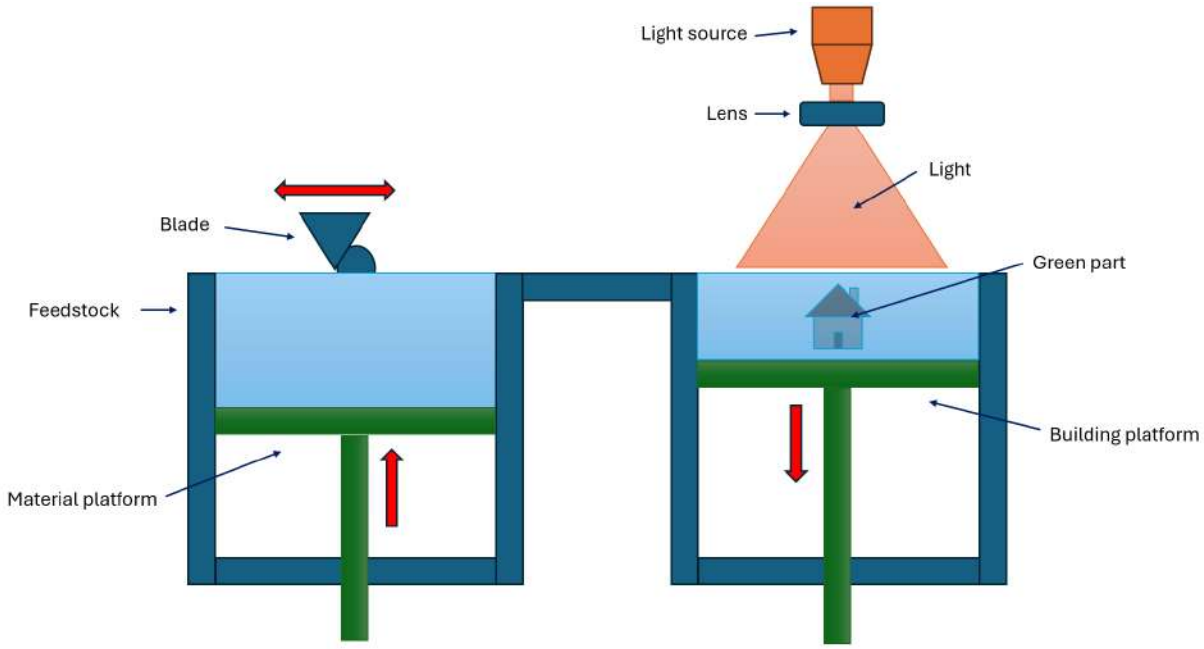

Figure 1: Schematic diagram of the LMM process used by the Hammer Lab35 [12].

2.2 Post-printing Processing

Following the LMM printing process, the resulting green bodies exhibit poor mechanical properties and are fragile [3]. During the photo-polymerization only the binder is cured, leaving the metal particles encapsulated in the polymer matrix. To minimize shrinkage during the subsequent sintering, the ratio of metal to binder in the feedstock must be high. The steel 316L feedstock used in this project contains 55% metal particles by volume and 88% by weight [3]. Consequently, the mechanical properties of the components are entirely dependent on the limited volume of cured polymer matrix, necessitating careful handling during subsequent stages.

Given the projects focus on internal channels smaller than 1.5 mm, de-caking of the green bodies is affected by several parameters. During the initial de-caking stage, heat is applied to separate the excess feedstock from the components. The feedstock used is solid at room temperature and has a melting point of 45 °C - 50 °C [3]. When subjected to temperatures above this threshold, the viscosity of the feedstock drops, allowing gravity to drain the excess away. However, there is an upper limit, temperatures exceeding 80 °C permanently degrade the feedstock preventing its reuse.

Furthermore, the draining of excess feedstock from geometries such as narrow channels and fin arrays introduces difficulties related to fluid dynamics. As the scale of the geometries decreases, the relative strength of forces such as the capillary action and surface tension becomes increasingly dominant relative to gravity, preventing efficient removal of excess feedstock [13]. These forces necessitate further mechanical and chemical agitation. A partial solution to this is IncuSOL, an isopropanol-based cleaning solvent developed by Incus specifically to remove excess feedstock [14]. IncuSOL reduces surface tension and dissolves feedstock, easing drainage. However, prolonged exposure to IncuSOL may damage the components when the binder is exposed. IncuSOL penetrates the porous surface, dissolving the cured binder beneath causing swelling also known as "blistering", as well as delamination [13].

2.2.1 Ultrasonic Cleaning

Another partial solution for removing excess feedstock is ultrasonic cleaning as an additional post-processing stage. Ultrasonic cleaners transmit high-frequency sound waves through a liquid solvent, inducing cavitation within the fluid [13]. The resulting shock waves can dislodge residual feedstock not only from external surfaces but also from narrow channels and internal geometries.

However, both the cavitation and the solvent pose a significant risk of damaging the components, as the green parts at this stage are only supported by the cured binder. Prolonged exposure may cause fractures and blistering as the polymer matrix degrades [13]. Edges and corners are especially vulnerable due to stress concentration effects.

2.2.2 Airbrush Cleaning

Airbrushing provides a combination of mechanical and chemical agitation to remove excess feedstock from the components. The process utilizes a stream of pressurized air that mechanically pushes melted feedstock off surfaces or out of narrow channels. To help overcome the strong capillary action and surface tension trapping material, the airbrush simultaneously applies a solvent, which chemically dissolves the binder and breaks the surface film.

The process must be carefully controlled to prevent damage to the components. Excessive pressure can easily deform thin geometries such as fin arrays. Furthermore, prolonged exposure to the solvent dissolves the binder not only in the excess feedstock but also in the component itself. Therefore, the application must be kept short and excess solvent must be removed.

2.3 Interview with Incus

Following an interview with Dr. Santiago Cano, representative of Incus GmbH, several recommendations relevant to the subsequent experimental work were identified and implemented into the testing procedure.

- Heating causes the polymer to continue reacting and binding surrounding material. This can lead to cross-binding within channels and between fin structures, inhibiting flow and negatively affecting cleaning performance. Components should preferably not remain in a heated state for more than 30 minutes and should not undergo repeated heating and cooling cycles, as thermal expansion and contraction may weaken the structure.
- IncuSOL can be applied directly onto components and remain for prolonged exposure times, up to approximately 15 minutes.
- Components should be stored in a dry and controlled environment to minimize moisture absorption, as moisture may weaken printed layers and increase the risk of delamination during cleaning.
- Components in an ultrasonic bath should be positioned above the bottom surface of the container to avoid contact with cleared feedstock. Continual movement of components during ultrasonic cleaning is also beneficial, as it promotes a flushing effect that helps remove residual feedstock.
- When using an airbrush, the IncuSOL should be heated to approximately 55 °C to avoid cooling the components and to improve solvent efficiency.
- The optimal frequency of the ultrasonic cleaner is approximately 40 kHz. Lower frequencies improve cleaning efficacy but increase the risk of component damage, while higher frequencies reduce damage but also decrease cleaning effectiveness.
- Feedstock that includes material such as copper can have the metal act as a catalyst, facilitating chemical reactions. This complicates cleaning procedures.

3 Method

The cleaning procedure was developed iteratively by first evaluating individual cleaning steps separately before combining them into an improved process. Cleaning efficacy was assessed through visual inspection and microscopy, with focus on residual feedstock and defect formation. The following sections present the test geometries, evaluation criteria, and experimental development of the cleaning process. Detailed lists of materials and equipment are provided in Appendix B *Material and Equipment*, while examples of observed defects are presented in Appendix C *Defects*.

3.1 Test Geometries and Sample Design

To evaluate the cleaning process, four different component types were designed with focus on geometries considered difficult to clean. These geometries were selected through discussions with supervisor Erika Tuneskog and included:

- Straight channels of varying diameters
- Curved channels of varying diameters
- Fin arrays of different thicknesses and heights
- Internal junctions of channels

The following components were designed as conventional tests to evaluate cleaning efficacy in relation to channel diameter and fin dimensions that could be reliably cleaned without leaving residual feedstock or causing component damage. Component A consisted of a 5 mm tall block containing straight channels with diameters ranging from 1 mm to 0.3 mm. Component C consisted of a thin block containing a fin array with a height-to-width ratio of 10:1. The fin widths ranged from 0.15 mm to 0.3 mm, while the heights ranged from 1.5 mm to 3.0 mm. Surfaces without easily distinguishable features were marked with numbers to simplify identification of individual specimens. Full drawings of component A and C can be seen in appendix F *Drawings of test components*.

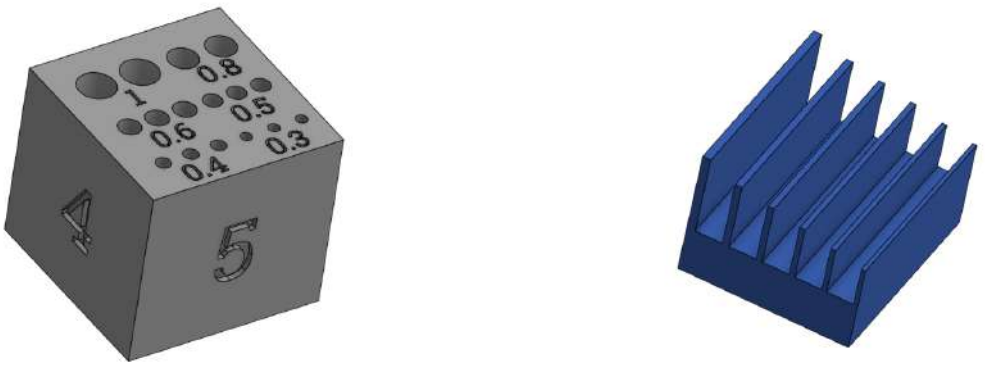

(a) Component A: Straight channels with varying diameters.

(b) Component C: Fin array with varying heights and widths.

Figure 2: Test geometries A and C used to evaluate cleaning of straight channels and gaps between fins.

The second set of components was designed to evaluate cleaning of increasingly complex internal channels. Component B consisted of a block containing curved channels with diameters ranging from 1.5 mm to 1 mm, where the bend radius was 3 mm. Component D consisted of a channel junction with one central 2 mm channel connected to four surrounding 1.25 mm channels positioned symmetrically around the center 1.25 mm from the lower side. Surfaces without easily distinguishable features were also marked with numbers to simplify later identification in figures. Full drawings of component B and D can be seen in appendix F *Drawings of test components*.

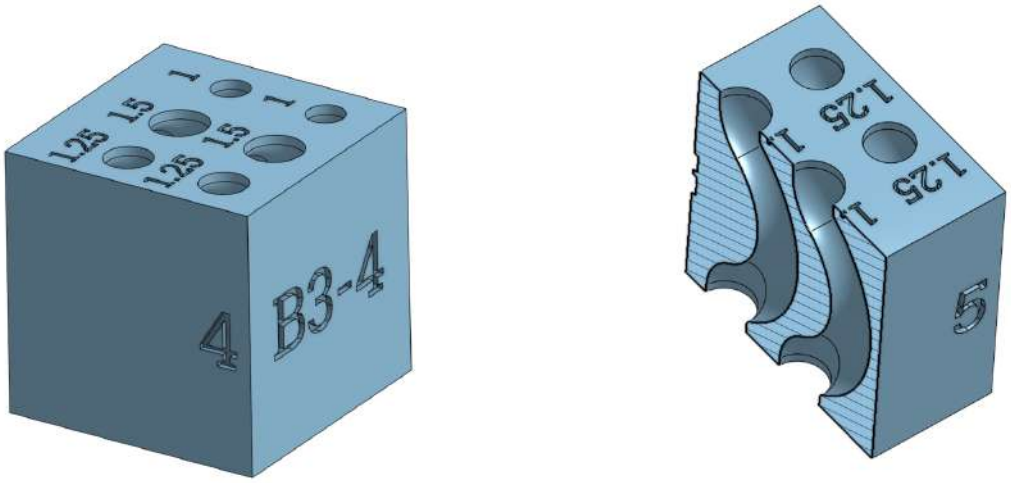

(a) Component B: Complex internal curved channel geometry of varying sizes.

(b) Component B: Cross-section showing internal flow paths.

Figure 3: Component B: Standard view of the component together with cross section view.

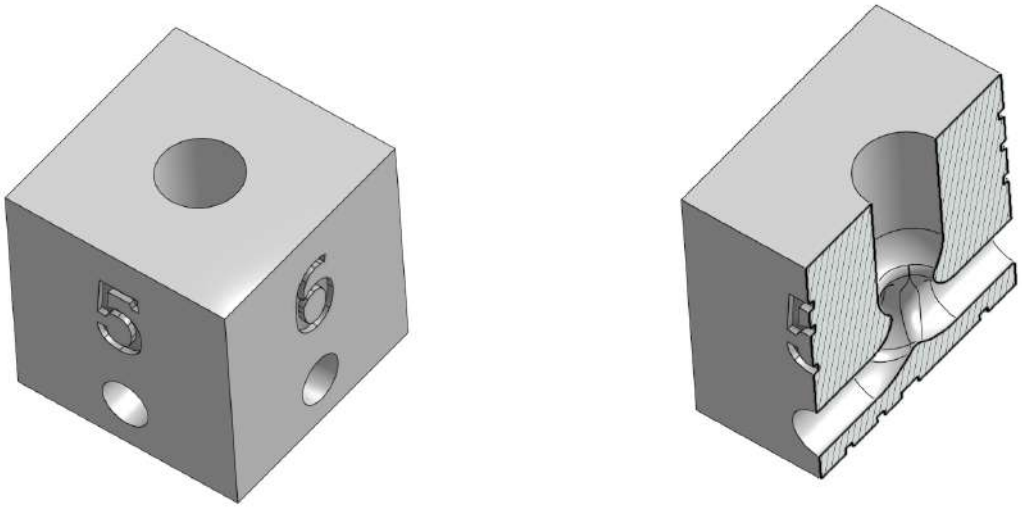

(a) Component D: Combined vertical and horizontal channels into a junction.

(b) Component D: Cross-section showing junction channels.

Figure 4: Test geometries B and D used to evaluate cleaning of complex and intersecting internal channels.

For each component type, four duplicates were printed to allow variations in the testing procedure to be evaluated. Initially, the spacing between components on the build plate was 1 mm. After batch three, this distance was increased to 1.5 mm to improve feedstock flow and reduce the risk of components sticking together. The components were positioned with a 400 µm offset from the build plate, resulting in a total print height of 7.4 mm as shown in Figure 5a. The overall build layout dimensions were 46 mm in length and 28 mm in width.

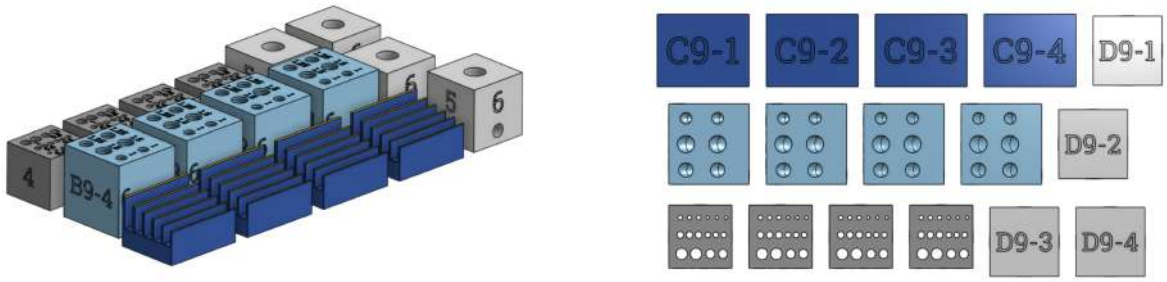

(a) Build plate layout in isometric view.

(b) View of the build plate showing component positions and sample groups.

Figure 5: Build plate layout showing component placement and sample identification used during printing.

3.2 Evaluation Criteria and Documentation

Each experimental stage was designed to evaluate specific aspects of the cleaning procedure and to guide the continued development of the method. Since the number of available print batches was limited to ten, observations from each stage were used to determine which parameters and cleaning strategies should be investigated further.

All cleaned components were examined using stereo microscopy. At least three sides of each component were photographed after cleaning, while additional images were taken when defects or residual feedstock were observed. The purpose of the documentation was to enable comparison between methods and to identify recurring patterns of damage or insufficient cleaning.

The evaluation focused on cleaning efficacy and visible damage. Particular attention was given to residual feedstock, blocked channels, bent fins, edge damage, and other defects affecting the geometry or surface quality of components.

3.3 Development of the Cleaning Procedure

Documentation and execution details for each experimental stage carried out during the project are presented in the following sections. Materials and equipment used throughout the experiments are listed in Appendix B *Materials and Equipment*.

The cleaning procedure consisted of multiple stages intended to remove excess feedstock from the components after printing. The initial de-caking stage was used to separate the components from the surrounding feedstock block. This was followed by one or more secondary cleaning methods, which were ultrasonic cleaning and airbrush cleaning with or without IncuSOL. Depending on the observed cleaning performance, these stages could be repeated or combined before the components were dried using either compressed air or passive air drying.

Figure 6 presents a simplified overview of the different cleaning and drying stages evaluated during development of the cleaning procedure and how the individual methods could be combined iteratively throughout the experimental batches.

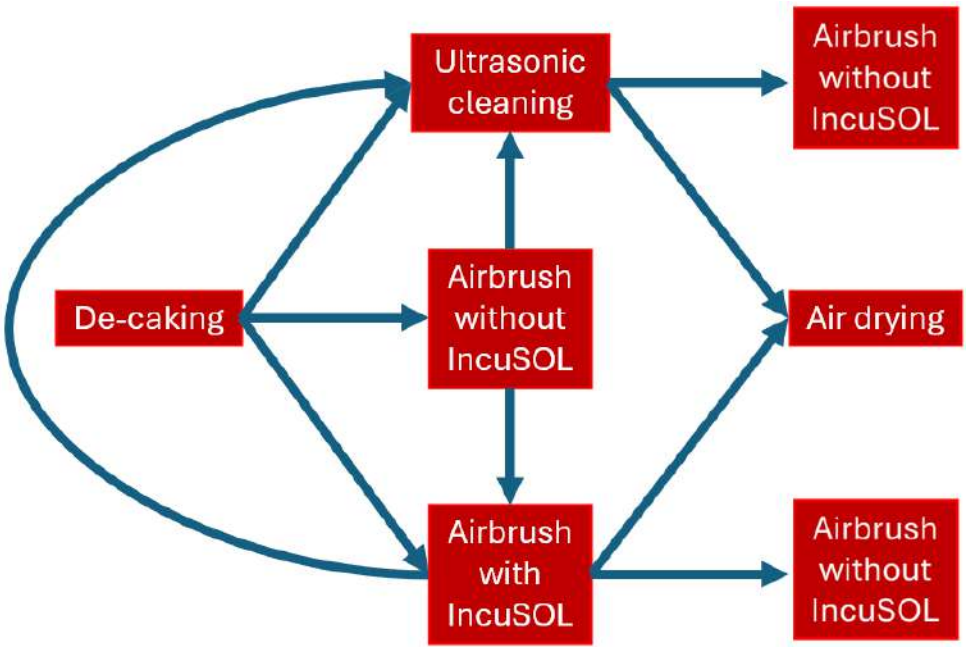

Figure 6: Flowchart illustrating the different cleaning and drying stages evaluated and combined during iterative development of the cleaning procedure.

3.3.1 Baseline Evaluation of the Existing Cleaning Method - Batch One

The initial batch was processed using the existing cleaning method in order to establish a baseline reference for later comparison. The purpose was to evaluate the effectiveness of the current procedure and to identify areas where improvements could be made.

Batch one included four sample geometries. For geometries A, C, and D, four specimens were printed, while three specimens of geometry B were included.

The cleaning procedure began with a de-caking step in which the feedstock block was placed on a plastic mesh positioned above a glass container as seen in Figure 7. Heat was applied using a handheld heat gun at setting two from a distance of approximately 60 cm, resulting in a temperature of about 60 °C. Due to the handheld operation, some temperature variation was expected. The de-caking stage lasted approximately 20 minutes, until no further dripping of excess feedstock was observed.

This was followed by ultrasonic cleaning in IncuSOL for two minutes. After cleaning, the components were removed one by one from the solution using tweezers. Finally, the components were placed on a paper towel and dried using compressed air.

Figure 7: Initial de-caking setup used, where heat was applied manually using a handheld heat gun.

3.3.2 Baseline Evaluation of the Existing Cleaning Method with Minimized Handling - Batch Two

This batch was conducted using the same baseline procedure as batch one, but with modifications intended to reduce direct handling of the components during cleaning. Reduced handling of components was considered beneficial due to the inherent risk of damage caused by operator error.

Batch two included the same set of geometries and number of specimens as batch one but with some modifications to the dimensions of the components. On the A-,B- and D-component, channel diameters were increased by 20-30 % in order to ease cleaning and more accurately gauge improvements stemming from changes to the cleaning procedure. Component A also had a slight adjustment to accommodate measurement specifications. Finally print orientation for components B was changed so that channels were vertically oriented, easing the escape of feedstock.

The de-caking stage was performed using the same handheld heat gun setup at approximately 60 °C for 20 minutes, until no further dripping of excess feedstock was observed. After de-caking, the entire build plate was transferred using metal tweezers into a larger beaker containing IncuSOL heated to 45 °C. The beaker was then placed in an ultrasonic cleaner for four minutes.

After ultrasonic cleaning, the solution was poured off and the components were poured onto a paper towel and dried. The main difference from batch one was therefore the reduced handling of individual components during the cleaning stage.

3.3.3 De-caking Parameter Study - Batch Three

To evaluate the entire cleaning process from start to finish, the first step was to establish suitable parameters for the initial de-caking stage. Therefore, batch three investigated the influence of heat exposure time during the de-caking stage of the cleaning process.

In this batch, four specimens of each geometry were printed, resulting in a total of 16 components. Size adjustments made it possible to fit a fourth B-component on the build plate, which enables identical number of testing procedures for all components. For this test, the C-components were modified and the thickness of the baseplate was increased from 1.25 mm to 1.75 mm to minimize damage during handling with tweezers.

During the de-caking stage, heat was applied using the heat gun mounted on a newly introduced stand seen in Figure 9. Unlike previous batches where the heat gun was handheld, this stand enabled a more consistent temperature by positioning the gun at distances up to 60 cm from the container holding the feedstock block. Prior to placing the feedstock block in the container, the temperature was measured using a FLUKE 53 II THERMOMETER with the probe placed on the plastic mesh to ensure that it reached and stabilized at approximately 60 °C or 80 °C, depending on the heating stage. This is visualized in Figure 8. The heat gun was operated at setting two out of three, and the desired temperature was achieved by adjusting the distance between the heat gun and the container.

Figure 8: Placement of temperature measuring probe during tests

Figure 9: Heat gun stand during de-caking with a glass container to catch excess feedstock.

Along with the newly introduced stand, the setup also utilized an adjustable tilting device shown in Figure B.8 in B.2.3 to hold the container. This device allowed the container to be set at inclinations between 0° and 45° to assist in drainage of excess feedstock. Throughout the experiment, the inclination was fixed at 15° which was the steepest angle possible to avoid components sticking together or colliding, which could cause damage.

All components were initially subjected to 40 minutes of de-caking at 60 °C to remove and recycle most of the excess feedstock. After initial de-caking the temperature was increased to 80 °C to attempt to decrease the viscosity of the feedstock. Simultaneously, the container holding the components was placed onto the tilting plate set at 15°. The container was then rotated 90° clockwise every 10 minutes on the tilting device to ease drainage of excess feedstock from the components. This rotation is visualised in Figure 10.

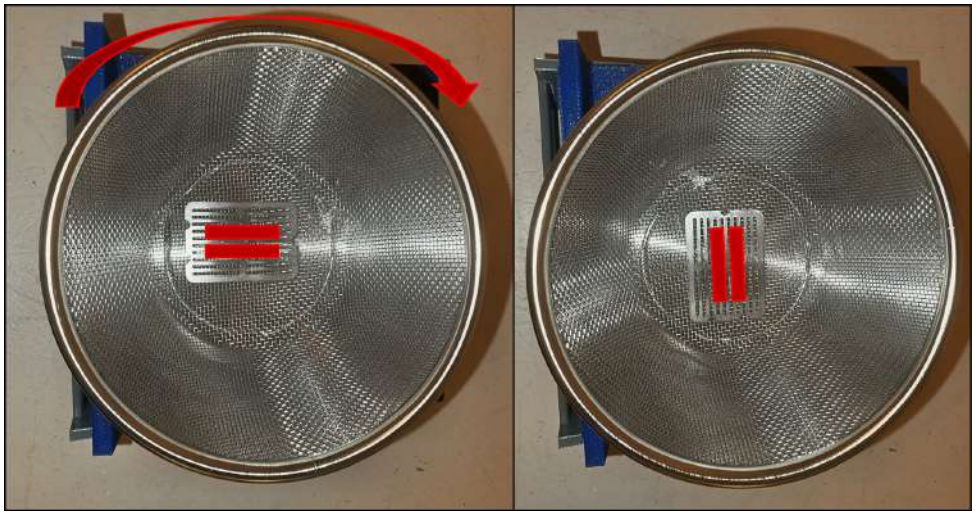

Figure 10: Container positioning during the secondary heating stage. Left: initial orientation. Right: orientation after a 90° clockwise rotation to improve drainage of excess feedstock.

The experiment was divided into 40-minute intervals, where each sample group was subjected to different exposure times according to Table 2. After each interval, one complete set of components was removed for further evaluation.

Upon completion of the heating intervals, the components were placed on a paper towel to cool down.

Table 2: Overview of batch three experimental design, including de-caking parameters and total heating exposure times for each sample group.

Sample Group	de-caking 60°C	Heating 80°C	Time (min)
1	40 min	15° incline, rotate 90° every 10 min	40
2	40 min	15° incline, rotate 90° every 10 min	80
3	40 min	15° incline, rotate 90° every 10 min	120
4	40 min	15° incline, rotate 90° every 10 min	160

3.3.4 Solvent-Assisted Cleaning Experiments - Batch Four

Based on the outcomes of the previous test, it was considered that introducing a solvent capable of breaking the surface film could further improve the cleaning results. Consequently, batch four investigates the effect of applying different amounts of IncuSOL directly onto the components while under the heat gun. The reasoning was that the lowered viscosity achieved by the heat, combined with the surface film breaking properties of IncuSOL, would facilitate an improved drainage of excess feedstock. IncuSOL was chosen primarily as it is developed specifically for this purpose by Incus.

Previous testing revealed a need to reduce the risk of surface damage during handling, consequently rubber-coated tweezers were introduced for removal of components from the build plate and transfer between cleaning steps. A figure of these can be found in appendix B.2.2 *Purchased Equipment*.

The de-caking step was performed with the components positioned horizontally rather than on an incline used in batch three, otherwise the experimental setup was identical to that of batch three.

During the test, IncuSOL was applied manually using a pipette while the components remained under heat exposure. The distribution of drops between the components is shown in Figure 11, while the full experimental procedure is summarized in Table 3. After the full 30 minutes of the test, the components were detached from the build plate using tweezers and placed on a paper towel to air dry at room temperature.

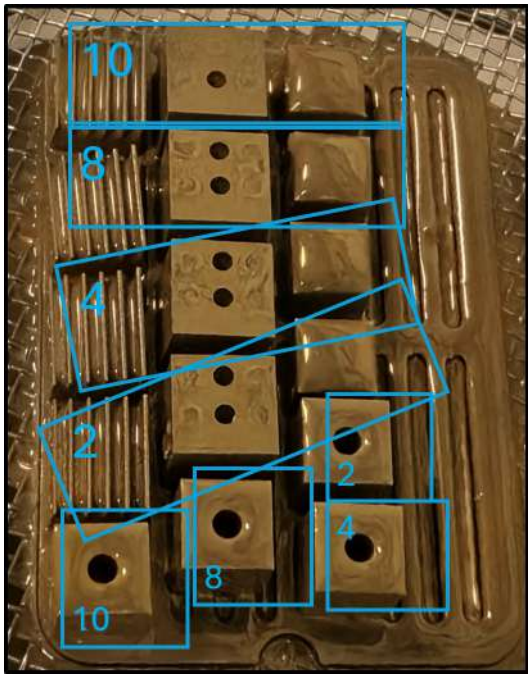

Figure 11: The layout after initial de-caking and which component received what amount of drops.

Table 3: Test procedure for batch four.

Parameter	Description
Application method	Manual application of IncuSOL using a pipette
Application interval	Every 5 minutes
Application times	5, 10, 15, 20, and 25 minutes
Total test duration	30 minutes
Rotation between applications	Container rotated 90° counter-clockwise after each application
Heat exposure	During de-caking 60 °C. During IncuSOL application 80 °C.
End of test	Components removed after 30 minutes and air dried on paper towel

3.3.5 Impact of Delayed Post-Processing - Batch Five

The initial objective of batch five was to evaluate airbrush cleaning. However, upon initiating the de-caking stage, it was observed that the prolonged 72-hour delay between printing and post-processing significantly altered the feedstocks melting behaviour. Instead of liquefying and draining as observed in previous batches, the material exhibited increased viscosity and resisted flow. Consequently, the components cleared far less efficiently, which compromised the baseline required to accurately evaluate the planned parameters. As reliable conclusions regarding the test could not be drawn, the planned test design was aborted. The batch was instead redirected towards evaluating the alternative cleaning equipment, as presented in Table 4.

De-caking was performed for approximately 15 minutes with the components positioned horizontally before the test was aborted and redirected to alternative methods. The components were then subjected to one of the following treatments: No additional cleaning, IncuSOL baths, ultrasonic cleaning, or airbrush. The IncuSOL bath and ultrasonic cleaning lasted 8 minutes after de-caking. During the bath treatment, the solution was stirred and components were moved back and forth in the direction of the channels. The airbrush experiment was conducted during heating and the components were repeatedly removed, airbrushed and then reinserted under the heating element over a period of 30 minutes, every 5 minutes. The airbrush was applied for approximately 30 seconds and used a small amount of IncuSOL. After the different tests were completed, components were placed on a paper towel to air dry at room temperature.

Table 4: Experimental design of batch five testing different cleaning equipment.

Sample Group	de-caking 60 °C	Method	Experimental procedure
1	15 min	None	Baseline
2	15 min	Ultrasonic cleaning	Submerged for 8 minutes
3	15 min	IncuSOL bath	Submerged for 8 minutes
4	15 min	Airbrush	Iterative process between heating and applying air with dispensed IncuSOL

3.3.6 Airbrush Cleaning Experiments - Batch Six

Previous testing in 3.3.5 batch five, demonstrated that the airbrush method yielded higher cleaning efficacy than the alternative techniques up until this point. To build upon this success, batch six was designed to investigate whether applying IncuSOL via airbrush during the secondary heating stage could further improve results by combining solvent exposure with mechanical agitation and directed airflow.

Components were subjected to the same 15-minute de-caking step as in batch five. After de-caking, the temperature was increased to 80 °C, and the container holding the components was placed on the tilting device at 15°. Secondary heating was then carried out for 40 minutes, during which the components were periodically removed for airbrush application with IncuSOL and then returned to the heating element.

The timing of the airbrush applications differed between the sample groups, as summarized in Table 5. Sample group one received one application after 40 minutes. Sample group two received two applications after 20 and 40 minutes. Sample group three received four applications at 10-minute intervals, starting after 10 minutes. Sample group four received eight applications at 5-minute intervals, starting after 5 minutes.

Following the airbrush application, all components were blown dry and placed on a paper towel.

Table 5: Test parameters for batch six.

Sample Group	de-caking	Secondary heating procedure (40min)	Airbrush application
1	15 min	15° incline, rotate 90° every 10 min	1 time
2	15 min	15° incline, rotate 90° every 10 min	2 times
3	15 min	15° incline, rotate 90° every 10 min	4 times
4	15 min	15° incline, rotate 90° every 10 min	8 times

3.3.7 Ultrasonic Cleaning in IncuSOL - Batch Seven

Previous testing indicated that prolonged exposure to ultrasonic cleaning caused surface defects to the components. Therefore batch seven was designed to evaluate the efficacy of short intermittent ultrasonic cleaning cycles in an IncuSOL bath. The objective was to determine if brief ultrasonic exposure could clean without causing the surface damage observed in earlier tests.

The components underwent an initial 20 minute de-caking at 60 °C. Following this, components A, B and D were subjected to a secondary heating stage at 80 °C on a 15° incline with 90° rotations performed every 10 minutes as presented in Table 6. The previous test revealed that the thin profiles of the C-components were at risk of bending when heated on the incline. To mitigate this, the C-components were heated at a lower temperature and only positioned parallel to the incline, preventing flowing feedstock from causing damage.

Table 6: Heating parameters used in batch seven for de-caking, showing the different secondary heating conditions applied to components C compared to A, B, D

Component type	de-caking 60°C	Heating at inclination 15° (40min)
A,B,D	20 min	Rotate 90° every 10 min at 80 °C
C	20 min	Rotate 180° after 20 min at 60 °C

During the secondary heating stage, the components were periodically removed and submerged in the IncuSOL ultrasonic bath for 10 second intervals. The total number of immersions varied across the sample groups over the course of the heating stage, as outlined in Table 7. This necessitated submerging one component at a time in the ultrasonic bath as seen in Figure 12.

Following ultrasonic cleaning, components A, B, and D were placed on a paper towel to dry and carefully rolled onto each side. Due to the inherent brittleness of component C, compressed air was instead used for drying at low pressure. The pressure was adjusted by closing the airflow completely and then reopening the airbrush control by two turns, resulting in only a weak airflow perceptible against the skin.

Figure 12: Short intermittent ultrasonic cleaning cycles performed in heated IncuSOL.

Table 7: Ultrasonic cleaning in IncuSOL, A-, B- & D- components not C:"Fins" - Batch 7

Sample Group:	Duration time:	Number of times in bath:	Cleaned after:
1	10 sec	1x	at 20min
2	10 sec	2x	at 10min and 30min
3	10 sec	4x	one each rotation
4	10 sec	8x	two times per rotation

3.3.8 Inverted Printing, Airbrush - Batch Eight

In batch seven the test showed that the build plate interfered with the de-caking process and restricted the drainage of excess feedstock. To address this limitation, the printing orientation was changed and the components were printed inverted. As shown in the left side of Figure 13, flipping the feedstock block upright for post-processing positioned the build plate above the components, allowing it to be removed immediately during the de-caking stage, seen in the right side of Figure 13. To prevent damage during separation, a 400 µm marginal layer was incorporated between the build plate and the components.

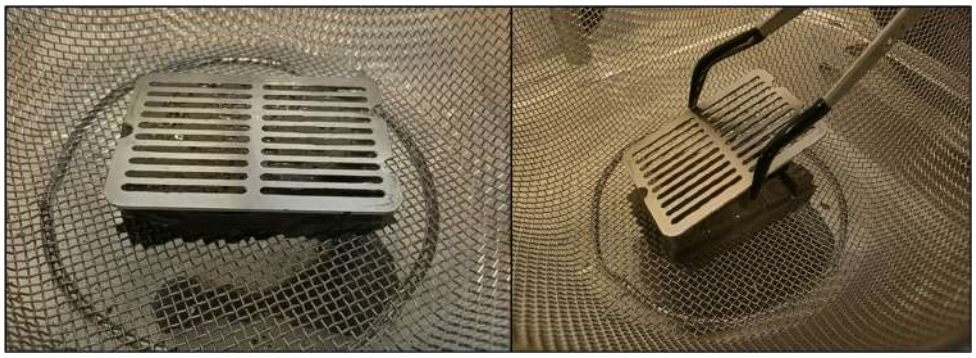

Figure 13: Left side shows the build plate attached to the feedstock block right after being removed from the printer. Right side shows just when the build plate is removed after a few minutes into the de-caking

The initial de-caking stage was identical across all four sample groups, consisting of a 20 minute heating period at 60 °C. Following de-caking, an initial airbrush cleaning cycle was performed on all components to establish a consistent baseline reference. This baseline cycle consisted of two full passes over all of the components with generous application of IncuSOL complemented with 2 minutes of heating at 60 °C.

Following the baseline cleaning, components A, B and D were subjected to a varying number of heat and airbrush cycles according to Table 8. Heat exposure was performed for 2 minutes at 60 °C for each cycle.

C-components were subjected to a separate process. During heating intervals, these components were positioned on their sides seen in Figure 14, to better utilize gravitational forces in facilitating drainage of excess feedstock from the spaces between the fins. The C-components were exposed to heating for two minutes at 60 °C for each cycle.

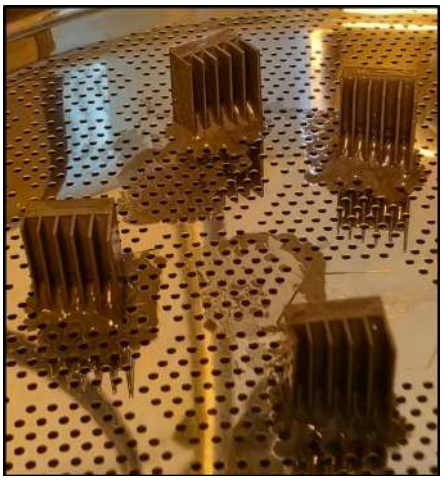

Figure 14: Side-oriented positioning of C-components during intermediate heating stages to utilize gravitational drainage between narrow fin structures.

Table 8: Airbrush iterations with IncuSOL - Batch 8.

Sample Group:	Number of times airbrushed:
1	1x (reference)
2	2x
3	4x
4	5x

Upon completion of the cleaning cycles, the components were dried using the airbrush and placed on a paper towel.

3.3.9 Airbrush without IncuSOL before Ultrasonic Cleaning - Batch Nine

Building on the successful use of the inverted build plate in batch eight, the same printing orientation was adopted for batch nine. In addition, batch eight showed that airbrushing could cause a thin layer of feedstock to remain on the components due to feedstock moving between surfaces. Batch nine was therefore designed to evaluate a combined cleaning strategy consisting of initial airbrush cleaning without IncuSOL, followed by ultrasonic cleaning in heated IncuSOL.

As in batch eight, the inverted build plate configuration enabled early removal of the build plate during the de-caking stage. The de-caking was carried out in 60 °C for approximately 15 minutes. After de-caking, all component C specimens were separated from the remaining samples and processed later due to their increased structural fragility. By separating them the risk of damage to the C-components, while cleaning the other components can be avoided.

Due to the limited cleaning performance observed during ultrasonic cleaning in batch seven, it was theorised that IncuSOL had a limited effect on improving cleaning performance in earlier batches employing the airbrush. Instead, the observed cleaning results were believed to primarily originate from the mechanical effect of the pressurized air. Therefore batch nine investigated whether additional removal of excess feedstock prior to ultrasonic exposure could improve the cleaning results. This was achieved by introducing repeated airbrush cleaning cycles, without IncuSOL, before ultrasonic treatment. Components A, B, and D were therefore subjected to eight intervals consisting of intermediate heating followed by airbrush cleaning without IncuSOL in order to gradually remove excess feedstock before immersion in the ultrasonic bath.

Components A, B, and D were placed in a strainer and submerged in a bowl containing IncuSOL heated to 45 °C, as shown in the right side of Figure 15. The bowl was positioned inside the ultrasonic cleaner. The sample groups were removed at predefined exposure intervals by lifting the strainer from the bath, illustrated in the left side of Figure 15, according to the intervals summarized in Table 9. After removal, each sample group was placed on a paper towel and allowed to air dry.

Figure 15: Ultrasonic cleaning setup used. The right side shows the components submerged in heated IncuSOL, while the left side shows removal of the strainer to remove one of A-, B- and D-component.

Table 9: Exposure times used for ultrasonic cleaning in heated IncuSOL.

Sample Group	Time of removal from ultrasonic bath
1	30 seconds
2	60 seconds
3	90 seconds
4	120 seconds

The C-components were positioned on their sides, as in batch eight seen in Figure 14, to promote drainage of excess feedstock between the fins. The components were first heated in a horizontal position at 60 °C for 15 minutes. Thereafter, two of the components were treated using airbrush application with IncuSOL, while the remaining two were treated using airbrush without IncuSOL. This procedure was repeated three times.

After completion of the airbrush cycles, the two components treated with IncuSOL were removed and placed on a paper towel for drying. The remaining two components were transferred to the strainer used in the previous stage and subjected to ultrasonic cleaning in heated IncuSOL. These components were removed after exposure times of 30 and 60 seconds respectively, and then placed on a paper towel.

3.3.10 Final Method Validation with Incus Recommendations - Batch Ten

The cleaning procedure for batch ten was developed based on observations from all previous batches regarding drainage, heating time, and the effectiveness of repeated mechanical and chemical agitation. In addition, several recommendations from an interview with a representative from Incus were incorporated into the procedure. This final validation of the method was done without sample groups as all components received an identical treatment.

One of the recommendations was to keep the entire process, from completed printing to cleaned components, below 30 minutes and at 60 °C in order to reduce binder cross-linking and maintain feedstock flow. To achieve this, the de-caking stage was performed using the inverted printing orientation at 60 °C until no visible dripping of excess feedstock remained.

Following de-caking, one cleaning cycle was performed using only pressurized air from the airbrush without the use of IncuSOL in order to remove excess feedstock prior to solvent exposure. Only a single cycle was performed to minimize the risk of structural damage caused by repeated heating and cooling cycles.

After reheating, three additional cleaning cycles were carried out using pressurized air together with IncuSOL heated to approximately 50 °C in order to minimize cooling of the components during cleaning. Between each cleaning cycle, the components were reheated for approximately 2–3 minutes to maintain feedstock flow and improve drainage.

Finally, the components were submerged in an ultrasonic cleaner containing heated IncuSOL (45 °C) for 60 seconds as a final cleaning stage intended to remove residual feedstock from internal channels and narrow geometries. During the ultrasonic cleaning the strainer was moved around in the IncuSOL after recommendations from Incus, see 2.3.

4 Results and Discussion

This section presents the results and discusses the core findings of the study. Every test conducted is labelled as a separate batch, consisting of multiple components. All batches are individually evaluated and key results are discussed.

4.1 Baseline Evaluation of the Existing Cleaning Method - Batch One

The first set of components were cleaned using the pre-existing cleaning process and yielded poor results. The original cleaning process is described in section 3.3.1. Residual feedstock remained, particularly within the channels as observed in Figure 16. Channels on B- and D-components were completely filled with excess feedstock. This is likely due to their complex inner channel structure which is more restricting to flow of residual feedstock in comparison to the straight channel components. For reference on channel structure, see section 3.1. The fins of the C-components were either badly damaged mostly due to manual handling, or had large amounts of residual feedstock between them.

The cubic structures of A-, B- and D-components were compromised, with significantly rounded corners. The damage was noted after ultrasonic cleaning, which aligns with information presented in [13]. The simpler A-components with straight channels had better results as the largest holes with a diameter of 1 mm were cleared through the component. The exterior of most components was well cleaned, see Figure 16 and 17. However some of the parts had defects arising from the manual handling of components between cleaning steps. The components are difficult to grip without damaging them using the plastic tweezers, especially in a heated state where they are easy to deform. Such handling errors result in damage, especially to the fragile finned components.

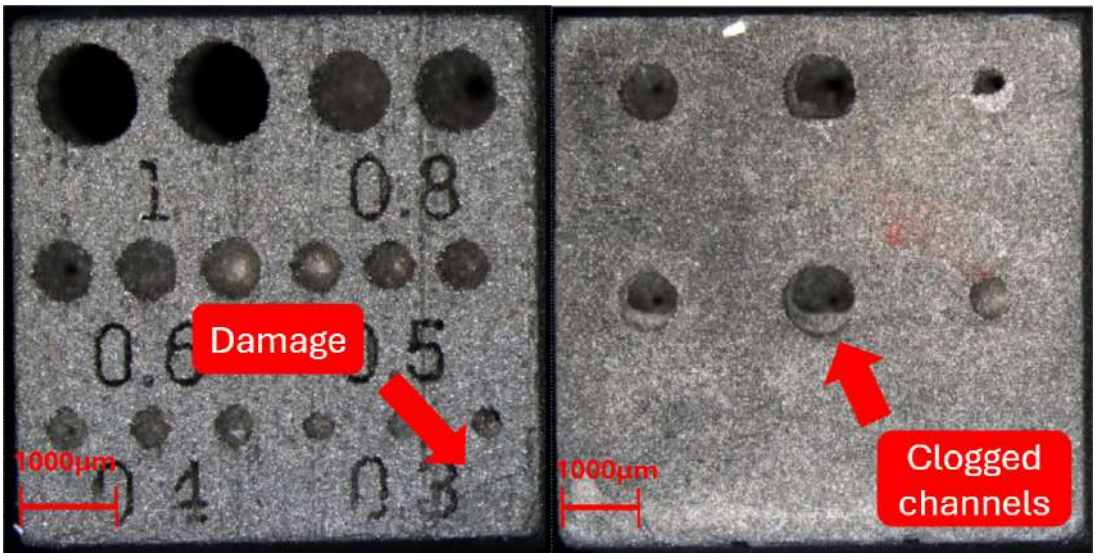

Figure 16: Component A and B. A-component shows structural damage to corners but successfully cleared the largest channels of 1 mm. However the smaller sizes from 0.3 mm to 0.8 mm were not cleared. B-component has no cleared channels and damage to corners.

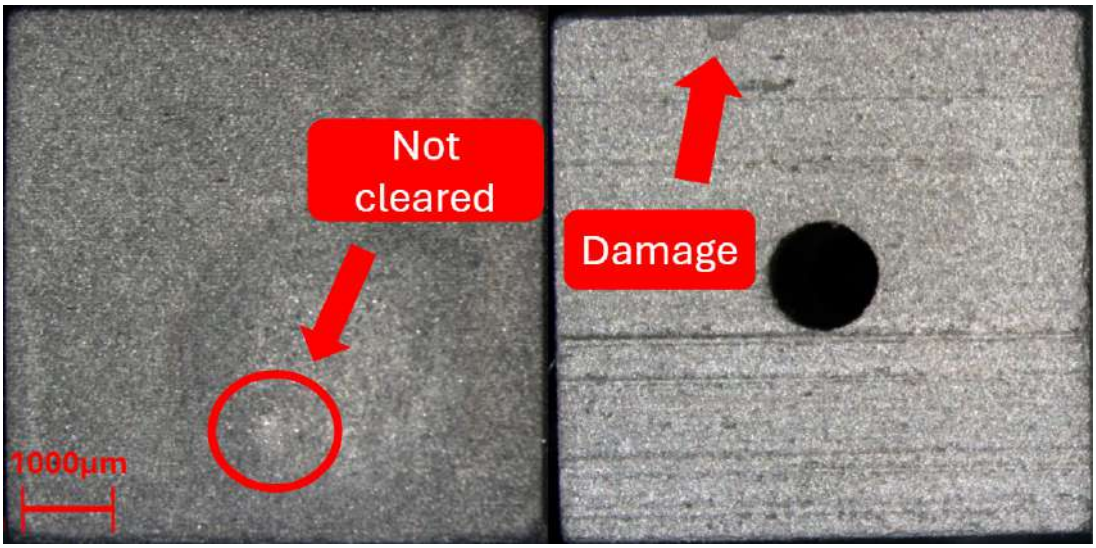

Figure 17: Component D, structural damage and no success in clearing side channels on the component.

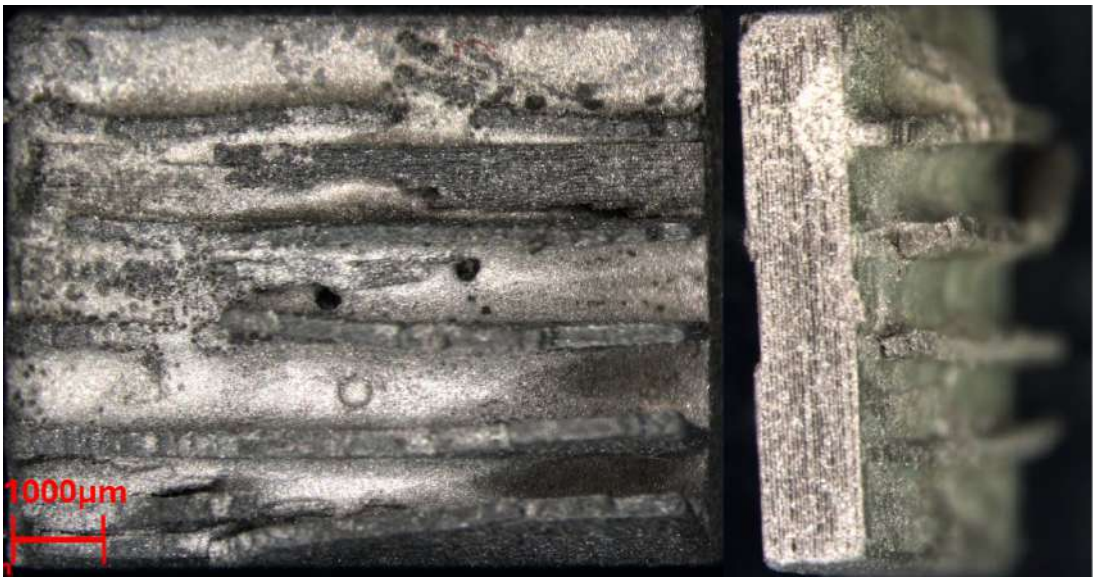

Figure 18: C-component, damage to the whole components and crushed fins

4.2 Baseline Evaluation of the Existing Cleaning Method with Minimized Handling - Batch Two

The damage seen in batch one was largely caused by repeated manual handling using the available equipment. In order to minimize this damage it was attempted to avoid moving individual components and instead transport the complete build plate between steps. In all other aspects the test was conducted identically to batch one. Results for A- B- and D-components were overall similar, however C-components had improved results with less damage. For all components the cleaning result is unsatisfactory and residual feedstock is left on the components.

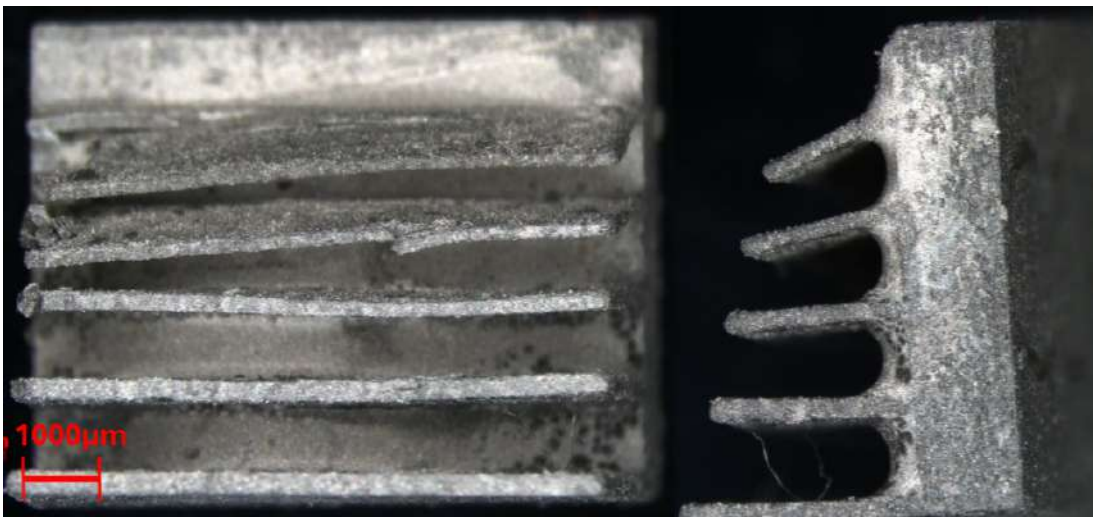

Figure 19: Damage on the fins of C-component.

The entire build plate was after initial de-caking submerged into the ultrasonic bath. This was achieved with a pair of tweezers grabbing the metal build plate and placing it into a beaker containing IncuSOL. This successfully kept all components intact during transportation, but due to the ultrasonic vibrations, components moved and some fell off the build plate during cleaning. This, in combination with the solution becoming opaque during cleaning, complicates removing the components from the beaker. Instead of picking up the components using tweezers, components were poured out of the beaker which caused extensive damage, especially to the finned components. This highlighted the need for an alternative method for removing the components from the beaker.

Finned components were difficult to grab in batch one and could not be reliably poured from the beaker in which they were ultrasonically cleaned, while maintaining their structure. The thin base plate complicates gripping the C-components without causing damage. Because of the evaluation being focused on the fins rather than the base plate, the thickness of the base plate on component C was increased from 1.25 mm to 1.75 mm, providing a larger surface area to grab, to ease further experimentation.

The second batch exposed the need for alternative equipment for transporting components. This led to the purchase of a bowl and sieve. The build plate is placed on the sieve and the bowl is placed underneath, catching excess feedstock. The sieve and bowl can easily be moved and IncuSOL can be poured into the bowl allowing for easy transportation to the ultrasonic bath without a need for a change of containers, minimizing handling. Since manual handling cannot be completely avoided when removing components from the build plate, rubber-coated tweezers were purchased to avoid causing surface damage or deformation of components. A vacuum pen was also purchased for the same reason, which after tests failed to lift the components as intended and was subsequently not used again.

In order to achieve more even heating of the components and avoid cleaning personnel manually holding the heat gun during the de-caking stage, a heat gun stand was introduced for future tests. Together with the thermometer available in the laboratory, this enabled more stable and repeatable temperature conditions during heating. However, the available thermometer was unable to measure the temperature of liquid solvents. Therefore, a digital probe thermometer capable of measuring liquids was purchased to accurately determine the temperature of the IncuSOL bath. Figures of the purchased equipment can be found in Appendix B.

4.3 De-caking Parameter Study - Batch Three

To determine if a dual stage heating regime and a tilted build plate could improve the drainage of excess feedstock, batch three was subjected to a prolonged and more intensive heat exposure. However, keeping the components at a 15° angle from the beginning of the de-caking procedure caused them to stick together as excess feedstock formed bridges between components. This is evident in Figure 20, where components can be seen to have a waist.

The issue with bridging persisted throughout the whole test and the bridge between components was not possible to clear. Bridging between components made it difficult to evaluate how much tilting the build plate assisted in clearing the components, and the maximum incline was limited to 15° before components started sliding. Bridging never materialized in earlier tests where the build plate was kept horizontal during the de-caking phase.

The feedstock block was left for 48 hours after printing. In an interview with Dr Santiago Cano (see 2.3), it was discovered that the cause for bridging is a process of polymerization in the unhardened feedstock that begins immediately after printing. The problem with bridging between components was almost certainly contributed to by the prolonged time between printing and cleaning, but there was no knowledge of such effects at the time and the test was conducted normally.

Heating the components to 80 °C seemed to have increased the effectiveness of the cleaning. Prolonging the heat exposure however, quickly resulted in diminishing returns, with limited reductions in the amount of feedstock removed after the secondary 40 minute heating stage. The problem with components sticking together also persisted, regardless of heating time. There was a pronounced difference between the components that only had exposure to the first stage of heating at roughly 60 °C , and those that spent time exposed to higher temperatures. The components heated at 80 °C for 40, 80 and 120 minutes showed very little difference in the amount of excess feedstock that was cleared.

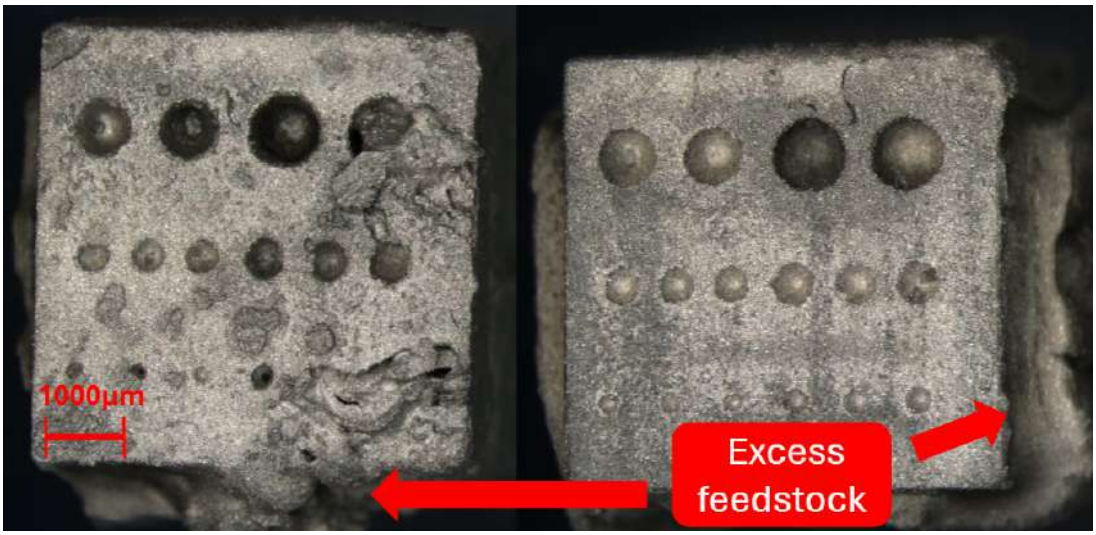

Figure 20: A-components, to the left heated for 40 minutes and to the right heated for 80 minutes.

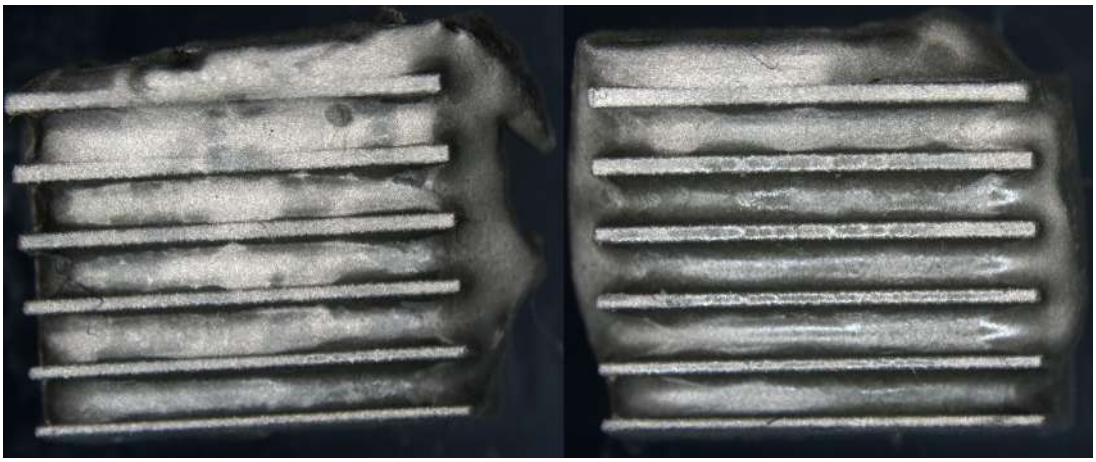

Figure 21: C-components, heated for 40 (left) and 160 (right) minutes. 160 minutes has resulted in visibly deeper grooves but the difference is not significant.

The experimentation with the third batch resulted in the distance between components being increased from 1 mm to 1.5 mm to ensure that bridging between components did not occur. It was also decided that during the first stage of heating, the build plate would be kept horizontal to stop components from sliding into each other and sticking together. There were difficulties in assessing the effectiveness of using the tilting table since the bridging between components left a layer of residual feedstock, hiding the side channels of the D-components and restricting the flow between fins in the C-components. It was also noted that surface tension between fins and capillary forces inside channels kept the feedstock from flowing out. In order to break these forces IncuSOL will be employed in future tests.

The heat gun stand freed operators to attend other activities in the lab such as cleaning the printer, while it also gave a consistent heat at the component level. Combined with the rubber-tipped tweezers that allowed for gentler handling and the curved tip allowed for easier handling of individual components. Finally the rubber-coated tweezer's soft tips minimized the risk of surface damage compared to the hard plastic tweezer used in batch one and two.

4.4 Solvent-Assisted Cleaning Experiments - Batch Four

The fourth batch was intended to determine if IncuSOL could be used to counter capillary forces and surface tension to provide a better cleaning result, with minimal damage to components. This was done using drops of IncuSOL on the components applied every 5 minutes during the secondary heating stage. The amount varied between from 2 to 10 drops, intended to test the difference between passively applying an IncuSOL layer on the components and flushing them. The solid cubic components displayed little benefit from the drops of IncuSOL. The results were most notable on the finned C-components as seen in Figure 22.

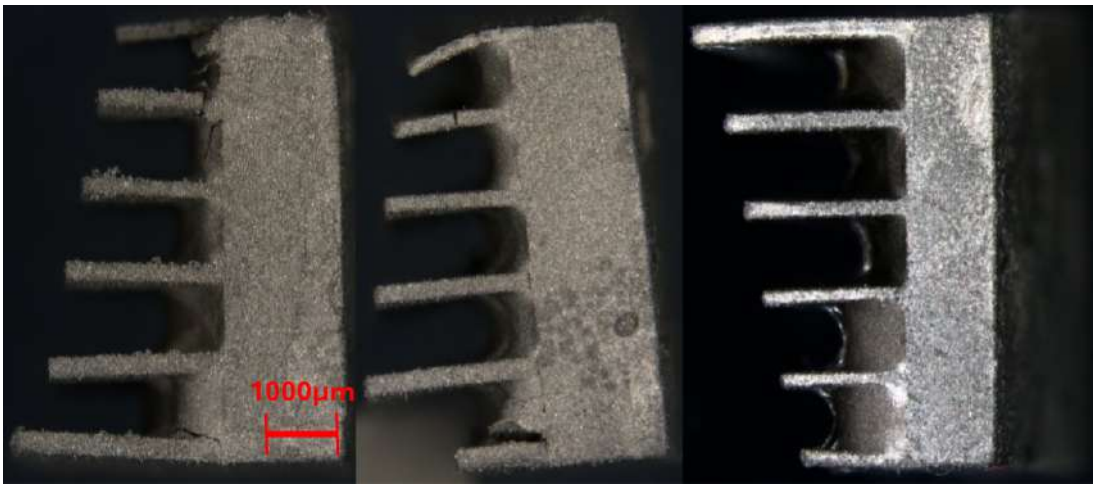

Figure 22: Comparison of cleaning efficacy and structural integrity on C-components after applying varying amounts of IncuSOL during secondary heating. To the left in the picture the C-component that received 10 drops of IncuSOL, in the middle 2 drops. The right component is a reference from batch 2 which is ultrasonically cleaned.

The introduction of IncuSOL and tilting the build plate has an impact on clearing feedstock from the C-components but larger amounts also have a negative impact on surface integrity as seen in Figure 22. It was observed that the finned component that received 10 drops of IncuSOL started to display surface damage, appearing coarse. The noted surface damage is likely due to the partial dissolution of the binder between the metal particles. Moreover, this damage can be explained by blistering in the thinner, more vulnerable parts of the component. Further, the finned component with 10 drops of IncuSOL exhibited increased deformation of the fins, which could originate from the increased amount of mass that was deposited onto it. However, in combination with the applied mass of IncuSOL, the heating temperature of 80 °C as well as chemical degradation of the binder resulting from prolonged IncuSOL exposure are also believed to have affected the extent of the bending. The difference in cleaning results between the 2-drop and 10-drop variants was also insignificant and as seen in Figure 22, more IncuSOL led to slightly worse results.

Displayed in Figure 23 the application of IncuSOL on the cubic components could not penetrate deeply into the vertical channels and formed a surface film on components.

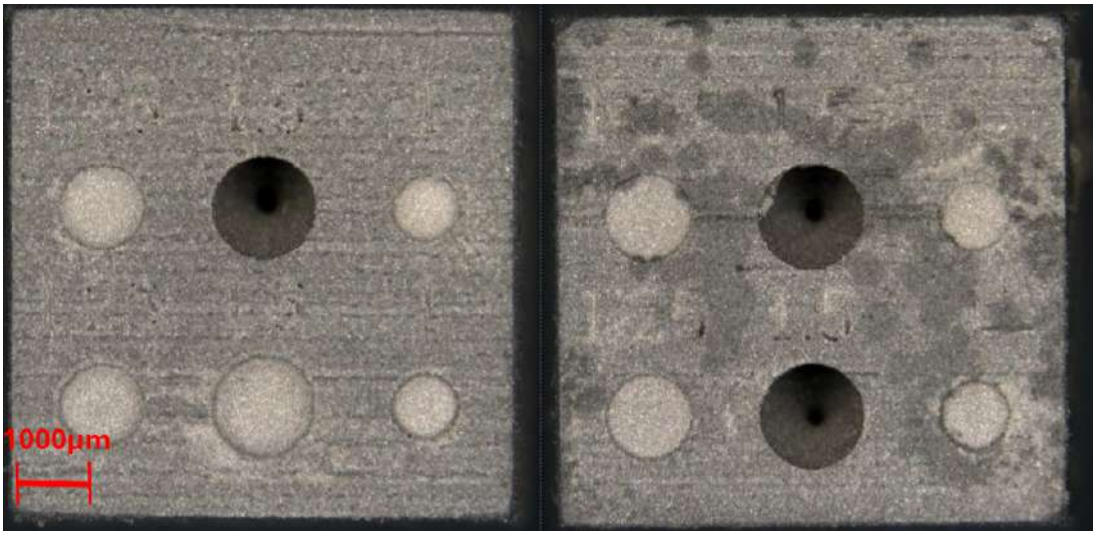

Figure 23: D-component comparison, 10 drops of IncuSOL to the left and 2 drops of IncuSOL to the right.

The conclusions drawn from batch four were that IncuSOL can be useful in breaking the surface tension of the feedstock but quickly forms a new surface tension consisting of the solvent instead. It is unable to penetrate into channels by passive application. For most components, this limits the efficacy of cleaning and risks creating undesired effects such as blistering, delamination and partial dissolution of the binder between the metal particles.

4.5 Impact of Delayed Post-Processing - Batch Five

Before cleaning commenced, the feedstock block was left in the printer for approximately 72 hours. As discussed in the interview with Incus in section 2.3, delaying the de-caking causes the binding polymer to start cross-linking, thickening the excess feedstock and inhibiting cleaning attempts. This was notable during the initial de-caking where residual feedstock remained trapped in channels where it had previously been cleared. This caused the test to be cancelled.

It can be observed that the bridging between components in batch three, section 4.3, was not seen on this batch of components. This is likely attributable to keeping the build plate flat during the initial de-caking phase and increasing the distance between components on the build plate during printing. This increased distance eases the flow of feedstock between components.

After the test's cancellation it was decided to instead assess different cleaning methods, as to not waste the material. The different experimentations on the components showed promising results with employing an airbrush to help clear channels and fin arrays without damaging components. As seen in Figure 24 below, both the ultrasonic bath and airbrush treatments significantly improved cleaning performance. However ultrasonic cleaning caused a significant amount of damage to components in the form of blistering and delamination without significant improvements to the cleaning performance.

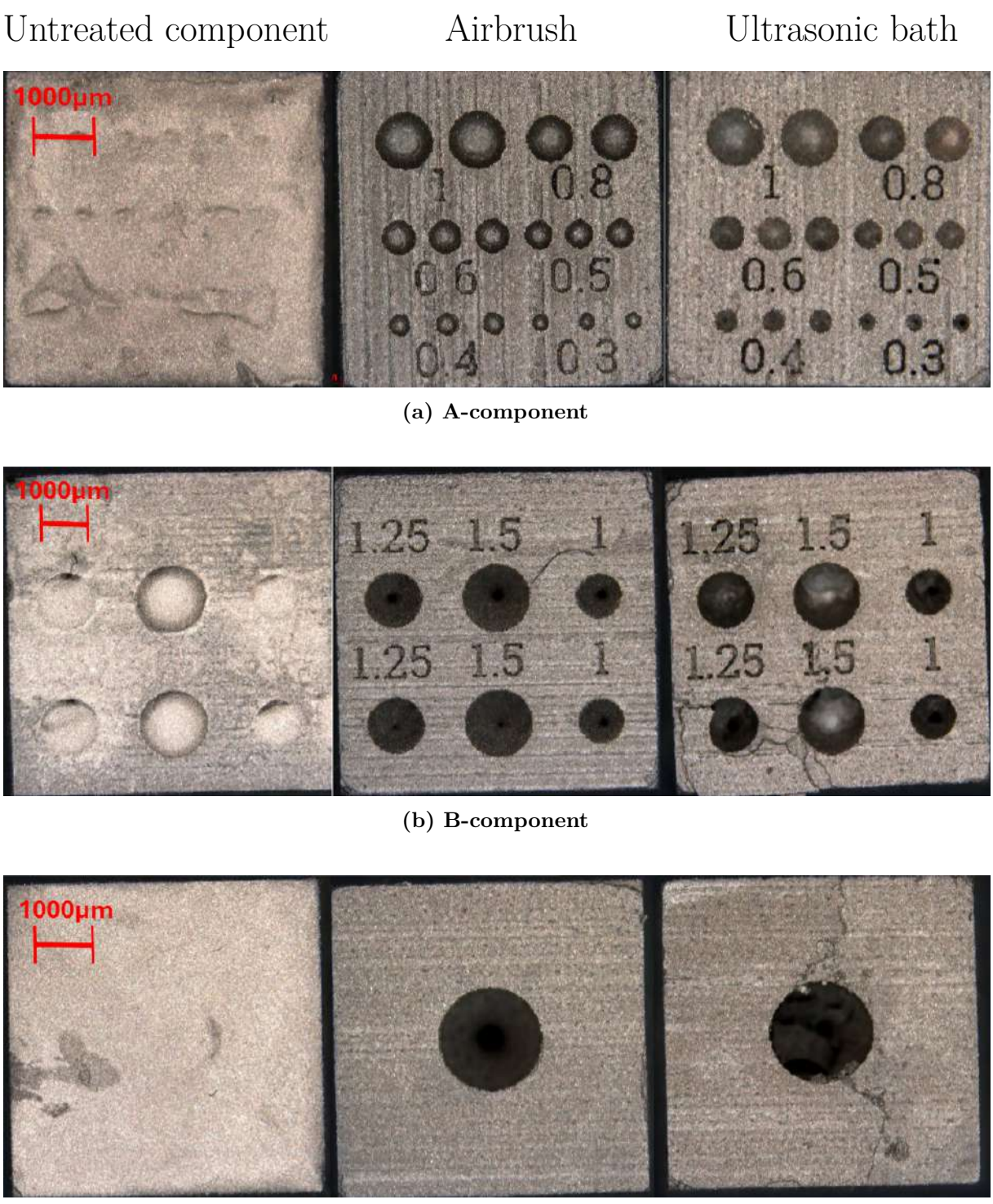

(a) A-component

(b) B-component

(c) D-component

Figure 24: Comparison of untreated, airbrush-cleaned and ultrasonically cleaned components. A, B and D are represented. The images illustrate differences in feedstock removal and surface integrity between the evaluated cleaning methods.

4.6 Airbrush Cleaning Experiments - Batch Six

The next step was to evaluate pressurized air with an IncuSOL mix in differing intervals, from just once, up to eight times during the secondary heating stage. Pressurized air was utilized to remove excess IncuSOL in order to stop it from damaging the component. It was evident that a larger number of airbrush cycles resulted in improved cleaning results on B- and D-components while also resulting in minimal damage to components. This is likely attributable to IncuSOL being removed from the components between airbrush applications, leaving minimal amounts of residual solvent to negatively affect binder material.

On A-components, all numbers were satisfactorily cleaned with no variation between specimens with different airbrush exposures as seen in Figure 25. Interestingly, the components with the most amount of airbrush exposure had a worse result clearing channels. This contrasts with the results of B- and D-components where a larger amount of exposure directly results in superior cleaning results. This indicates that a separate factor is inhibiting the flow in the A-components channels. During later experimentation the placement of channel openings on the build plate was found to affect the flow of excess feedstock. It was also noted that the first cleaning cycle using the airbrush removed significant amounts of residual feedstock but every following cycle had diminished returns.

Later in the project during the interview with Incus, section 2.3, Dr Santiago Cano explained that cross-linking polymerization is a constant process, that over time thickens feedstock and negatively impacts cleaning efficacy, particularly in smaller channels. It also accelerates during heating, especially when temperatures exceed 60 °C.

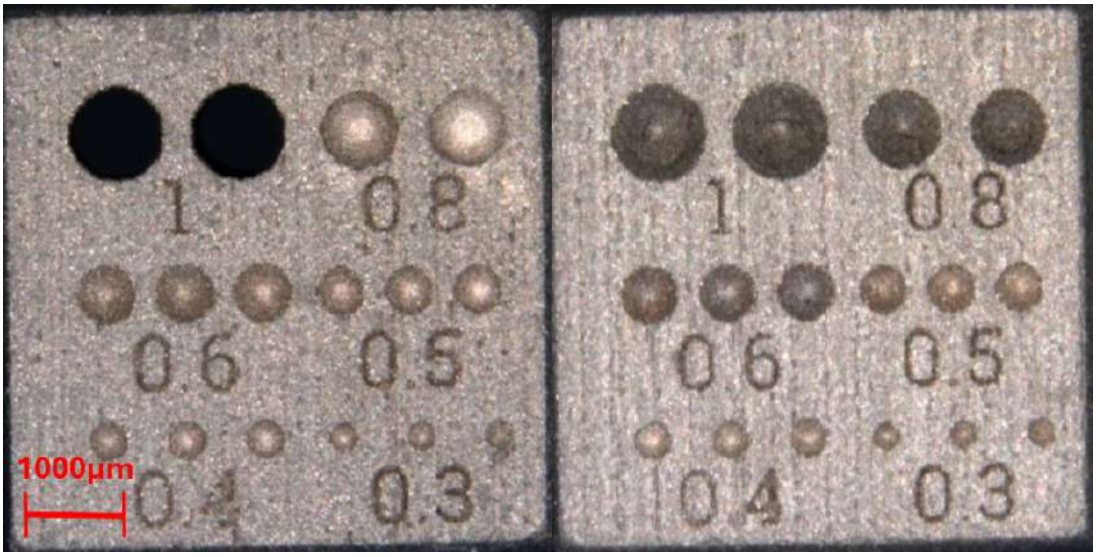

Figure 25: Component A with airbrush application 2 times to the left and airbrush application 8 times to the right.

For B-components the larger channels both 1.5 mm and 1.25 mm were cleared all the way through, which was verified by cutting the components in half, see Figure 26. The smaller 1 mm channel was not fully cleared through the component, but significant progress was made with both channel openings appearing cleared.

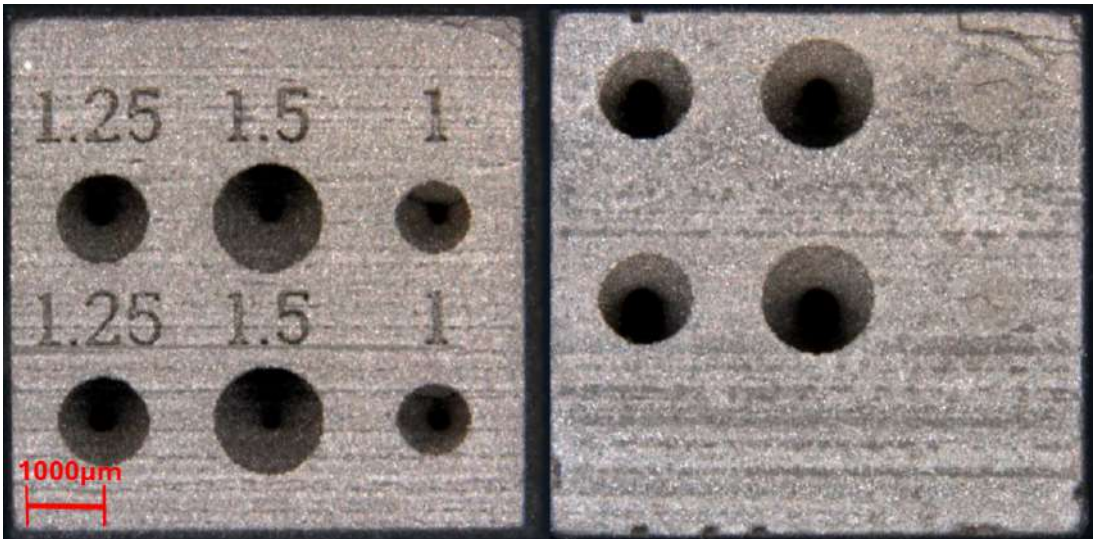

Figure 26: B-component cleaned with airbrush on the left and with the middle cross-section of the same component on the right.

On C-components the fins were slightly deformed as a result of the application of pressurized air as well as handling errors, but had similar cleaning results to those in batch four, section 4.4, without the negative repercussions of prolonged IncuSOL exposure. Residual feedstock remains between the fins, as seen in Figure 27.

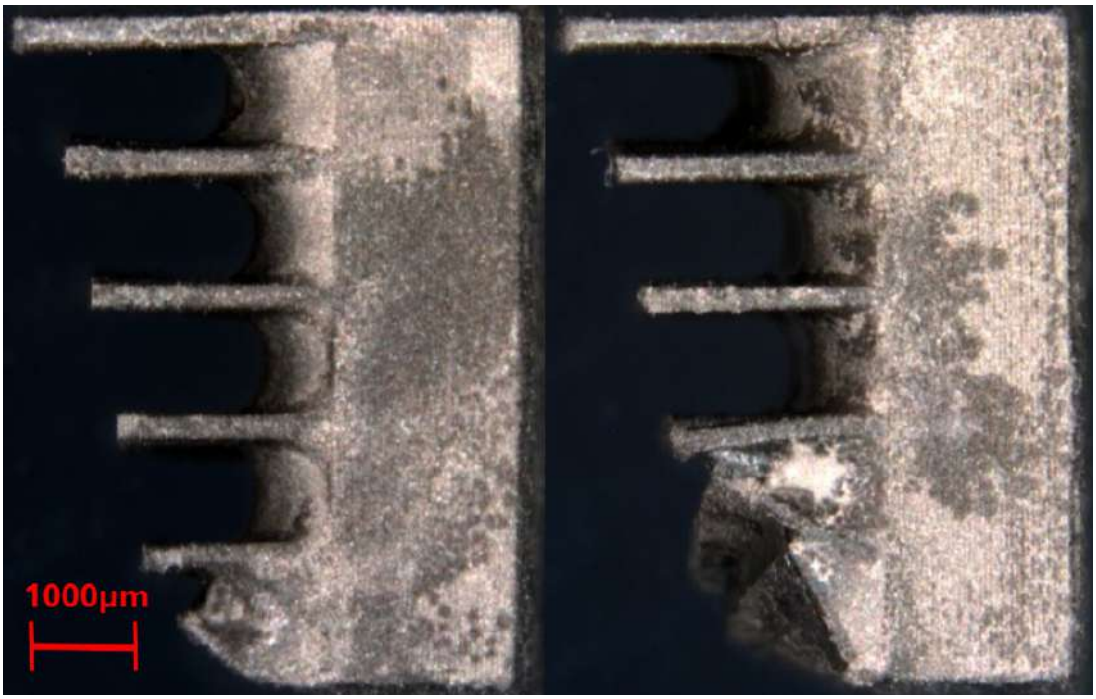

Figure 27: C-components cleaned with airbrush. Damage to the fins can be seen in the thinnest and shortest fins for both specimens.

On D-components all of the side channels were completely cleared of excess feedstock. The components appear intact with minimal damage and good surface integrity. The result is a satisfactory cleaning of the component, as seen in Figure 28.

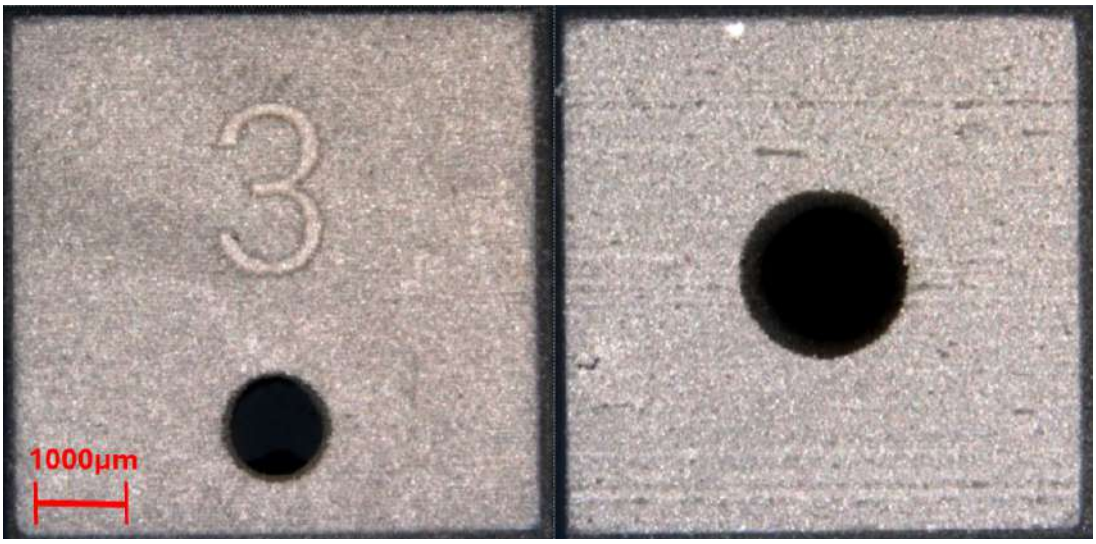

Figure 28: D-component, on the left a side view of one of the four side openings, and on the right the larger top opening.

4.7 Ultrasonic Cleaning in IncuSOL - Batch Seven

The previous experimentation with the airbrush successfully cleared larger channels of the B- and D- components. There was however limited progression made in A-components, with results similar to those observed in batch one, section 4.1, although with less damage in the corners. There was some success in penetrating deeper into the channels on A-components than observed in batch six, although the channels remained blocked. No damage was noted for the components that were exposed for the longest total duration (80 seconds) but the results were worse than those observed in batch six, section 4.6 for all cubic components in relation to how effectively channels were cleared.

The results could indicate that more intensive ultrasonic treatments would be necessary to clear channels. However, the relative difference between how well A-, B- and D-components were cleared of excess feedstock was mostly negligible between 40 and 80 second exposures, indicating that progression declines rapidly. There is however, a clear improvement on cleaning performance on the A-, B- and D-components between those cleaned for 10 and 80 seconds, as seen in figures 30, 31 and 33. On the finned C-components seen in Figure 32, there is no noticeable difference in cleaning performance between components exposed to a single bath of ultrasonic cleaning, and those exposed to eight. The larger amount of manual handling, exposure to ultrasonic bath, and repeated heating cycles has caused components to crack between layers.

It was noted that during the initial heating stage that more channels were cleared and draining seemed more complete than in earlier tests. The contrast between the feedstock block that had a delayed cleaning of 72 hours and the one that was cleaned immediately after printing provided evidence that delaying cleaning was hindering cleaning effectiveness. This was confirmed in the interview with Incus representative Dr Santiago Cano in section 2.3.

Figure 29: Build plate after initial heating, note how clearing of channels corresponds with placement on the build plate.

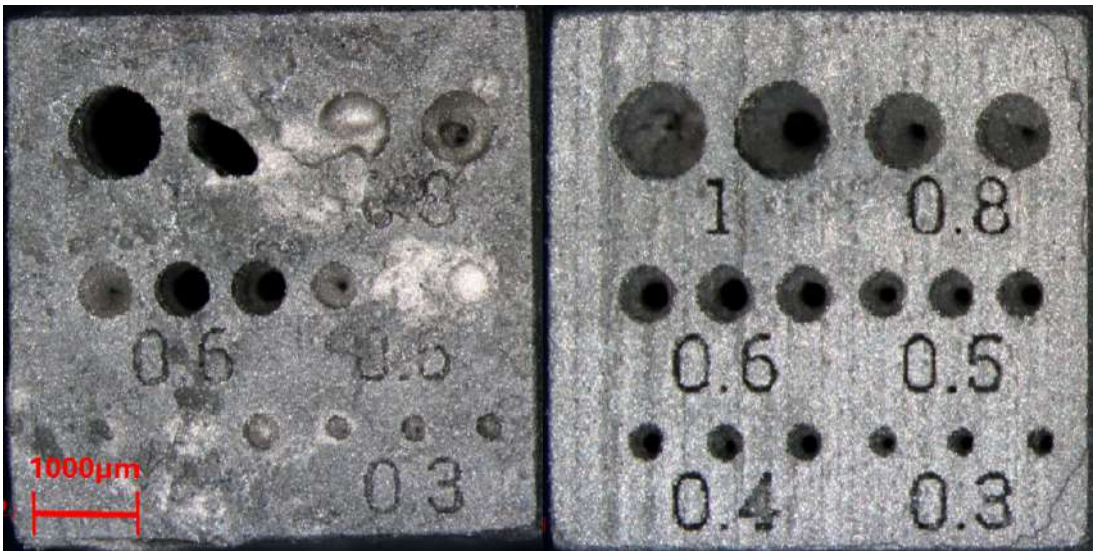

Figure 30: Component A, 10 and 80 second ultrasonic bath.

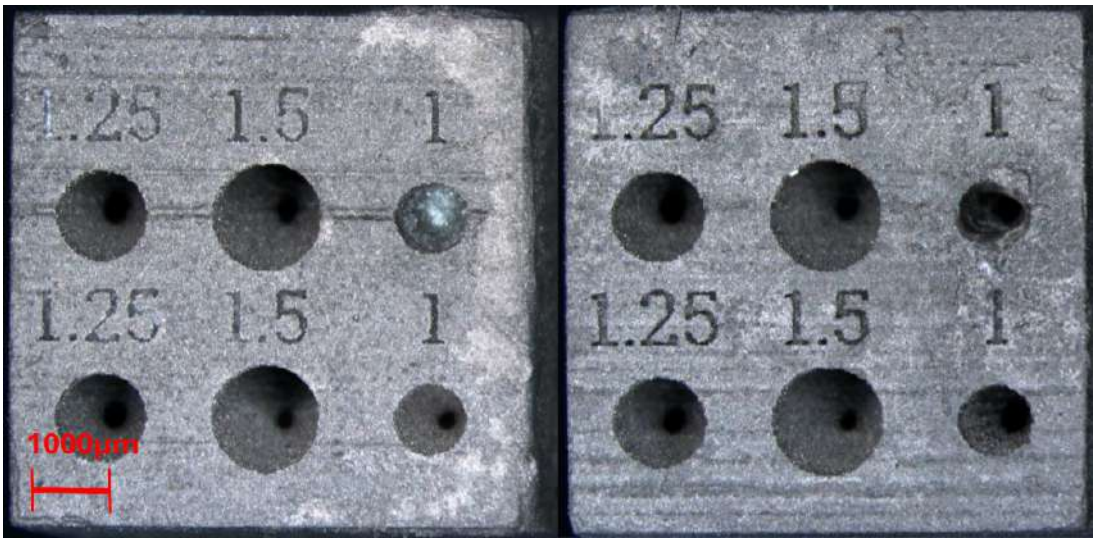

Figure 31: Component B, 10 and 80 second ultrasonic bath.

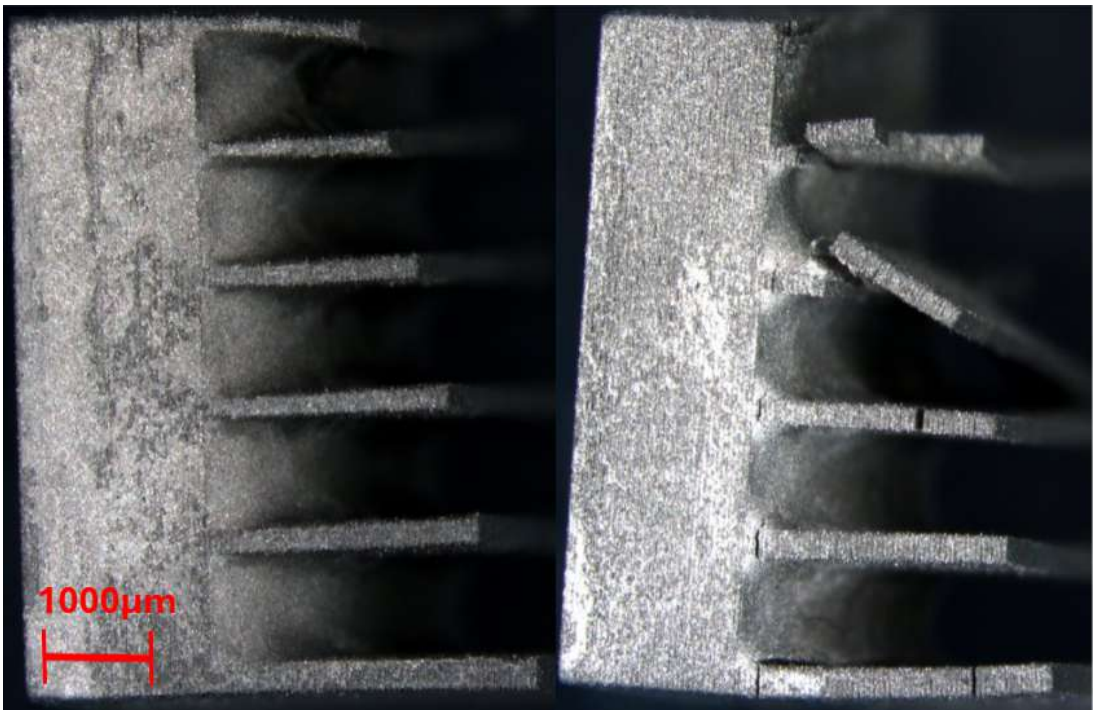

Figure 32: Component C, 10 and 80 second ultrasonic bath.

Figure 33: Component D, 10 and 80 second ultrasonic bath.

4.8 Inverted Printing, Airbrush - Batch Eight

It was noted in batch 7, section 4.7, that the ribs of the build plate inhibit the flow of excess feedstock in channels. When the print was inverted (see Figure 13), and the build plate removed during the initial de-caking stage, it was found that results were even across identical components as seen in Figure 34. This was the first time after de-caking that uniform results were noted.

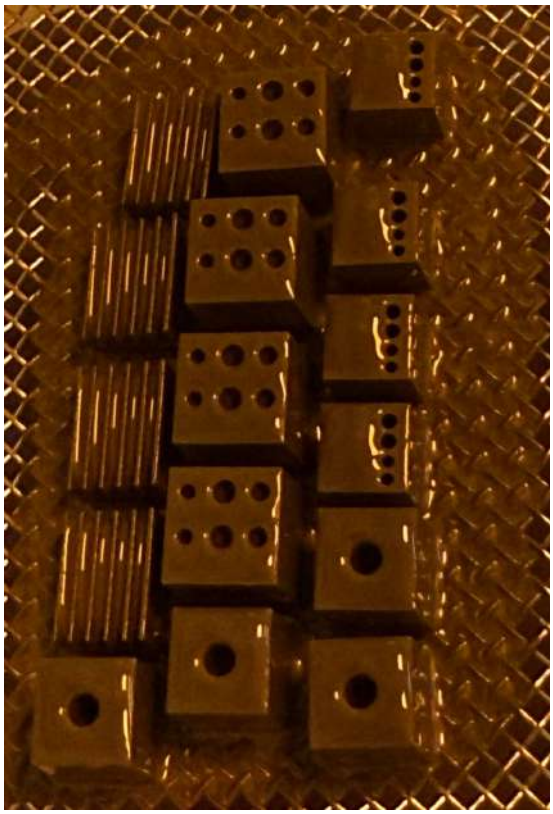

Figure 34: Components without build plate, unrestrictive flow through channels.

During the secondary heating stage components were intermittently airbrushed which has proven the most effective in experiments, primarily in batch six, section 4.6. Inverting the printing and using the airbrush with IncuSOL improved results for B-components with curved channels as seen in Figure 36. D-components with the junction, had all channels cleared as in batch six. The combination of inverting the build plate and using pressurized air with IncuSOL produced the cleanest results yet, for all components.

The cleaning of the A-components, seen in Figure 35, were improved but not fully satisfactory. Both the 1 mm and 0.8 mm channels were cleared all the way through, other channels remain blocked. The airbrush application had the adverse effect of causing excess feedstock, extracted from channels, to stick on the component. The exit of channels had a ring shaped deposit of excess feedstock around it, causing numbers and text to partially refill with new residual feedstock. Components that were repeatedly exposed to the airbrush had channels <0.8 mm more deeply penetrated, but the feedstock from these channels stuck to the surface.

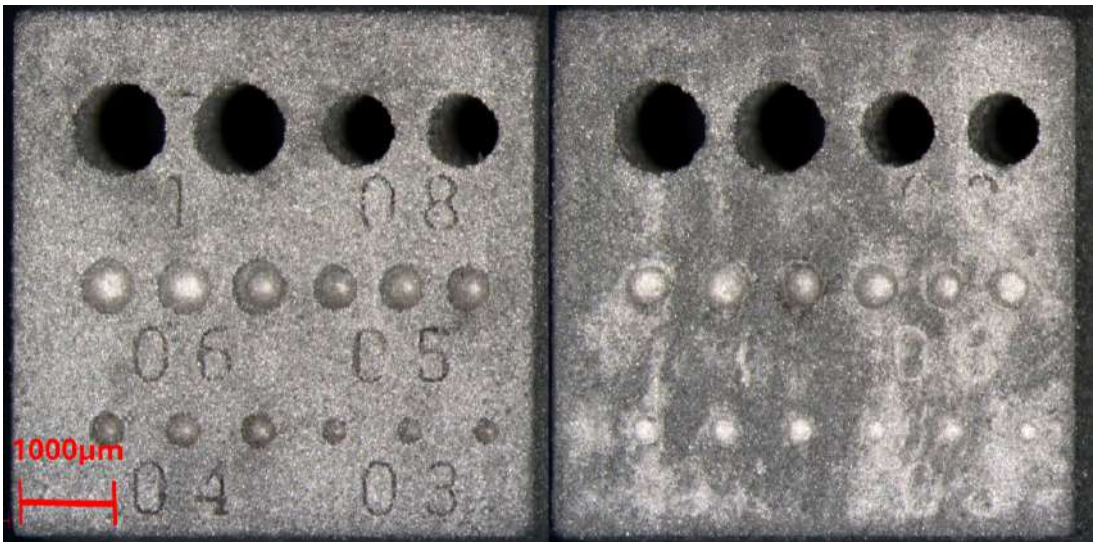

Figure 35: A-components. On the left the reference component which had only one airbrush exposure. On the right the component with the most airbrush applications.

All channels on component B were satisfactorily cleared, which was verified by cutting the components in half, as seen on the right side of Figure 36. Some excess feedstock remained in the engraved numbers and text due to a combination of the airbrush pressing out excess feedstock onto the components surface and manual handling forcing residual feedstock into these crevices.

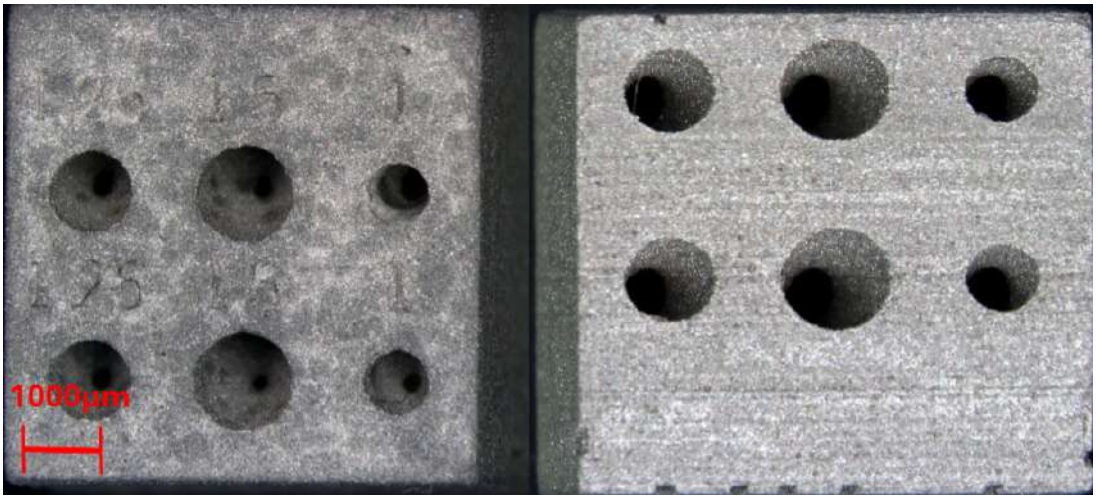

Figure 36: B-component, with its middle cross-section to the right.

The C-components were placed on their side to facilitate the flow of residual feedstock, as seen in 37. This has helped produce a satisfactory result in clearing the feedstock from between the top of the fins but excess feedstock has instead accumulated at the bottom of the components. The components remain largely intact but with the thinnest fins cracked. This likely stems from the heat cycles experienced due to heating and airbrush cycling where temperature rapidly shifts in the component.

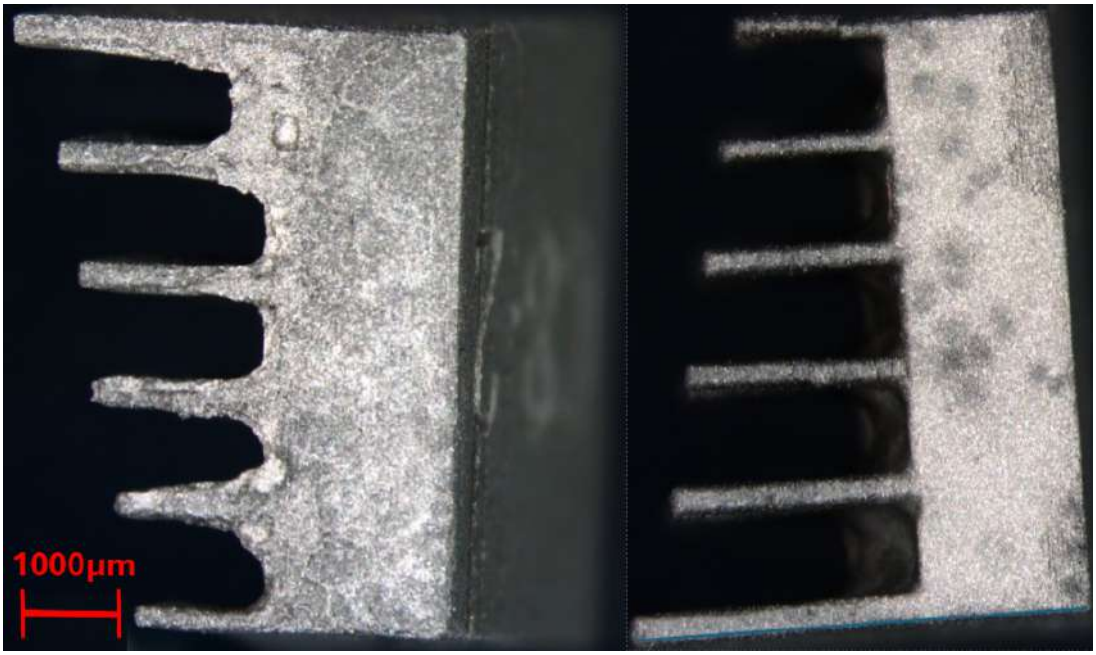

Figure 37: C-components, bottom view of the component to the left and top view of the component to the right.

4.9 Airbrush without IncuSOL before Ultrasonic Cleaning - Batch Nine

In batch seven, section 4.7 using the ultrasonic bath, it was found less effective than the airbrush. This, in combination with the results of batch 4, section 4.4, led to the assumption that the main reason for the effectiveness of the airbrush was the application of pressurized air rather than the accompanying IncuSOL. The pressurized air pushes residual feedstock through the channels clearing them partially or completely. To further explore this possibility and minimize the potential damage caused by IncuSOL, it was decided to use the airbrush without IncuSOL.

Partial success was found in clearing the channels and fins but overall the experiment proved less effective than airbrush employed with IncuSOL, despite the extra step including the ultrasonic bath with heated IncuSOL. This disproved the hypothesis that the application of IncuSOL during airbrushing had a limited effect on cleaning results.

During batch nine it was also evident that some hardening occurred during the clearing of the feedstock. When pressurized air was first applied, a significant amount of feedstock was able to be cleared. The amount of feedstock that could be cleared sharply reduced as time progressed during de-caking. The explanation for this is binder polymerization, which was revealed during the interview with Dr Santiago Cano, in section 2.3. This highlights the importance of limiting the time taken during the de-caking stage, preferably below 30 minutes.

A combination of IncuSOL, gravitation and applied air pressure has proved most efficient in clearing feedstock from channels and between fins. However, during the first application of pressurized air, without IncuSOL, components were still cleared of significant amounts of excess feedstock. It could be beneficial to limit the exposure to solvents which can negatively affect binder material. In future tests, the first airbrush application will be used without IncuSOL.

For A-components, seen in Figure 38 the cleaning results were similar but slightly worse than the results in batch eight, section 4.8. The ultrasonic bath was not able to clear indentations in the numbers, but did penetrate deeper into channels <0.8 mm, than was achievable relying solely on the airbrush.

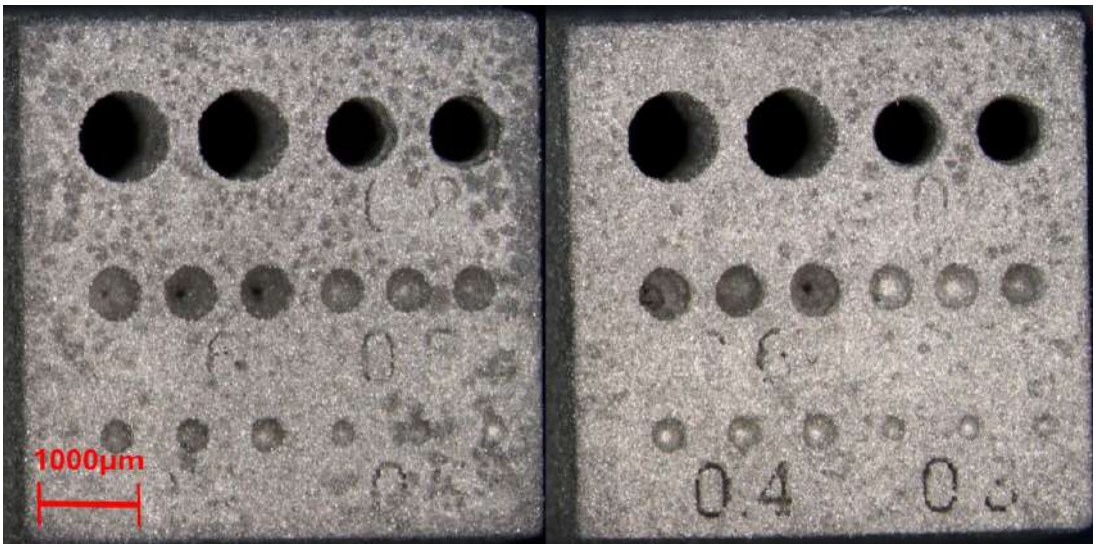

Figure 38: A-components cleaned from batch nine. To the left the component has been cleaned in 30 seconds in the ultrasonic bath and for the right component 120 seconds.

The B-components showed markedly worse results than when only the airbrush with IncuSOL was applied. The channels were not cleared all the way through which had been accomplished in batch eight.

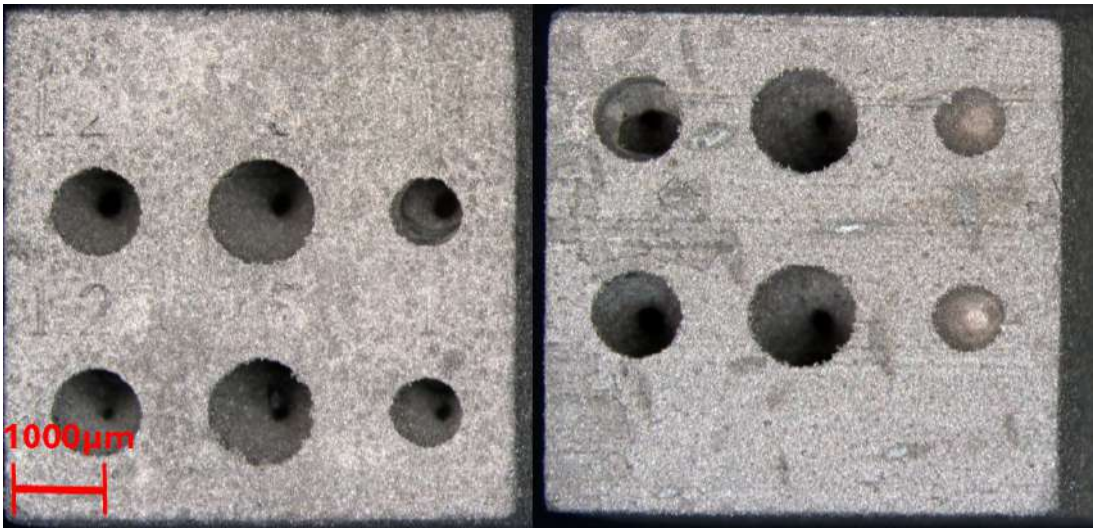

Figure 39: B-components cleaned from batch nine. For the left the component has been cleaned in 30 seconds in the ultrasonic bath and for the right component 120 seconds.

On C-components the cleaning between fins showed no significant improvement in cleaning between components with and without the ultrasonic bath. Residual feedstock that accumulated at the bottom of the component during de-caking still remained, despite the ultrasonic cleaning. Some signs of delamination were noted on components exposed to the ultrasonic bath as seen in the left side of Figure 40.

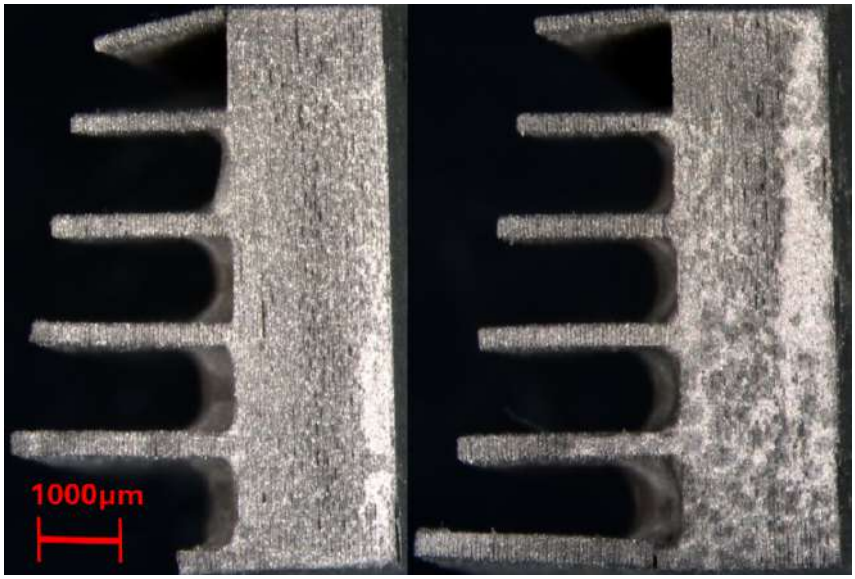

Figure 40: C-components from batch nine. To the left the component has been cleaned in 30 seconds in the ultrasonic bath and the right component 60 seconds.

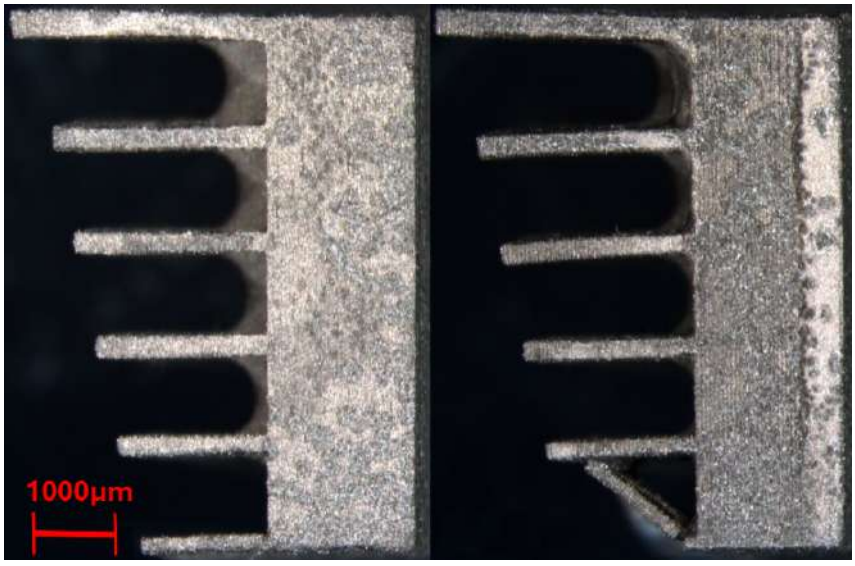

Figure 41: C-components cleaned with only airbrush in batch nine.

On the D-components in batch nine the results were significantly worse than those achieved in batch eight. The exact cause for the poor results seen in both Figure 42 and 43 is mainly believed to be explained by the fact that IncuSOL was not used in the airbrush step. Relying solely on airbrush for clearing channels and evacuating feedstock from the complex inner structure on D-components, only one channel opened and diverted airflow, leaving all other channels blocked. This is visible in Figure 42 and 43, the cleaning was drastically worsened despite the ultrasonic bath, regardless of exposure time.

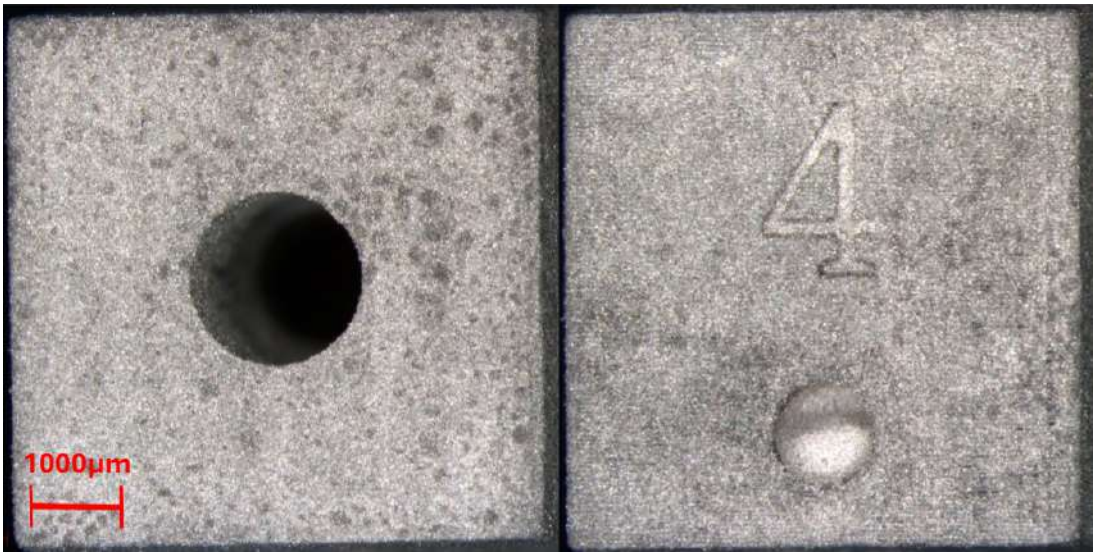

Figure 42: D-component cleaned in batch nine. To the left, top view of the larger channel and to the right, a side view on one of the four side channels.

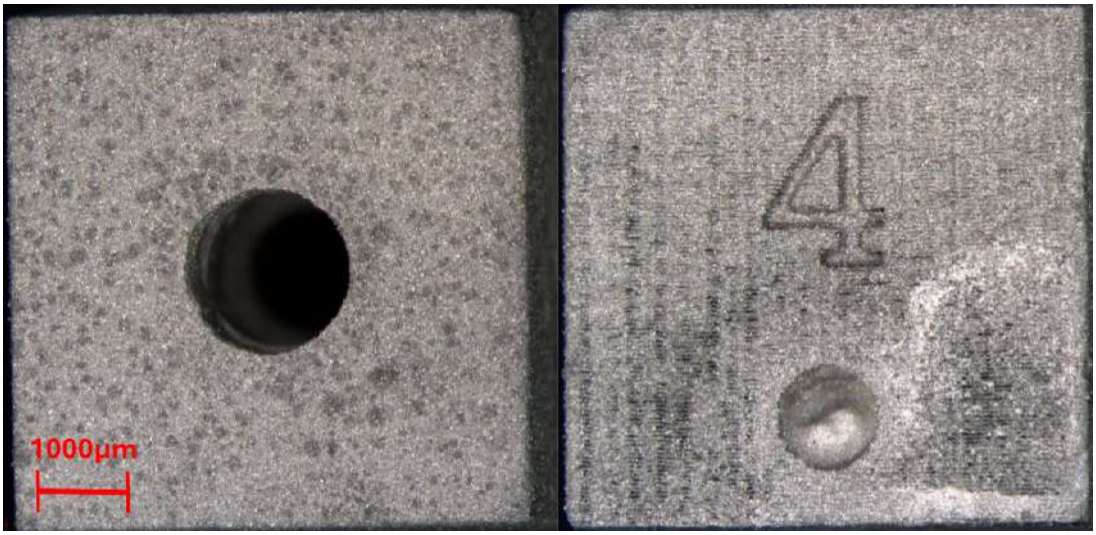

Figure 43: D-component cleaned in batch nine. To the left, top view of the larger channel and to the right, a side view on one of the four side channels.

4.10 Final Method Validation with Incus Recommendations - Batch Ten

It was noted in earlier experiments that all types of IncuSOL application had a negative impact on components but the extent and effect varied. To mitigate these adverse effects components were first airbrushed without IncuSOL to remove residual feedstock deposited on the top of components and were then exposed to three subsequent airbrush applications with heated IncuSOL, as recommended by Dr Santiago Cano in the interview in section 2.3. Finally all components were subjected to 60 seconds of ultrasonic cleaning in heated IncuSOL.

The results were comparable to those in batch eight for all components except for C, however with less residual feedstock stuck in text and number indentations. Both B- and D-components had satisfactory results with all channels being cleared. A-components had only the 1 mm and 0.8 mm channels cleared, which had been achieved in earlier testing. It appeared that greater progress had been made in clearing the 0.6 mm channel, although complete clearing was not achieved.

Delamination was noted on the components, which was not observed in earlier testing using only the airbrush. The material that was used for printing had been recycled and stored for an unknown amount of time, which might have impacted the testing results and exaggerated the delamination and blistering seen on components. In earlier testing, longer exposure times to the ultrasonic cleaning did not result in delamination.

On A-components, as shown in Figure 44, channels smaller than 0.8 mm remain blocked. In Figure 45 the identification text is clean and sharp without excess feedstock attached to the surface. None of the A-components from batch ten show significant damage, indicating that a more aggressive cleaning method could be used. Development of the cleaning steps could involve a more extensive use of the airbrush, since earlier testing indicates that longer ultrasonic cleaning exposure produces limited improvement. Therefore, the proposed development of the cleaning step would involve increasing the air pressure for the airbrush as well as experimenting with larger amounts of IncuSOL applied.

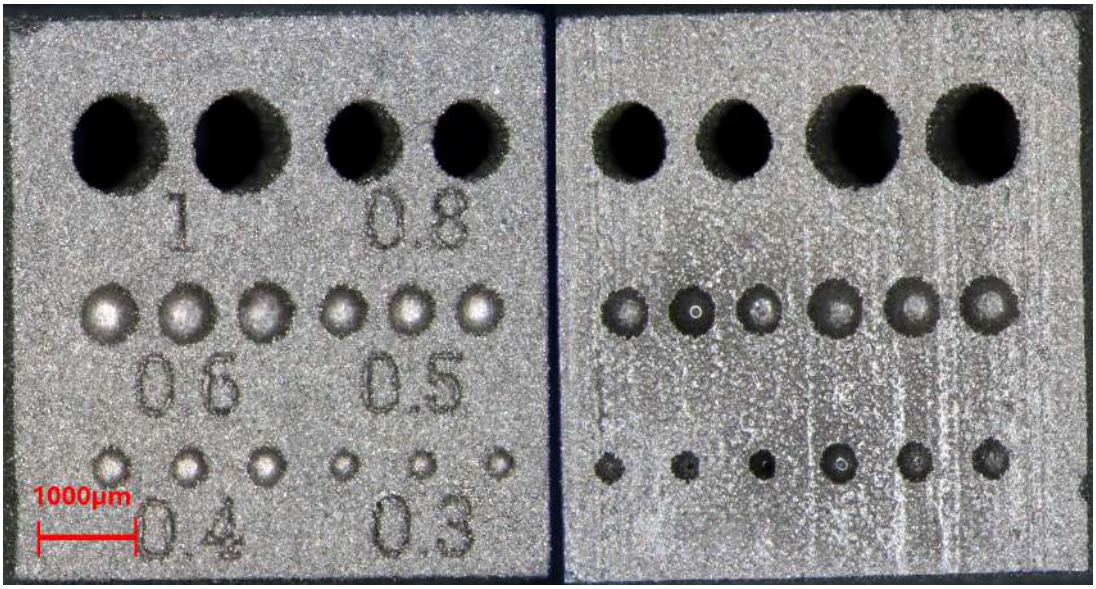

Figure 44: A-component from batch ten, the specimen from the sample group with the best cleaning result. To the left the top view of the channels and to the right the bottom view.

Figure 45: A-component, the same specimen as in Figure 44 from batch ten, showing cleared identification text.

The channels in the B-components were completely cleaned through as seen in Figure 46. These results were satisfactory, however, some damage can be seen in the bottom side corners of the component, to the right in Figure 46. The damage seen on the component might be from handling and could therefore possibly be avoided with more careful handling of the component.

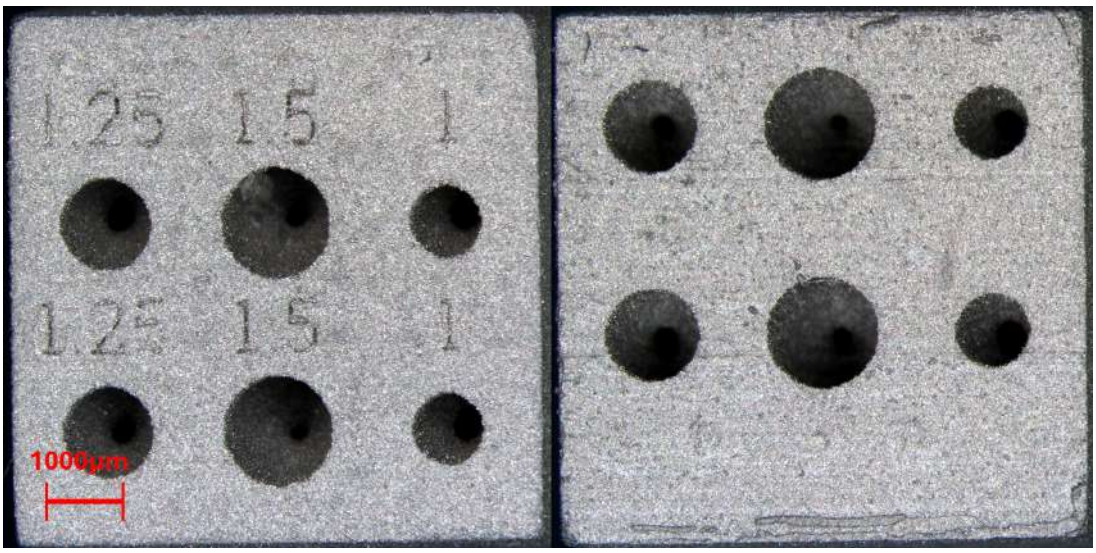

Figure 46: B-component from batch ten exhibiting the best observed cleaning result. The left part shows the top view of the channels, while the right part presents the corresponding bottom view.

In the left view of Figure 47, dark striations can be observed along the printing layers, indicating delamination. Since batch ten was printed using recycled feedstock, the recycled material may have negatively affected the integrity of both the printed layers and the overall component structure.

Figure 47: B-component from batch ten showing the same specimen as in Figure 46. To the left, one side of the component and to the right another side with the identification text.

The C-components in batch ten had the best cleaning results for C-components in the entire study. However, they also sustained more overall damage than C-components in both batch eight section 4.8 and batch nine section 4.9. The specimen shown in Figure 48 was the least damaged from batch ten, nevertheless the four specimens had similar cleaning performance in feedstock clearance.

The observed damage is believed to primarily originate from the ultrasonic cleaning stage, where all C-components were placed together in the bath. During ultrasonic exposure, component movement and collisions likely caused deformation and structural damage to the fragile fin structures. To minimize this, removal of the C-components prior to ultrasonic cleaning would likely be beneficial, allowing them to instead be cleaned using only airbrush and heated IncuSOL. Another possible solution would be to ensure sufficient spacing between components during ultrasonic cleaning by positioning them horizontally and introducing dividers to prevent interaction and collisions between specimens.

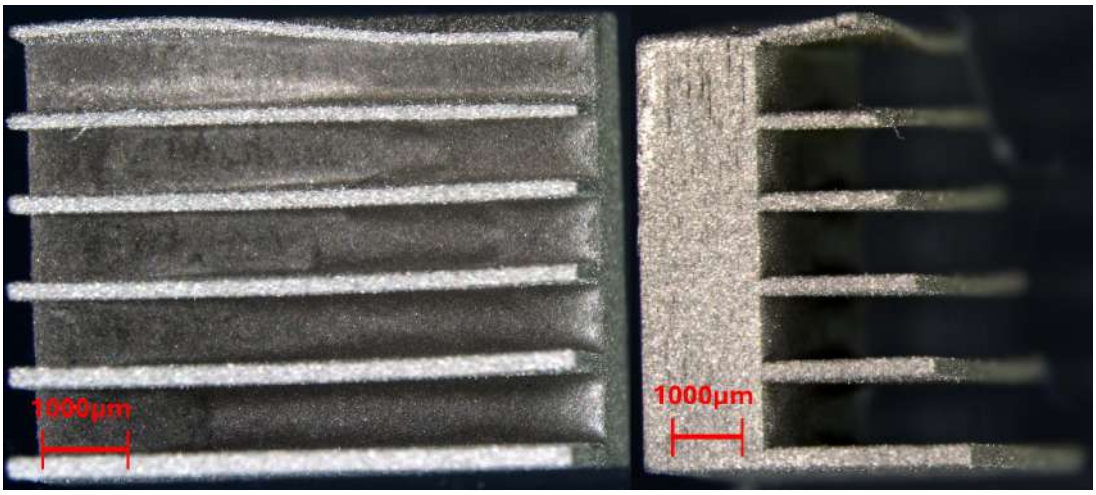

Figure 48: C-component from batch ten exhibiting the best overall cleaning result. The left side shows a top view of the fin structure, while the right image presents a side view.

Figure 49: Bottom surface of the C-component shown in Figure 48. The sharp and clearly visible part identification indicates effective removal of residual feedstock from the surface.

D-components in batch ten had channels and junctions completely cleared with satisfactory results, seen in Figure 50 and 51. Overall the four D-components in the batch were undamaged and had great cleaning results.

The successful cleaning of D-components indicates that the combined cleaning strategy was sufficient to clear both vertical channels and internal junctions without causing structural damage. Compared to the finned C-components, the thicker walls and more structurally stable geometry of the D-components likely reduced the risk of deformation during ultrasonic exposure and handling.

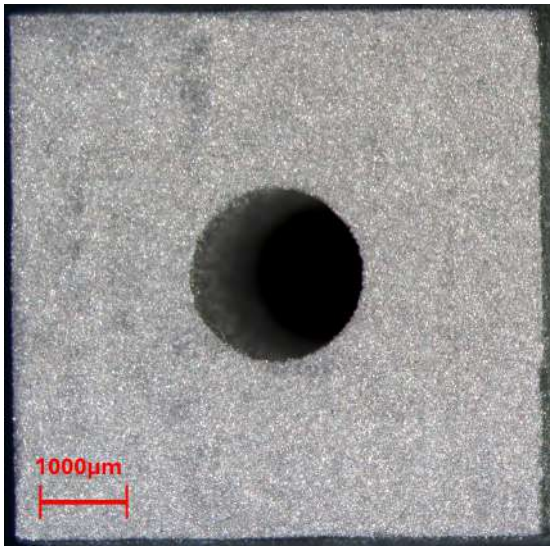

Figure 50: D-component from batch ten exhibiting the best overall cleaning result. The image shows the top inlet channel above the internal junction structure.

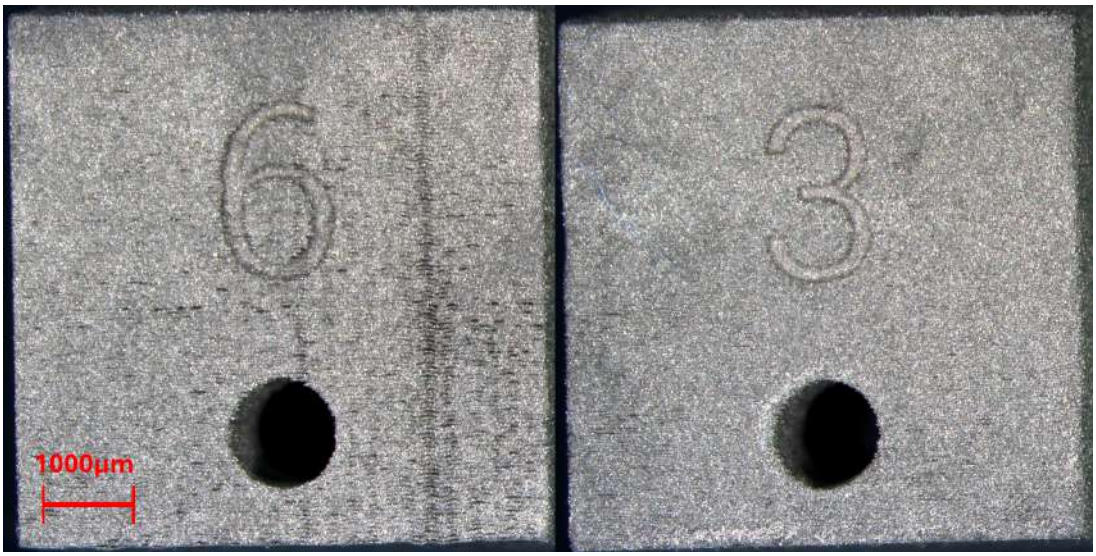

Figure 51: Side views of the D-component shown in Figure 50, displaying two of the cleaned outlet channels connected to the internal junction.

4.11 Method Limitations

The iterative testing method used in this project provided valuable insight into the cleaning of LMM manufactured components. However, several limitations influence the scope and precision of the results.

- The experimental methodology was constrained by a hard limit of ten available print batches. This limit restricted the number of parameter combinations and alternative cleaning techniques that could be comprehensively evaluated.
- Testing was limited to stainless steel 316L provided by the laboratory. Because different materials and feedstocks exhibit varying properties, the optimal cleaning parameters identified in this study may not directly apply to other LMM materials without further adjustment.
- The cleaning procedures relied heavily on manual handling, including the use of tweezers and airbrush applications. This introduced unavoidable human errors, variance in applied pressure and accidental structural damage to fragile features.
- A mix of new and recycled material was used. In one aspect, this recreates a real world production environment where material is continually reused. However, it makes it difficult to assess how tests were affected by their mix of previously used material and how many times it was reused.

4.12 Future Work

To further develop the findings of this study, several areas require additional investigation:

- **Print Parameters:** No adjustments were made to the printer parameters during this study. In the interview with Incus in section 2.3, it was explained that the precision of the projector has limitations, causing a certain amount of light to bleed onto adjacent feedstock. This agitates the binder within the channels, initiating unwanted cross-binding and severely restricting the flow of residual feedstock, especially in small channels. While changes to the settings of the projector might mitigate this effect, such adjustments fell outside the scope of this project. Alterations to the projector could prove beneficial in the cleaning of small channels and should be explored in future investigations.
- **Environmental Control:** The ambient humidity and temperature of the laboratory were neither controlled nor monitored during post-processing. Humidity can have severe repercussions on the binder material, as components that absorb moisture become prone to delamination. Consequently, when defects such as delamination occurred, it was difficult to determine whether the damage was caused by environmental factors or cleaning methods, and must therefore be investigated further.

- **Feedstock Degradation:** The prints were conducted using an uncontrolled mixture of new and recycled material, with an unrecorded number of reuse cycles. While this simulates a real world production environment where material is continually reused, it makes it difficult to isolate how feedstock degradation affects cleaning results. An independent study assessing how degradation of reused material affects cleaning performance would be necessary. An investigation would also have to assess how degradation differs between feedstock compositions.
- **Sintering:** Since components were evaluated prior to sintering it is unknown what adverse effects could be experienced by the final components as a result of the cleaning procedure. Future testing should include a final sintering stage to verify that components are intact and functional, as well as to determine which pre-sintering defects are inconsequential to the final components.
- **Materials:** Testing was conducted exclusively using a feedstock containing stainless steel 316L. Feedstocks containing different metals require varying binder compositions, which may result in differing melting and draining behaviours. Furthermore, specific metal particles can alter chemical interactions, for instance copper can act as a catalyst when exposed to heat and solvents. Therefore, it remains unknown how the cleaning procedure will translate to other materials. To further develop the study, a larger amount of materials will have to be studied, to ensure that the cleaning procedure and recommendations are generally applicable to components created with LMM technology.

5 Conclusions

This study aimed to establish a standardized and reproducible post-processing cleaning method for complex components manufactured via LMM. Through iterative testing of ten component batches, individual cleaning stages were evaluated to identify cleaning equipment and methods that maximize the removal of residual feedstock while minimizing the risk of structural damage and surface defects.

5.1 Design for Cleaning and Handling

To successfully answer how a standardized cleaning procedure can be established, specific conditions regarding component design and print layout must be met to create optimal conditions for cleaning.

- **Design for Cleaning:** Components must be designed and oriented to allow residual feedstock to flow out. Specifically, printing components in an inverted orientation allows for the early removal of the build plate, which reduces flow restrictions during the initial de-caking stage. Furthermore, a distance of 1.5 mm is recommended between the components on the build plate to prevent excess feedstock from causing components to stick together during heating.
- **Design for Handling**: The fragility of LMM components in the green state necessitates that manual handling is minimized. However, where handling is required, components must be designed with surfaces capable of withstanding forces exerted by tools such as tweezers. Incorporating such surfaces ensures that components can be securely handled without damaging delicate geometries such as fins.

5.2 Optimal Cleaning Process

The results indicate that the most effective cleaning procedure relies on a combination of mechanical and chemical agitation. The success of the cleaning process is highly dependent on time and temperature. Delayed post-processing allows the binder to cross-bind, which thickens the excess feedstock and severely inhibits cleaning attempts. Therefore, the cleaning process should begin as soon as possible after a completed print, and the entire cleaning process should be kept under 30 minutes.

The established process differs slightly depending on the geometry of the component.

- **Channels:** The most effective procedure for clearing narrow, intersecting channels utilizes a sequenced combination of thermal, chemical, and mechanical agitation. Initially, the components undergo a de-caking stage of 15 minutes at 60 °C to facilitate the initial flow of residual feedstock. Subsequently, an iterative secondary stage of agitation and heating is initiated. The components are kept at 60 °C during heating and are intermittently removed to apply pressurized air combined with IncuSOL, preheated to 50 °C. Between airbrush applications, components must be returned to the heating environment to ensure that feedstock remains liquid. This cycle is repeated every 3 minutes for a total of 4 applications.

  As a final step to dislodge any remaining feedstock, the components are submerged for 60 seconds in an ultrasonic cleaner containing IncuSOL heated to 45 °C. The ultrasonic cleaner should be set to a frequency of roughly 40 kHz, lower frequencies increase the risk of structural damage while higher frequencies fail to yield sufficient cleaning. Experimentation showed that internal channels exhibit sufficient structural integrity to withstand the forces exerted by the airbrush. Therefore, provided the surrounding walls are not excessively thin, pressurized air can be applied continuously during this stage without inducing damage.

- **Thin-Walled Components:**

  The most effective procedure for clearing features such as narrow fin arrays also utilizes a sequenced combination of thermal, chemical and mechanical agitation, but requires some modifications to account for structural vulnerabilities. Initially, the components undergo a de-caking stage of 15 minutes at 60 °C to facilitate the initial flow of residual feedstock. Subsequently, an iterative secondary stage of agitation and heating is initiated. The components are kept at 60 °C during heating and are intermittently removed to apply pressurized air combined with IncuSOL, preheated to 50 °C. Between airbrush applications, components must be returned to the heating environment to ensure that feedstock remains liquid and to prevent rapid cooling, which is critical as thin-walled structures are sensitive to stress from repeated heat cycles. Unlike other geometries, it is important to vary the rotation of the components during this heating phase. Specifically, components should be positioned so that the leading edges of the fins are vertical, thereby improving drainage of feedstock. This cycle is repeated every 3 minutes for a total of 4 applications.

  As a final step to dislodge any remaining feedstock, the components are submerged for 60 seconds in an ultrasonic cleaner containing IncuSOL heated to 45 °C. The ultrasonic cleaner should be set to a frequency of roughly 40 kHz, lower frequencies increase the risk of structural damage while higher frequencies fail to yield sufficient cleaning. Experimentation showed that thin-walled components lack sufficient structural integrity to withstand the forces exerted by the airbrush. Therefore, to prevent structural damage, pressurized air must be applied cautiously, utilizing reduced pressure and maintaining an increased distance between the nozzle and the components.

5.3 Defect Identification and Categorization

By breaking the proposed cleaning procedure into stages, specific damage mechanisms could be isolated and linked to their causes. For example, evaluating the ultrasonic bath as an isolated variable proved that prolonged exposure to cavitation and solvent directly caused corner rounding and layer delamination. Similarly, the airbrush stage revealed that applying pressurized air caused deformations, especially when components were hot. Beyond mechanical damage, isolating these stages highlighted chemical and thermal vulnerabilities. Applying unheated solvent via airbrush induced thermal stress that cracked fragile fins, while prolonged exposure to the solvent itself dissolved the internal binder, causing surface blistering. Furthermore, isolating the time and temperature variables during de-caking proved that prolonged heating accelerates binder cross-linking, blocking internal channels.

References

[1] RISE, Research Institute of Sweden. "Upptäck additiv tillverkning." No publication date, Accessed: Jan. 27, 2026. [Online]. Available: https://www.ri.se/sv/am-center/vart-erbjudande/upptack-additiv-tillverkning.

[2] Loughborough University Additive Manufacturing Reasearch Group. "About additive manufacturing vat photopolymerisation," Accessed: Apr. 14, 2026. [Online]. Available: https://www.lboro.ac.uk/research/amrg/about/the7categoriesofadditivemanufacturing/vatphotopolymerisation/.

[3] R. Melentiev, A. Wagih, A. Lagerweij, G. Mitteramskogler, G. Lubineau, and C. A. Grande, "Unlocking multiscale metallic metamaterials via lithography additive manufacturing," *Virtual and Physical Prototyping*, vol. 19, no. 1, e2339368, 2024. DOI: 10.1080/17452759.2024.2339368.

[4] Loughborough University Additive Manufacturing Reasearch Group. "About additive manufacturing the 7 categories of additive manufacturing," Accessed: Apr. 14, 2026. [Online]. Available: https://www.lboro.ac.uk/research/amrg/about/the7categoriesofadditivemanufacturing/.

[5] Loughborough University Additive Manufacturing Reasearch Group. "About additive manufacturing material extrusion," Accessed: Apr. 14, 2026. [Online]. Available: https://www.lboro.ac.uk/research/amrg/about/the7categoriesofadditivemanufacturing/materialextrusion/.

[6] Loughborough University Additive Manufacturing Reasearch Group. "About additive manufacturing powder bed fusion," Accessed: Apr. 14, 2026. [Online]. Available: https://www.lboro.ac.uk/research/amrg/about/the7categoriesofadditivemanufacturing/powderbedfusion/.

[7] Loughborough University Additive Manufacturing Reasearch Group. "About additive manufacturing material jetting," Accessed: Apr. 28, 2026. [Online]. Available: https://www.lboro.ac.uk/research/amrg/about/the7categoriesofadditivemanufacturing/materialjetting/.

[8] Loughborough University Additive Manufacturing Reasearch Group. "About additive manufacturing binder jetting," Accessed: Apr. 28, 2026. [Online]. Available: https://www.lboro.ac.uk/research/amrg/about/the7categoriesofadditivemanufacturing/binderjetting/.

[9] Loughborough University Additive Manufacturing Reasearch Group. "About additive manufacturing directed energy deposition," Accessed: Apr. 28, 2026. [Online]. Available: https://www.lboro.ac.uk/research/amrg/about/the7categoriesofadditivemanufacturing/directedenergydeposition/.

[10] Loughborough University Additive Manufacturing Reasearch Group. "About additive manufacturing sheet lamination," Accessed: Apr. 28, 2026. [Online]. Available: https://www.lboro.ac.uk/research/amrg/about/the7categoriesofadditivemanufacturing/sheetlamination/.

[11] Incus. "We have a passion for technology." No publication date, Accessed: Mar. 25, 2026. [Online]. Available: https://www.incus3d.com/about-us/.

[12] Incus. "The incus approach. supreme metal am. consistency & flexibility." No publication date, Accessed: Mar. 25, 2026. [Online]. Available: https://www.incus3d.com/technology/.

[13] Z. Xing, H. Zhou, W. Liu, J. Nie, Y. Chen, and W. Li, "Efficient cleaning of ceramic green bodies with complex architectures fabricated by stereolithography-based additive manufacturing via high viscoelastic paste," *Additive Manufacturing*, vol. 55, p. 102 809, 2022. DOI: 10.1016/j.addma.2022.102809.

[14] R. Melentiev, A. Wagih, G. Lubineau, and C. A. Grande, "3d printing, debinding and sintering of stainless steel metamaterials via lithography metal manufacturing: Processing, microstructure and properties relationships," *Materials & Design*, vol. 256, p. 114 352, 2025. DOI: 10.1016/j.matdes.2025.114352.

[15] Incus. "Finely-detailed metal 3d prints from the incus hammer lab35," Accessed: May 13, 2026. [Online]. Available: https://www.incus3d.com/articles/finely-detailed-metal-3d-prints-from-the-incus-hammer-lab35/.

[16] Micro MIM. "Lmm 3d printer: Hammer lab35," Accessed: May 13, 2026. [Online]. Available: https://www.micro-mim-europe.com/services/3d-printing.

[17] Incus. "Frequently asked questions," Accessed: May 13, 2026. [Online]. Available: https://www.incus3d.com/faq_v2_old/?fbclid=IwZXh0bgNhZW0CMTEAc3J0YwZhcHBfaWQPNDM3NjI2MzE2OTczNzg4AAEe3h_RSqGYR9v0anUC9vMtGZVblMM3shiqx7ayAhjRiLTjzWsEZoL94w7Xkms_aem_lWCXDDMQ7h8II04RfmwJBA.

[18] Incus. "Metal powders," Accessed: May 13, 2026. [Online]. Available: https://www.incus3d.com/materials/.

[19] Siemens. "Vat photopolymerization," Accessed: May 3, 2026. [Online]. Available: https://www.siemens.com/en-us/technology/vat-photopolymerization/.

[20] Siemens. "Material extrusion," Accessed: May 3, 2026. [Online]. Available: https://www.siemens.com/en-us/technology/material-extrusion/.

[21] Siemens. "Powder bed fusion," Accessed: May 3, 2026. [Online]. Available: https://www.siemens.com/en-us/technology/powder-bed-fusion/.

[22] Siemens. "What is material jetting?" Accessed: May 3, 2026. [Online]. Available: https://www.siemens.com/en-us/technology/material-jetting/.

[23] Siemens. "Binder jetting," Accessed: May 3, 2026. [Online]. Available: https://www.siemens.com/en-us/technology/binder-jetting/.

[24] RISE. "Ded - enabling remanufacturing," Accessed: May 4, 2026. [Online]. Available: https://www.ri.se/en/am-center/equipment-and-expertise/ded-enabling-remanufacturing.

[25] DASSAULT SYSTEMES. "Sheet lamination," Accessed: May 4, 2026. [Online]. Available: https://www.3ds.com/make/guide/process/sheet-lamination.

A Hammer Lab35 Specification

Hammer Lab35 Specification

Release date	2019
Build volume (dimensions)	89.6 × 56 × 120 mm
Build volume (total)	$0.6\,\mathrm{L}$
Maximum resolution (XY)	$0.035\,\mathrm{mm}$
Maximum resolution (Z)	$0.01\,\mathrm{mm}$
Print speed	100 cm^3/h
Slice thickness	10 - 100 $\mu\mathrm{m}$
Building velocity	Up to 250 slices/h
Feedstock format	Liquid

Compatible Materials

- Metal
  - Diamond
  - Gold
  - Cobalt chrome
    - Cobalt chrome MP1
    - CoCr28Mo6
  - Copper
    - Cu
  - Silver
    - Sterling silver 925
  - Steel
    - Stainless steel: 17-4PH, 316L
  - Titanium
    - Ti64
  - Tungsten
    - Tungsten Carbide Cobalt
  - Brass

Figure A.1: Technical specifications and supported metallic materials for the Hammer Lab35 system [15–18].

B Materials and Equipment

This appendix presents the materials and equipment used during the study. Standard laboratory equipment available at Chalmers was complemented by borrowed, purchased, and custom-made tools introduced to support the experimental development of the cleaning procedure.

B.1 Laboratory Equipment

- Hammer Lab35
- Heat gun: STEINEL Type 3481 $230V \sim 1800W$

Figure B.1: Heat gun used for de-caking and heating of the components.

- Glass container
  - Used to collect feedstock during initial de-caking.
- Mesh screen
  - Stretched over the glass container to allow excess feedstock to flow through during de-caking.
- Beaker
  - Used for handling and temporary storage of cleaning solutions.

- Ultrasonic cleaner: VWR Symphony serie

Figure B.2: Ultrasonic cleaner used for the study.

- Tweezers
- Compressed air cleaning station, from Incus
- Timer
- Paper towels
- Small build plate ($46 \times 30\,mm$)
- Pipette

B.1.1 Cleaning Solutions

- IncuSOL (oil-based cleaning solution)
  - Used for removal of residual feedstock during cleaning.

Figure B.3: IncuSOL and Ethanol containers.

- Ethanol
  - Used to clean tools and equipment during and after component cleaning.

B.2 Additional Equipment Introduced During the Study

Additional tools were introduced during the study to improve process control, handling, and documentation.

B.2.1 Borrowed Equipment

Some equipment available at Chalmers was borrowed for use in the study.

- Heat gun stand
  - This is a stand borrowed from the chemistry lab.
- Stereo microscope: ZEISS SteREO Discovery.V20
  - After each batch the microscope was booked and used for image-based documentation of results.
- Thermometer: FLUKE 53 II THERMOMETER with a type K thermocouple
  - Used to measure the air temperature around the components during de-caking and heating.

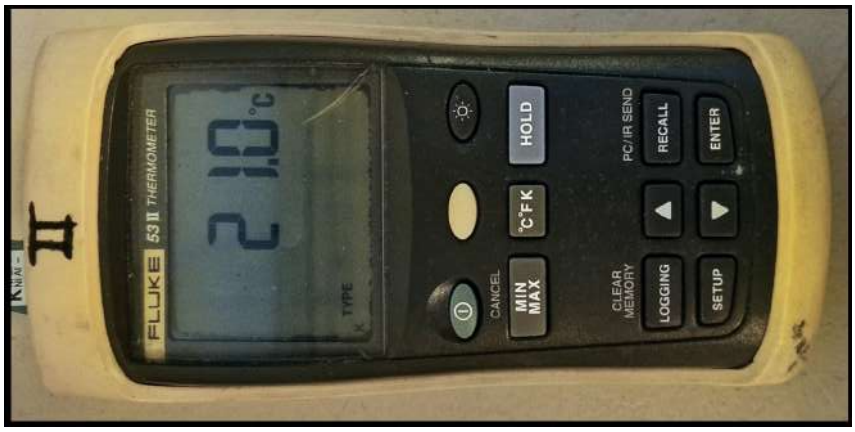

Figure B.4: FLUKE 53 II THERMOMETER with a type K thermocouple used during heating experiments.

B.2.2 Purchased Equipment

When suitable tools were not available for borrowing at Chalmers, the required equipment was purchased.

- Rubber-coated metal tweezer set
  - Used to reduce the risk of surface damage during handling.

Figure B.5: Rubber-coated metal tweezer set used for manual handling of components.

- Bowl and sieve
  - Used to minimize direct handling of components using tweezers and replaced the mesh screen.

Figure B.6: Strainer with container.

- Strainer with container
  - Used to minimize direct handling of components using tweezers and replaced the mesh screen.

Figure B.7: Strainer with container kit including a shallow stainless steel mesh beaker.

- Thermometer: Melissa digital food thermometer (up to 250°C)
  - Purchased to measure the temperature of liquids.
- Vacuum pen
  - Evaluated for component handling, but was not suitable for the intended application.

B.2.3 Custom-Made Equipment

- Tilting device (3D printed)
  - Used to provide controlled component inclination during heating experiments.

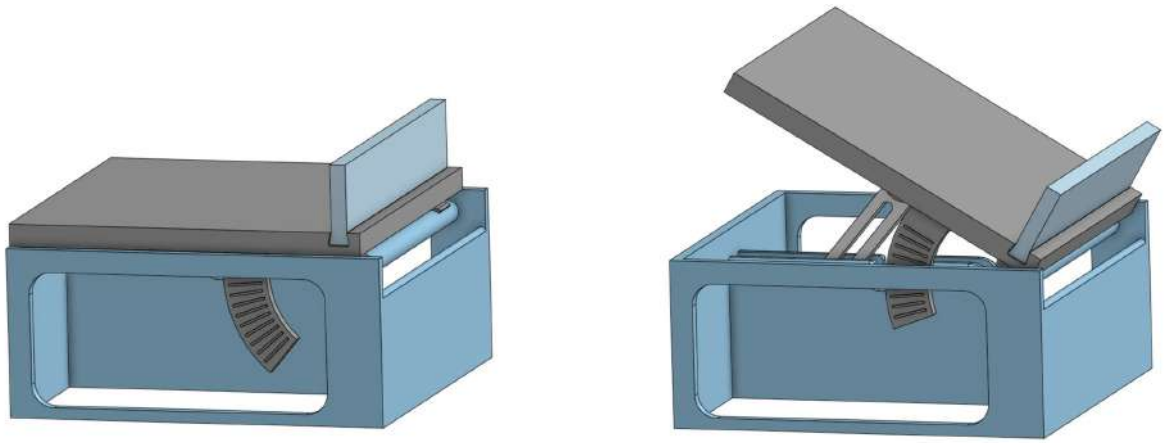

(a) Lowest position **(b)** Inclined position

Figure B.8: Custom-made tilting device used to control component inclination during heating.

C Defects

This appendix provides a brief overview of the defects observed during the project and outlines the measures taken to avoid them.

C.1 Residual Feedstock

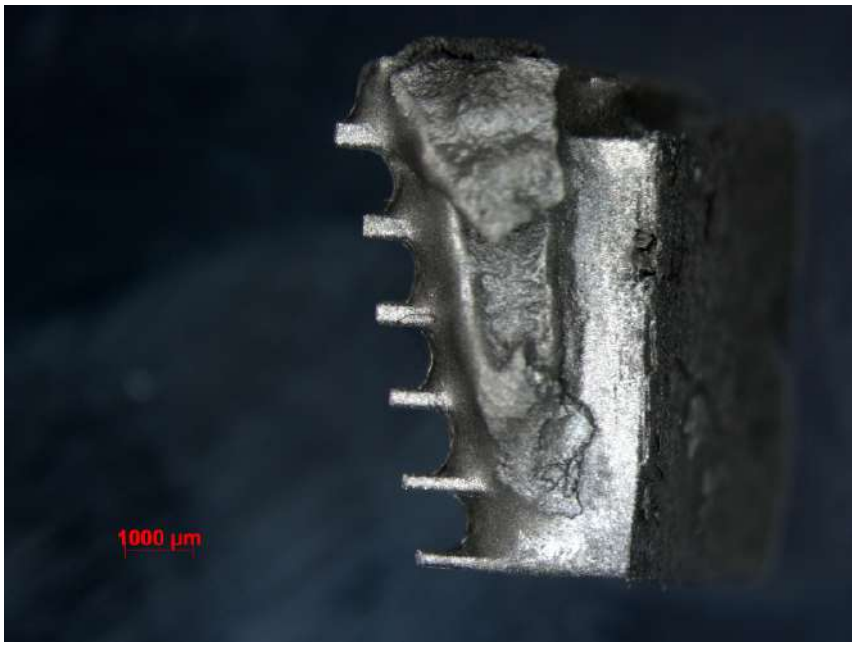

Figure C.1: Residual feedstock remaining on a component after the de-caking stage, caused by premature polymer binding within the unhardened material.

The figure depicts excess feedstock on components that remains after the de-caking stage. This problem arises due to polymer binding occurring inside of the residual feedstock. Polymer binding occurs naturally after printing and it is therefore advisable to begin cleaning as soon as possible after printing. The process of polymerization speeds up during heating and a higher de-caking temperature increases the progression further. To avoid this from happening cleaning should preferably begin immediately after completed printing, the entire cleaning procedure should be kept under 30 minutes and heating temperatures should not exceed 60 °C.

C.2 Cracks

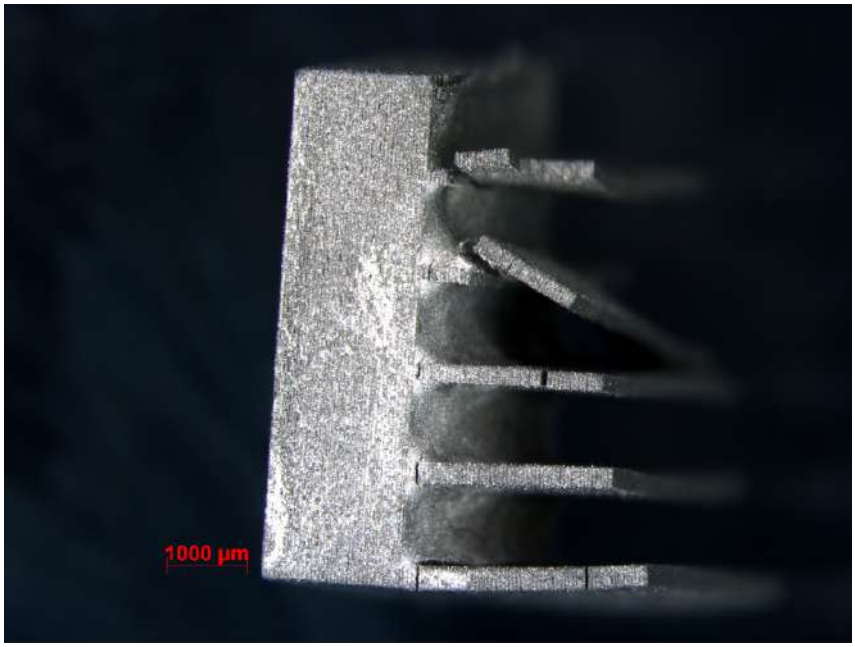

Figure C.2: Cracks formed on fragile fins after exposure to unheated solvent and pressurized air.

The figure illustrates crack formations on the delicate fins. This defect emerged as a result of repeated, brief airbrush applications using unheated IncuSOL. Consequently, both the solvent and the pressurized air struck the part at room temperature. Even though the heating was relatively low 60 °C, the repeated thermal cycling induced sufficient stress to fracture the thin fins. To prevent this, a stable temperature must be maintained during post-processing, in order to avoid the binder material continually expanding and shrinking.

C.3 Rounded Edges

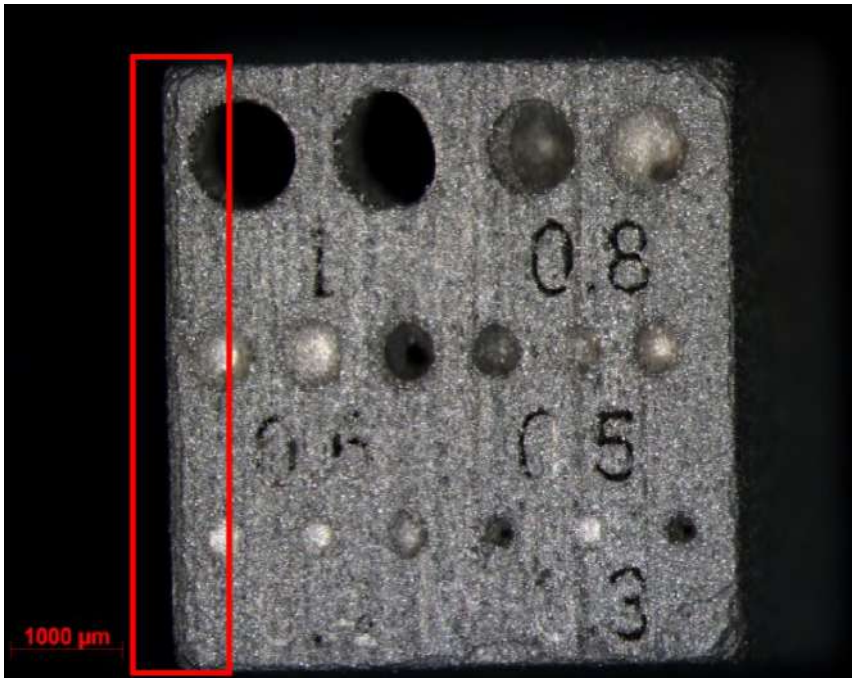

Figure C.3: Disintegration of component corners caused by localized pressure spikes during prolonged exposure in the ultrasonic bath.

Pressure spikes arise in the corners of square components in the ultrasonic bath. As seen in the figure above, the corners have disintegrated as a result of being left in the ultrasonic bath for a prolonged period of time. To mitigate this, time in the ultrasonic bath must be limited, or the vibration frequency increased. Both of these negatively affect cleaning performance but limit damage.

C.4 Surface Scratches

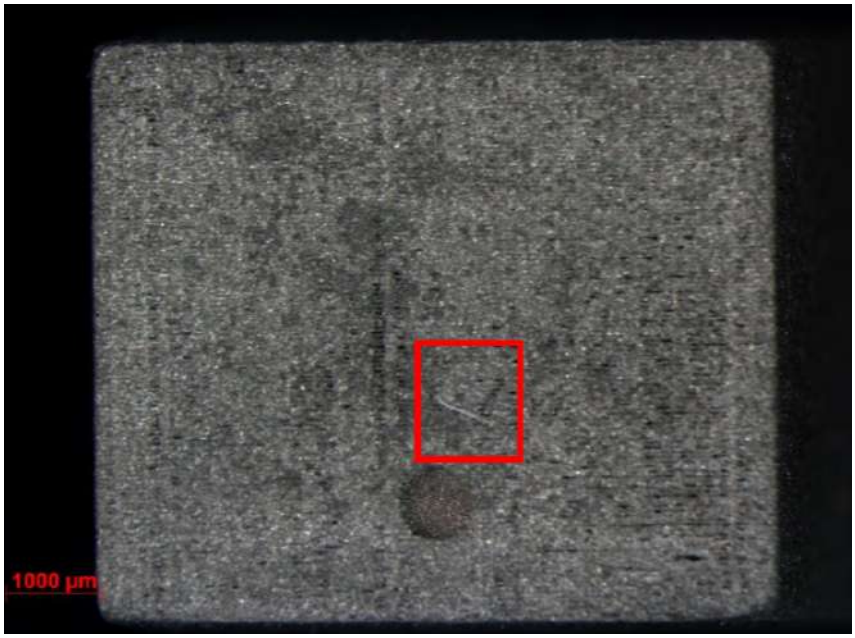

Figure C.4: Surface scratches on a component resulting from manual handling and transportation steps during the cleaning process.

Scratches to surfaces occur during manual handling of components. To avoid this, manual handling must be limited and the number of transportation steps reduced. When handling is unavoidable, caution must be taken and appropriate equipment be used to protect the fragile surfaces.

C.5 Delamination

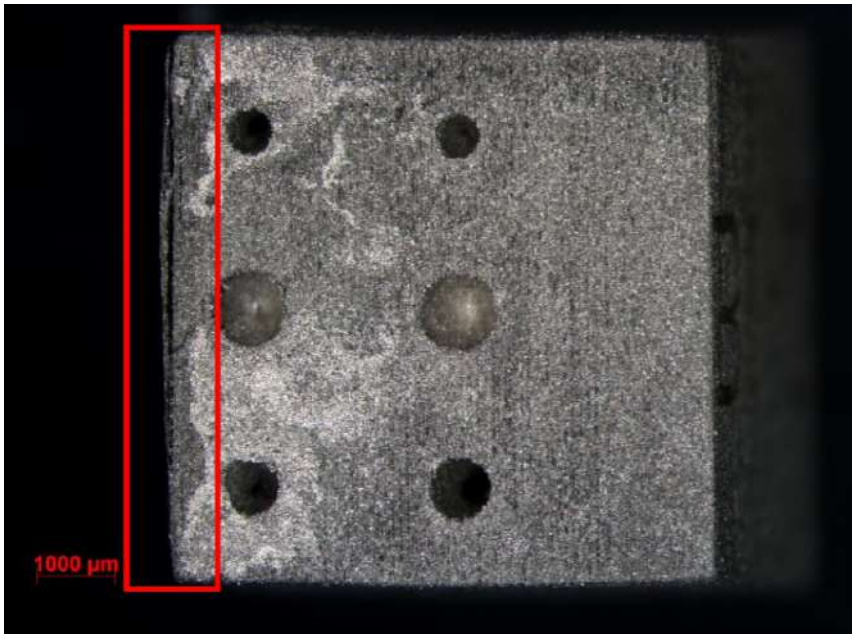

Figure C.5: Disintegration of printed layers observed after exposure to the ultrasonic bath for more than two minutes.

When components are created, a thin film of feedstock is spread over the build plate, layer by layer. This creates a layered structure that fuses into a solid component during sintering. During cleaning this layering remains sensitive and can disintegrate under unfavourable conditions. From the testing conducted this principally occurs during ultrasonic cleaning where both mechanical and chemical stress are experienced between the layers.

D Advantages and Disadvantages of the Different AM-methods

This section presents a structured overview of the advantages and disadvantages of the seven AM manufacturing methods. The information is compiled from literature sources and summarizes key aspects such as quality, speed, material compatibility, and post-processing requirements.

The purpose of this appendix is to provide a comparative reference supporting the selection and evaluation of manufacturing methods discussed in the main body of the report. The presented data should be interpreted as general characteristics, as performance may vary depending on machine configuration, material selection, and specific application.

D.1 VPP

Table D.1: Advantages and disadvantages of VPP

Aspect	Advantage	Disadvantage
Quality	VPP provides high dimensional accuracy and a smooth surface finish [2]	–
Speed	VPP is characterized by rapid print speeds[2] [19]	–
Suitability area	Large components and prototypes can be produced [19]	
Build size example	Objet 1000: 1000 x 800 x 500 and max model weight of 200 kg" [2] 3D Systems ProX 950, 1500 x 750 x 550 mm with max part weight of 450 kg [2]	–
Cost	–	"Relatively expensive" [2]
Materials	–	LU-AMRG states that the material selection is limited due to the use of photo-resin [2]
Structural properties	–	Often requires post curing for parts to have enough strength for structural use [2] VPP components have generally weak structural strength and can degrade over time [19]
Support structure		Support structure is needed [2]
Post processing	–	Generally time consuming for post processing and removal from resin [2]

D.2 MEX

Table D.2: Advantages and disadvantages of MEX

Aspect	Advantage	Disadvantage
Quality	–	Quality is dependent on the radius for the nozzle, which effect the print quality [5] For achieving good quality constant pressure of feeding material is required in order to have a steady flow [5]
Speed	–	The accuracy and speed for MEX are low compared to other AM processes [5] [20]
Suitability area	Inexpensive and commonly be used for producing prototypes as well as possible to scale up build area to print vehicle-sized parts [20] MEX is the most popular AM method for hobby 3D printing at home [20]	–
Build size example	Insstek MX3 1000 x 800 x 650 mm, build volume 520 liter [5]	–
Cost	MEX is a widespread and inexpensive process [5]	–
Materials	MEX can use ABS plastic which is easily accessible [5]. Further polymer materials are Nylon, PC and AB [5]	–
Structural properties	ABS plastic used which have good structural strength [5]	–
Support structure	–	–
Post processing	–	–

D.3 PBF

Table D.3: Advantages and disadvantages of PBF

Aspect	Advantage	Disadvantage
Quality	–	The final component finish is dependent on the grain size of the powder used for printing [6]
Speed	–	PBF has a relatively slow speed especially for Selective Heat Sintering (SHS) [6]
Suitability area	PBF is suitable for creating visual models and prototypes components [6] PBF is possible to integrate the technology into small scale, office sized machine [6]	–
Build size example	3S Systems ProX 500, 381 x 330 x 457 mm, layer thickness 0,08 - 0,15 mm with print speed of 2 liters/hour [6]	SHL has size limitations according to LU-AMRG [6]
Cost	The AM method is relatively inexpensive for printing [6]	PBF has a high power usage [6]
Materials	A large range of material is compatible with PBF [6] Example of materials that can be used as powder is metal, ceramic and polymer [21]	–
Structural properties	–	PBF has generally lack of structural properties in materials but varies between if polymer or metal is used [6]
Support structure	The excess powder acts as support structure for the component [6]	–
Post processing	–	Clearance of excess powder from the part is needed [6] For certain applications and subcategories of PBF post processing such as CNC work or further sintering is used to improve the components [6]

D.4 MJT

Table D.4: Advantages and disadvantages of MJT

Aspect	Advantage	Disadvantage
Quality	MJT can achieve a high accuracy [7] [22] Further MJT can create fine details and smooth surfaces [22]	–
Speed	–	MJT can be time consuming based on the low layer thickness, could be lower than 20 μm. The layer thickness results in a larger amount of layers needed, however this can be solved with multiple printing heads [22]
Suitability area	The printing technique is suitable for realistic models, visual or haptic prototypes, tooling and casting [22]	–
Build size example	Objet 500 Connex 3, 490 x 390 x 200 mm, layer thickness 16 μm, 46 number of colours [7]	–
Cost	Due to high accuracy in the deposition of droplets MJT results in low material waste and is therefore cost effective [7]	–
Materials	Multiple material parts can be printed as well as a large amount of colours under one process [7]	Materials are limited to polymers and waxes [7]
Structural properties	–	Since MJT is cured photopolymer the physical strength is low for functional- or load bearing components [22]
Support structure	–	MJT often requires structural support material [7]
Post processing	–	–

D.5 BJT

Table D.5: Advantages and disadvantages of BJT

Aspect	Advantage	Disadvantage
Quality	–	–
Speed	BJT is generally a faster printing technique than others [8]	–
Suitability area	Architecture mockups or decorative models [23]	–
Build size example	Spectrum Z 500, layer thickness 0,089 - 0,203 mm, 2 layers / minute [8]	–
Cost	BJT is generally an inexpensive printing technique [23]	Post processing might add overall cost [23]
Materials	Can use a range of materials such as metals, polymers and ceramics [8] Components can be printed with a range of different colours" [8] Two material method in the same components creates possibility for different mechanical properties due to a large amount of binder-powder combinations [8]	–
Structural properties	–	BJT is not always a prefered method for creating structural parts due to the use of binder material [8]
Support structure	–	–
Post processing	–	The need for additional post processing afterward printing can add significant time to the overall process [8]

D.6 DED

Table D.6: Advantages and disadvantages of DED

Aspect	Advantage	Disadvantage
Quality	With DED high quality and functional parts can be printed due to a large controllability of the grain structure [9]	–
Speed	The printing technique has a direct balance between printing speed towards surface quality, high accuracy and predetermined microstructure in the material, cited in [9]). With repair work using DED the printing speed is often sacrificed for quality [9])	–
Suitability area	Use cases for DED is repair, addition of features, metal coating and near-net-shape components [24]	Further research is needed for a more mainstream positioning of the fusion process used in DED [9] DED is a more complex printing technique cited in [9])
Build size example	Insstek MX3 1000 x 800 x 650 mm, layer thickness 0,089 - 0,203, print speed two layers per minute [9]	–
Cost	–	–
Materials	For electron beam melting electrons is used [9] Metals are Cobalt Chrome, Titanium cited in [9])	The printing technique has a limited selection of materials [9]
Structural properties	The printing technique can create parts with functional strength properties [9]	–
Support structure	For repairwork support structure is unneeded [9] DED can be used with powder which in that case the excess powder acts as support structure [9] [6]	–
Post processing	–	Large section of prints require post processing to achieve the desired result, however the finish depends on paper or plastic material [9]

D.7 SHL

Table D.7: Advantages and disadvantages of SHL

Aspect	Advantage	Disadvantage
Quality	–	–
Speed	Due to only cutting the outline shape the cutting speed can be very fast [10] The speed is beneficial, cited in [10])	–
Suitability area	Ergonomic studies, topography visualization, architecture models for paper-made SHL printed components [25] Functional, lightweight technical components for the aerospace and automotive industry for a very competitive cost [25]	Further research is needed for a more mainstream positioning of the fusion process used in SHL [10]
Build size example	MCor Matrix 300 plus, 256 x 169 x 150 mm, layer thickness 0,1 - 0,19 mm, it is using A4-paper [10]	–
Cost	The printing technique has low cost, cited in [10]) [25]	–
Materials	Paper and metal [10] For metals aluminium, copper, stainless steel and titanium can be used [10] Carbon fiber sheets and various composites can be used for material [25]	–
Structural properties	–	Strength and integrity of models printed with SHL is reliant on the adhesive used, cited in [10])
Support structure	–	–
Post processing	–	Post processing is needed to extract the part from the surrounding sheets of material after printing [10] Post processing can be needed to achieve the desired effect [10] Finish is varying depending on paper or plastic material [10]

E Cleaning Guide - LMM

Cleaning Guide - LMM

Hammer Lab35 Post-Processing

Originally created by: N. Bergvall, J. Pölder, M. Nilsson, L. Thorstensson during bachelor thesis
Last updated: June 3, 2026

Requirements

- **IncuSOL:** Solvent pre-heated to 50°C in the airbrush dosing bottle.
- **Airbrush:** For combined mechanical and chemical agitation.
- **Heat Gun:** Calibrated to approximately 60°C air temperature. Temperature is adjusted by changing the vertical position of the heat gun on the stand.
- **Thermometer:** To measure IncuSOL temperatures.
- **Rubber-coated Tweezers:** To prevent surface scratches and deformation.
- **Stopwatch:** For monitoring de-caking and exposure times.
- **Container with mesh insert x2:** First container used in the initial de-cake step and second container used for continued cleaning where IncuSOL residue might drop down into the container.

  The first container will catch the residual feedstock that melts during the initial de-caking step and is suitable for recycling. The second container will catch residual feedstock that has been exposed to IncuSOL and therefore not suitable for reuse.

Important Considerations

! **Immediate Start:** Begin cleaning immediately after the print is completed to prevent viscosity changes. The photopolymerisation continues after the print.

! **The 30-Minute Rule:** Try to keep the total cleaning procedure under 30 minutes. After printing the photopolymerisation continues which causes binder cross-linking.

! **IncuSOL Limits:** Minimize IncuSOL exposure. Prolonged exposure during airbrush or ultrasonic baths cause "blistering" and delamination of printed layers.

Design for handling

The fragility of LMM components in the green state necessitates that manual handling is minimized. However, where handling is required, components must be designed with surfaces capable of withstanding forces exerted by tools such as tweezers. Incorporating such surfaces ensures that components can be securely handled without damaging delicate geometries such as fins, seen in Figure E.1. The base plate on this component is 1.75 mm in order to be able to grab it with tweezers.

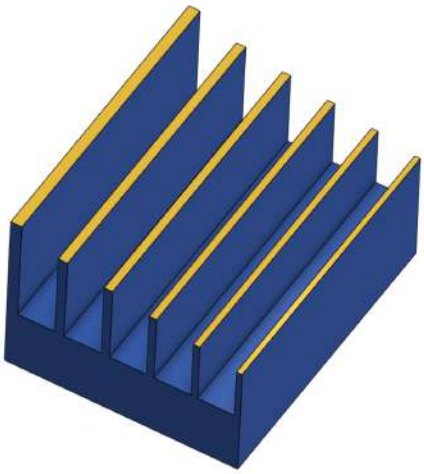

Figure E.1: Fin array with base plate enlarged so that tweezers can lift the components without causing damage

Design for cleaning

Components must be designed and oriented to allow residual feedstock to flow out. Specifically, printing components in an inverted orientation, as seen in Figure E.2, allows for the early removal of the build plate, which reduces flow restrictions during the initial de-caking stage. In order to limit interference between build plate and components in the removal stage a distance of 400 µm is recommended. Furthermore, a distance of 1.5 mm is recommended between the components themselves on the build plate to prevent excess feedstock from causing components to stick together during heating.

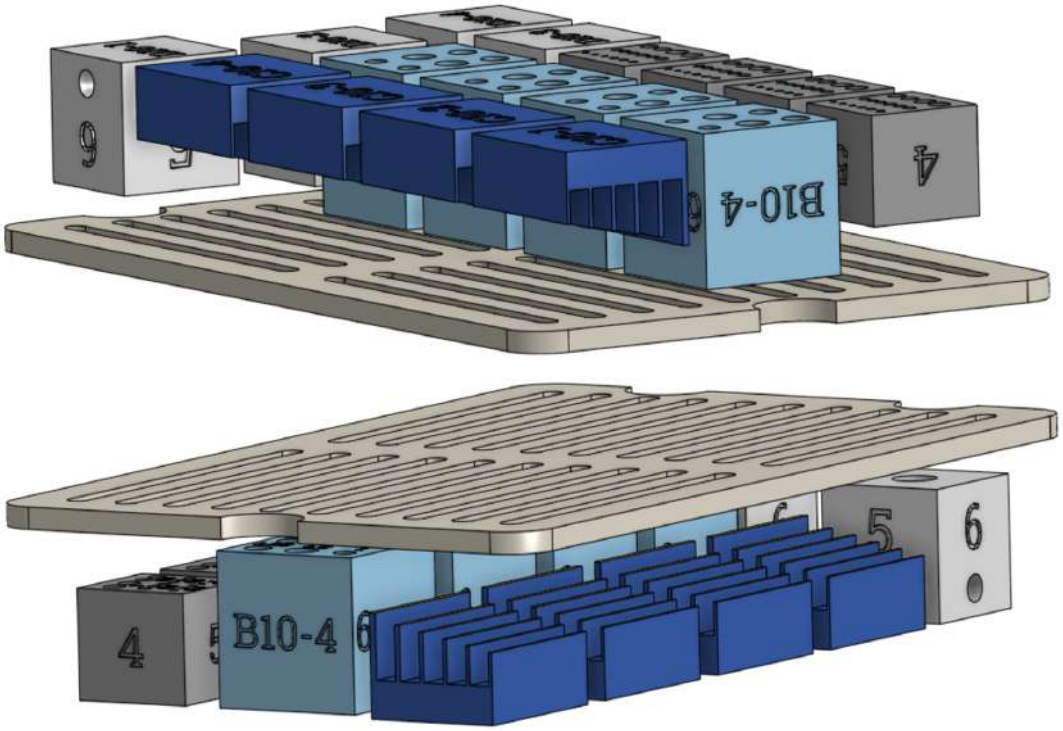

Figure E.2: The inversion of printed components, in order to remove the build plate and aid the flow of feedstock. The upper figure shows the printed orientation with the build plate on the bottom. The lower figure shows the placement of the feedstock block in the sieve during de-caking, with the build plate on top and components in the correct orientation

Brief Overview

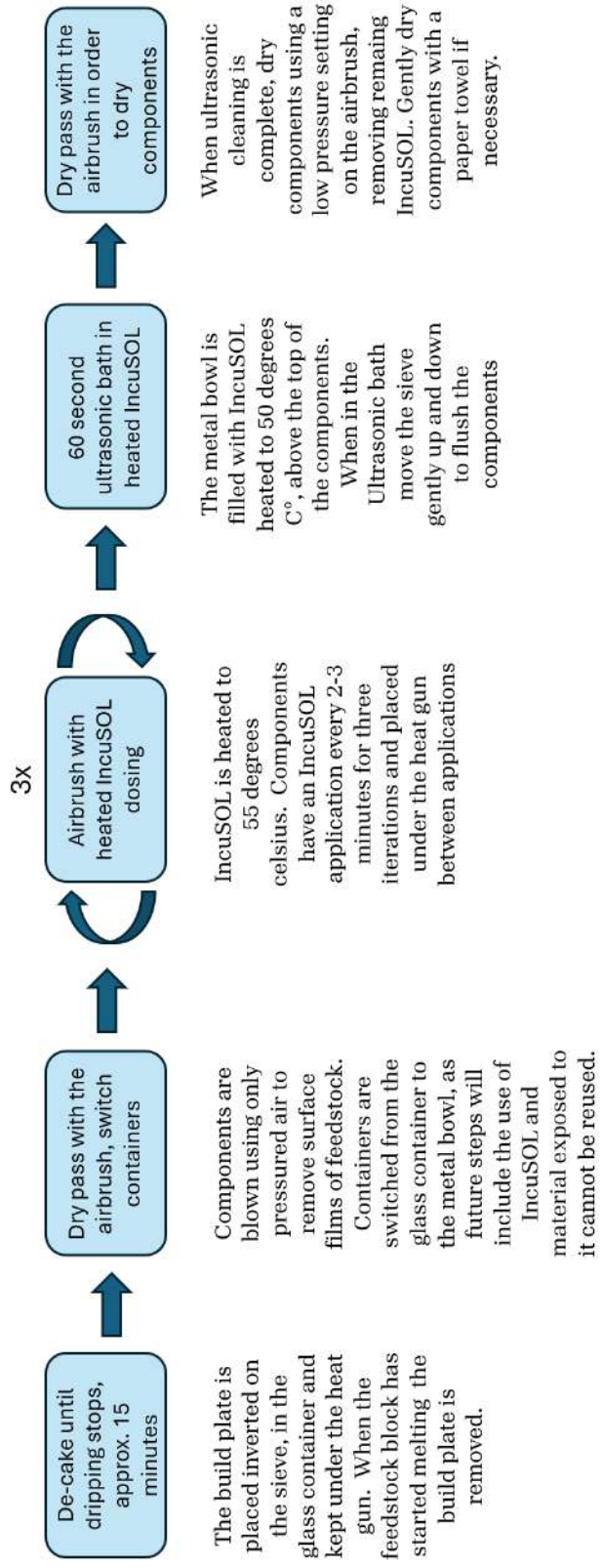

Figure E.3: A brief overview of the cleaning method

Step-by-Step Instructions

Step 1: Printing and de-cake

- Print components in an inverted orientation on the build plate (see Figure E.2). This allows for easy removal of the build plate from the top (see Figure E.4) when rotating the feedstock block to orient the components for de-caking.

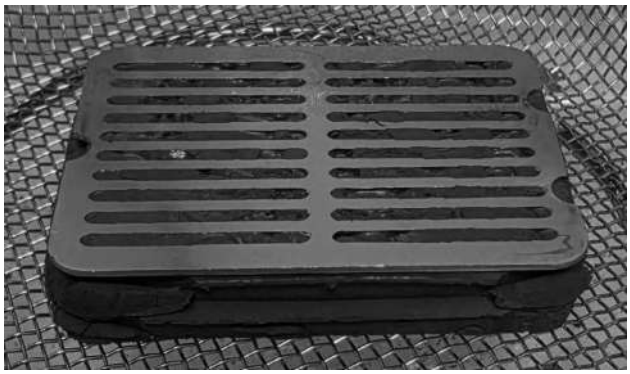

Figure E.4: Build plate on top of the untreated feedstock block.

- Start the de-caking process by applying heat using a heat gun (60 °C), see Figure E.5. This will initiate the melting of excess feedstock. Temperature varies depending on the container height and it is therefore necessary to measure the temperature at component height (see Figure E.6). The heat gun stand is marked with guides, but adjustments are necessary to ensure temperatures stabilize between 55 °C to 60 °C.

Figure E.5: Hot air gun used during testing.

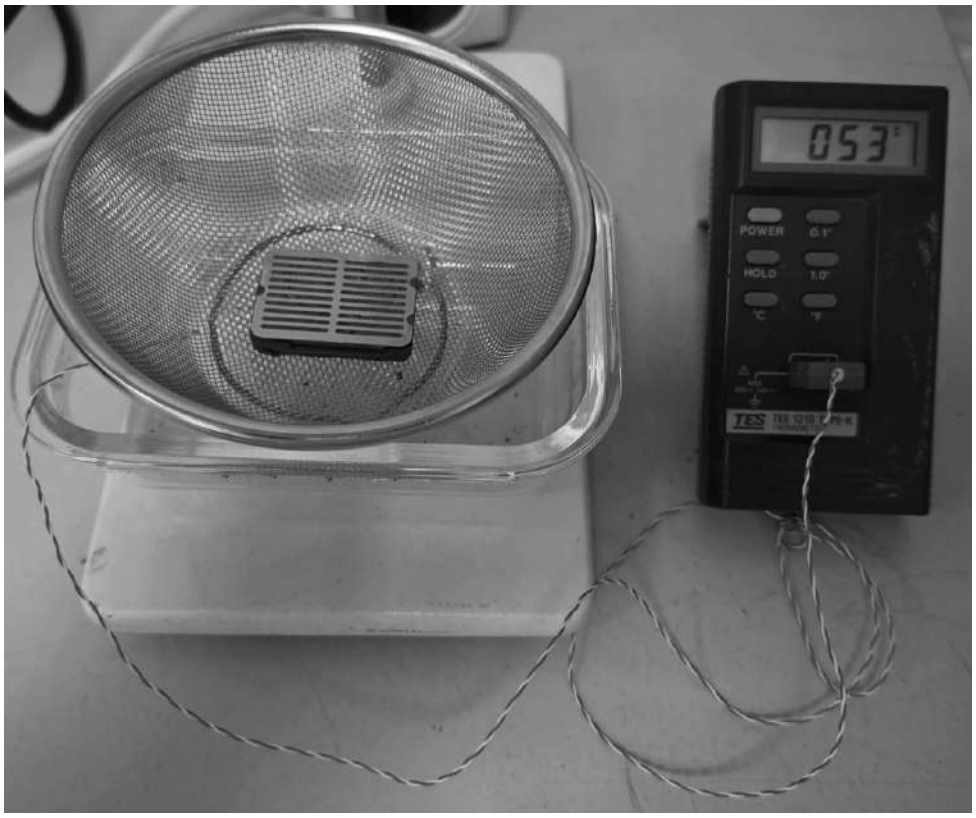

Figure E.6: Shows the start of de-caking where the melting is about to start.

- Remove the build plate early during the de-caking stage so that it does not damage the components.

Figure E.7: Removal of build plate early in the de-cake process.

Figure E.8: Removed build plate, de-caking will continue until dripping stops in this stage.

- The build plate remains under the heat gun until dripping stops. This takes approximately 15 minutes.
- Once residual feedstock has stopped dripping, switch containers in order to recycle collected feedstock, as IncuSOL will be used in the next steps and will contaminate the excess feedstock.

Figure E.9: Moving into a new fresh container to save de-caked feedstock from IncuSOL contamination.

Step 2: Cleaning Cycles (Airbrush)

- After the initial de-caking, the sieve containing all components is moved intermittently between the heating station and the Incus airbrush cleaning station.
- The first round of airbrush application should be done without IncuSOL since a large amount of residual feedstock can be removed without it in this stage.

Figure E.10: Airbrush with IncuSOL container attached.

- Following rounds use airbrush in the Incus cleaning station to apply pressurized air mixed with IncuSOL. The IncuSOL should be pre-heated to 55°C. After IncuSOL use, dry the component to free them from IncuSOL with the airbrush before returning the component for heating.

  ! Delicate structures, such as thin fin arrays, are highly susceptible to damage. Even at the lowest pressure setting available on the Incus airbrush station, the airflow can deform the component if applied from an incorrect angle.

- During airbrush application aim the nozzle directly into narrow channels and between fin structures. It is recommended to lower the pressure and move the nozzle closer for more precise application.

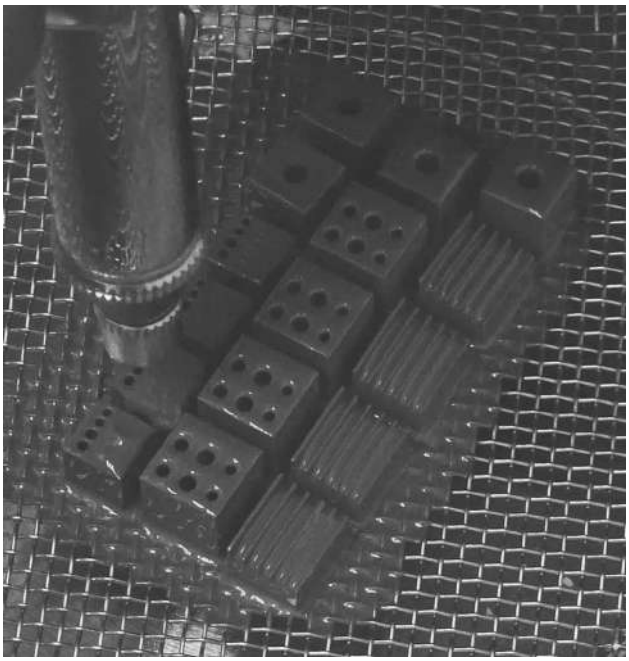

Figure E.11: Shows airbrush use up close on channels.

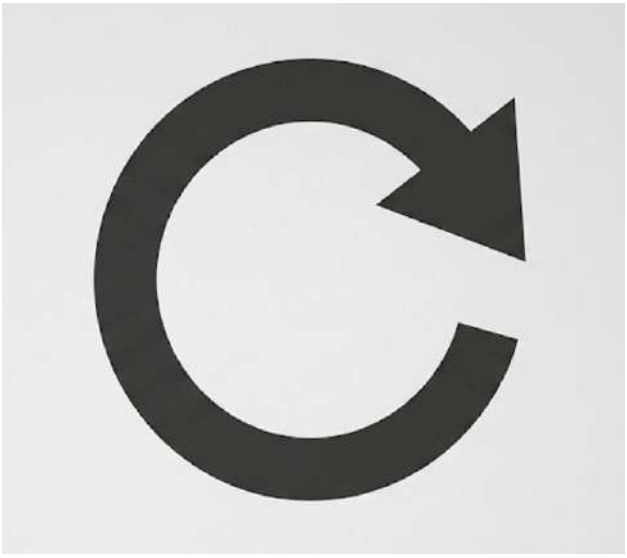

Figure E.12: Repeat symbol.

- Repeat airbrush steps 4 times with roughly 2 seconds of application per component. The air pressure depends on component geometry and the appropriate pressure differs on all components. Stable components with thick walls can handle larger pressures and the nozzle positioned close to the component. Weaker structures require a larger distance between component and nozzle and a lower pressure. No general rule has been established that is applicable to all components.

! If excessive amounts of IncuSOL is used this may cause blistering or delamination.

! When detaching the IncuSOL container from the airbrush, blow the airbrush dry for a few seconds afterwards, otherwise IncuSOL may remain in the airbrush.

Step 3: Ultrasonic cleaning

Figure E.13: Ultrasonic cleaner.

- For the last step in the cleaning sequence ultrasonic cleaning can be applied. Higher frequencies are less aggressive, however it also have negative effect in cleaning efficiency. The ultrasonic cleaner in the lab runs at 37 kHz. Incus recommends approximately 40 kHz.

! Thin walled components such as fins have a high possibility of being damaged in the ultrasonic cleaning process due to collisions.

! Ultrasonic cleaning may cause rounded corners and delamination.

- Submerge for 60 seconds. Continually move the sieve up and down to cause a flushing effect over the components. After ultrasonic treatment, gently dry the components with the airbrush. The cleaning is now complete!

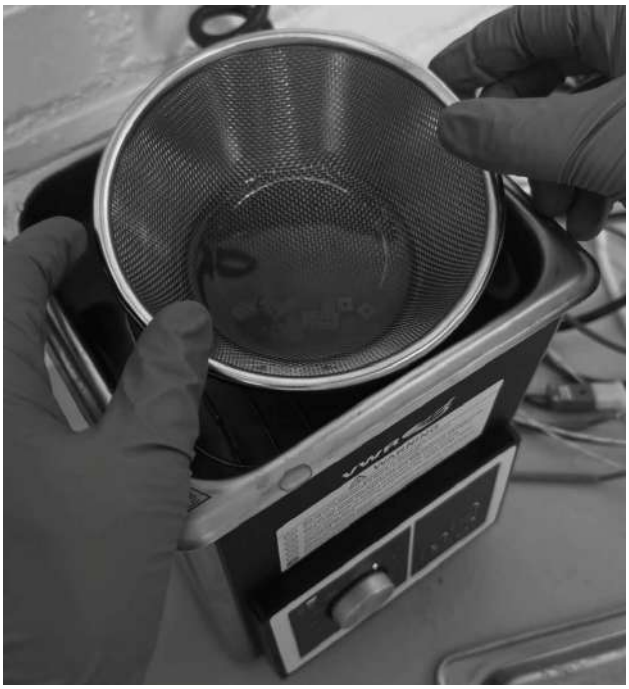

Figure E.14: Ultrasonic cleaning step.

F Drawings of test components

This appendix contains the full drawings of the test components.

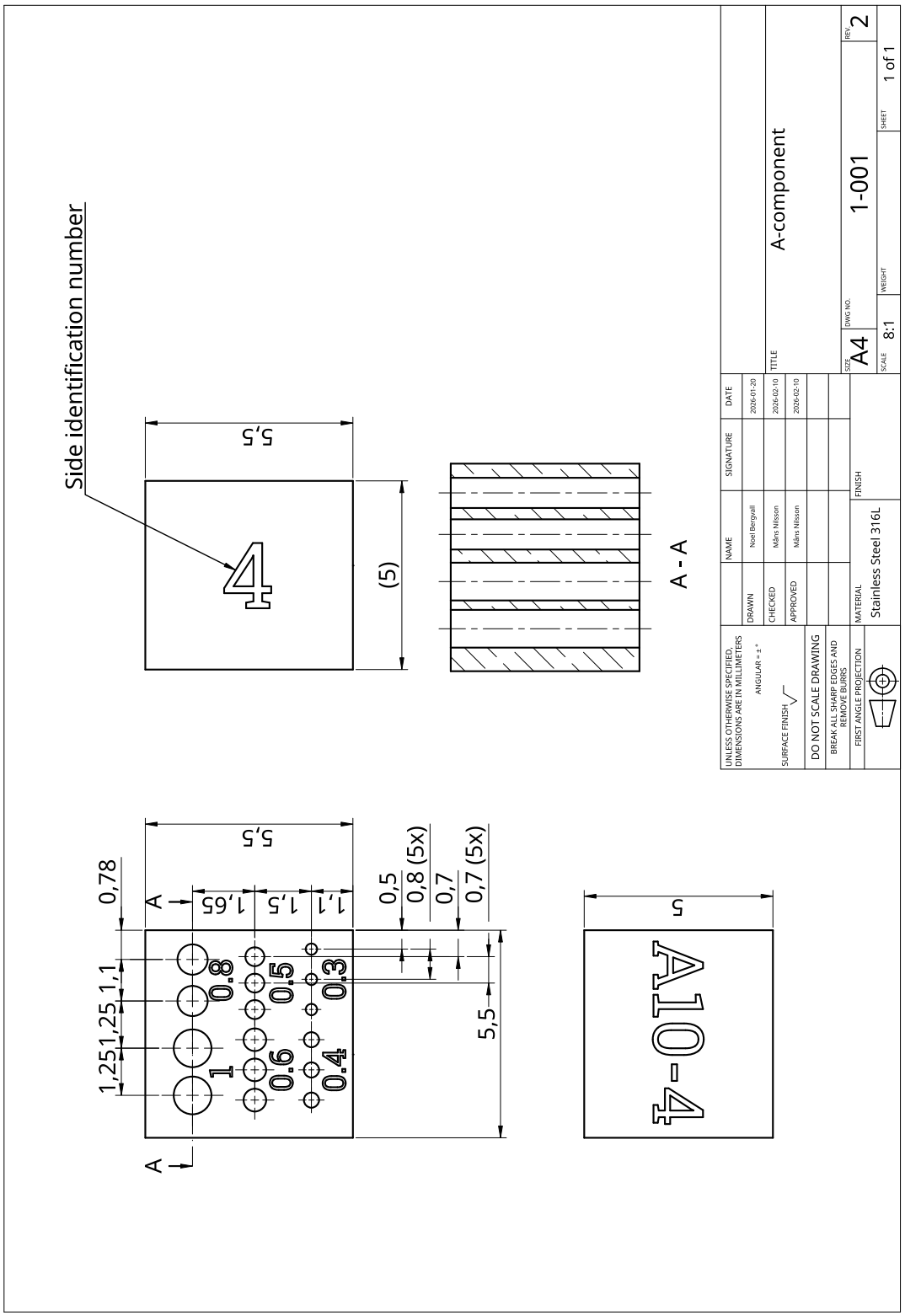

Figure F.1: Technical drawing of component A.

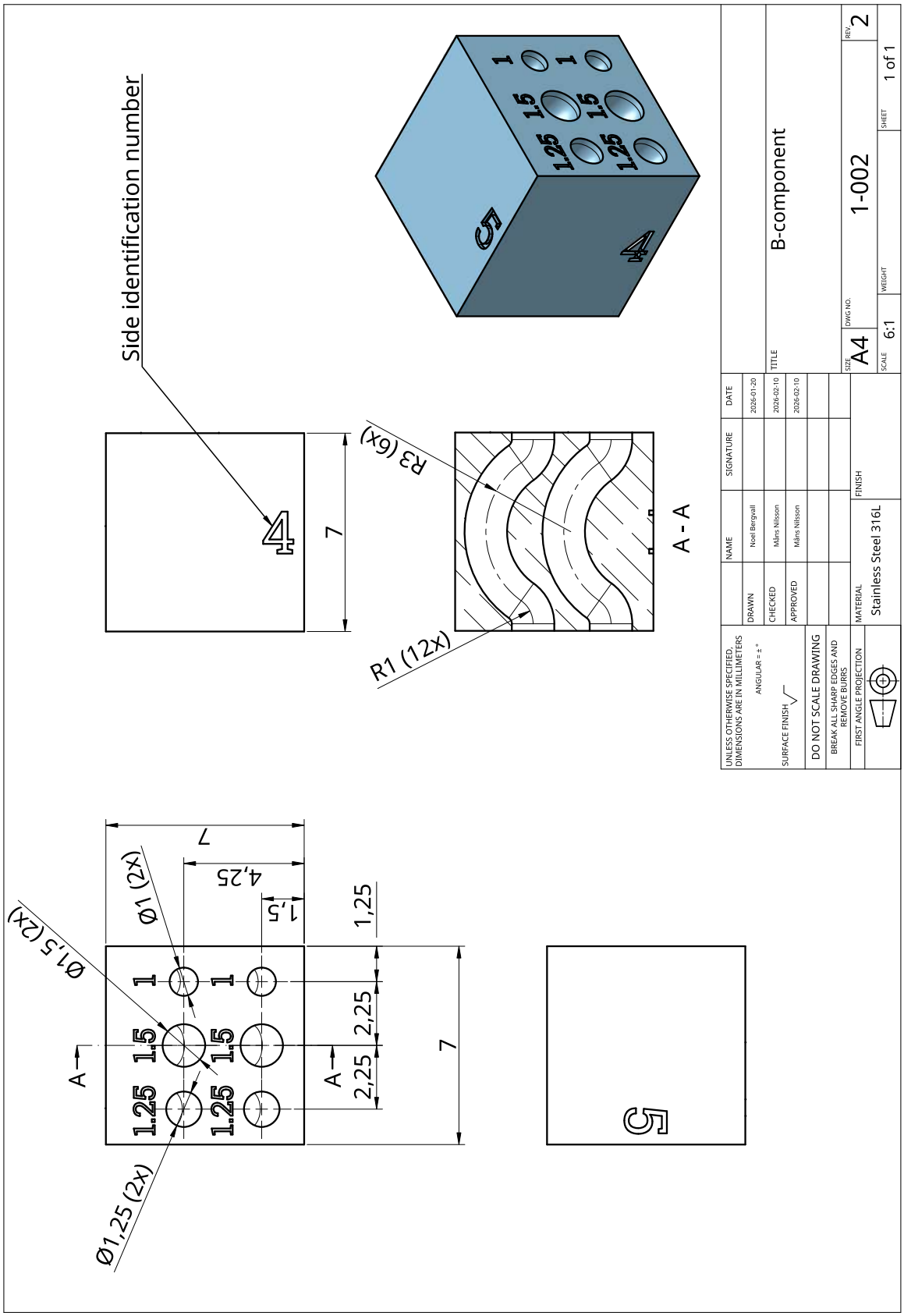

Figure F.2: Technical drawing of component B.

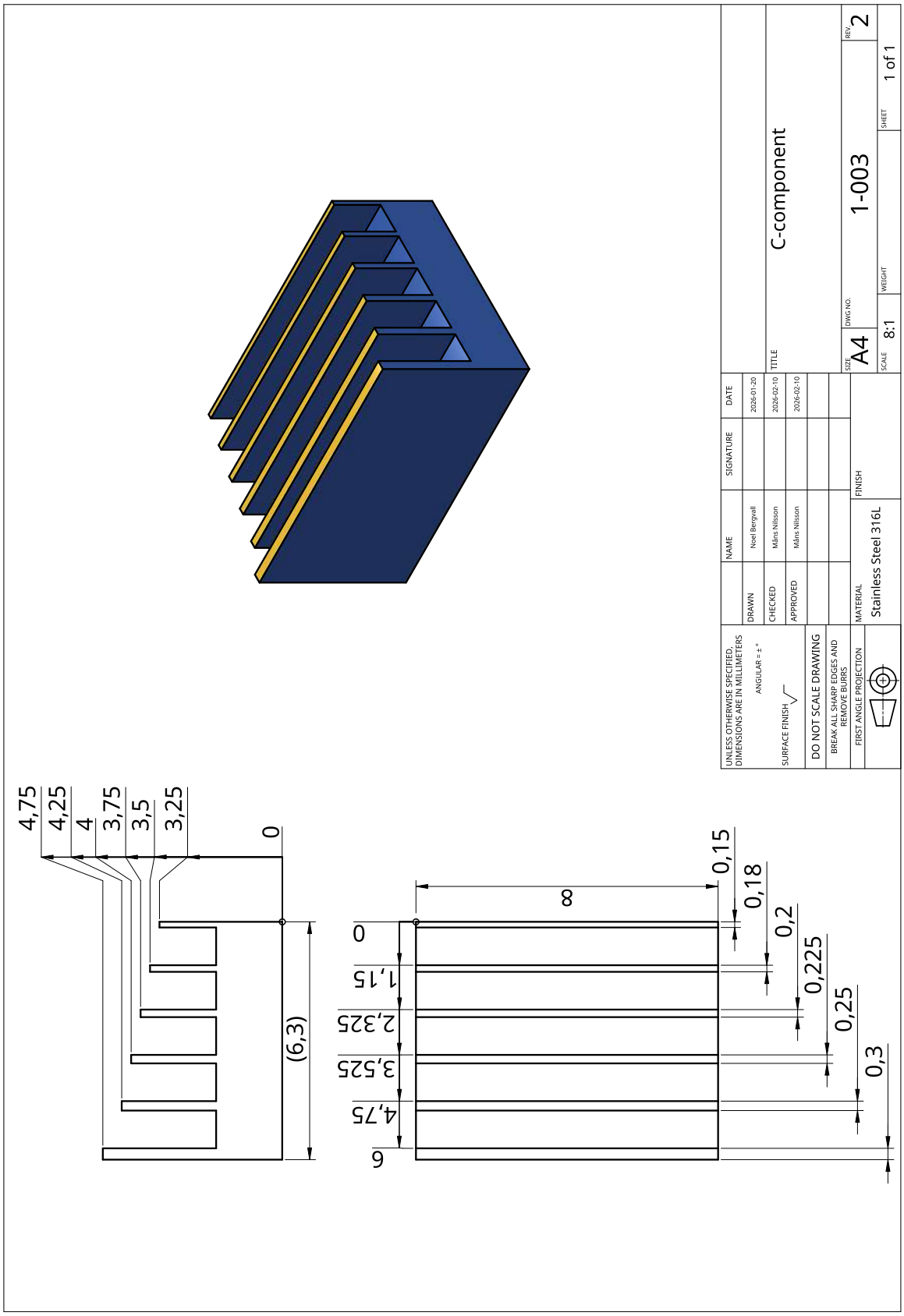

Figure F.3: Technical drawing of component C.

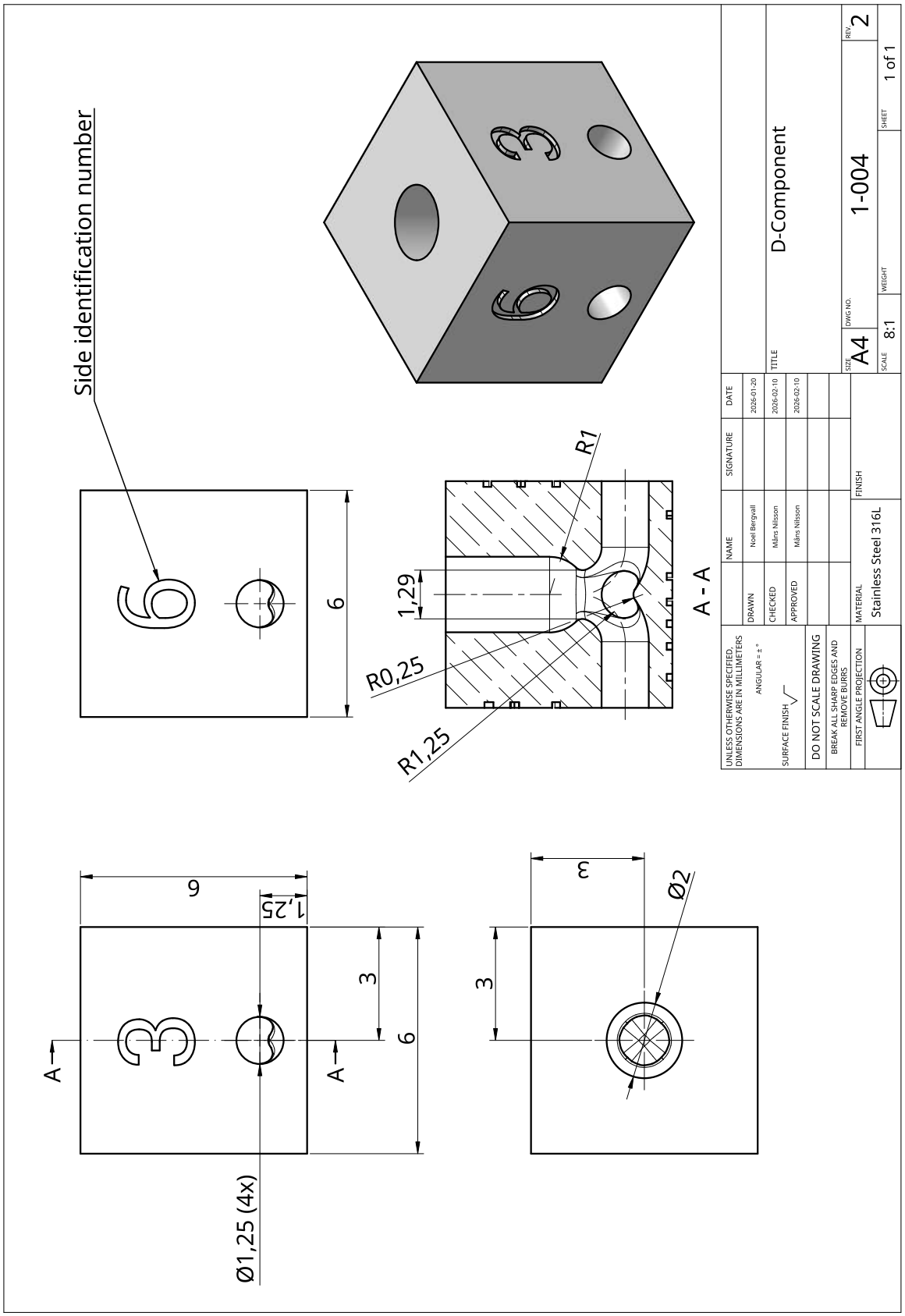

Figure F.4: Technical drawing of component D.